IMPROVING SCFV STABILITY THROUGH FRAMEWORK ENGINEERING

A Thesis Submitted to the College of

Graduate Studies and Research

In Partial Fulfillment of the Requirements

For the Degree of Master of Science

In the Department of Biochemistry

University of Saskatchewan

Saskatoon

By

Wayne I Hill

PERMISSION TO USE

In presenting this thesis in partial fulfillment of the requirements for a Postgraduate degree from the University of Saskatchewan, I agree that the Libraries of this University may make it freely available for inspection. I further agree that permission for copying of this thesis in any manner, in whole or in part, for scholarly purposes may be granted by the professor or professors who supervised my thesis work or, in their absence, by the Head of the Department or the Dean of the College in which my thesis work was done. It is understood that any copying or publication or use of this thesis or parts thereof for financial gain shall not be allowed without my written permission. It is also understood that due recognition shall be given to me and to the University of Saskatchewan in any scholarly use which may be made of any material in my thesis.

Requests for permission to copy or to make other use of material in this thesis in whole or part should be addressed to:

Head of the Department of Biochemistry
University of Saskatchewan
Saskatoon, Saskatchewan, S7N 5E5

ABSTRACT

The availability of cost-effective high throughput screening assays combined with an enhanced understanding of oncogenesis has driven the development of more potent, specific, and less toxic anti-cancer agents. At the forefront of these advances are immunoglobulin molecules and their fragments. However, difficulties in producing antibodies in sufficient quantity and quality for commercial application have driven the development of alternative systems that can produce antibodies efficiently and cost-effectively. This thesis focuses on the engineering of an antibody fragment referred to as a single chain variable fragment (scFv), which consists of antibody light and heavy chain variable domains fused together by a peptide linker.

Although the use of scFvs circumvents many of the issue of full-length antibody production, they still possess their own unique set of difficulties, including stability. In this thesis, we explored the following strategies to increase scFv stability. First, we increased the number of linkers used to join the variable light and heavy domains. We constructed two linear and two cyclic permutated scFvs that contained additional peptide linkers. Two linear permutated scFvs, named Model 1 and Model 3, showed increased stability with calculated melting temperatures (T_ms) exceeding that of the unpermutated scFv. The two cyclic scFvs were less stable with T_ms less than that of the unpermutated scFv. Second, we mutated light and heavy variable domains by introducing prolines or mutating glycine to alanine in the variable domain framework regions. Sites for proline mutations and glycine to alanine mutations were identified and scFvs containing the mutations were purified and their thermal stability tested. Unfortunately, there were no discernible differences between purified scFv mutants and the control scFv. Third, we designed a new selection/screening strategy using phage display and yeast two-hybrid assays to identify complementarity determining regions on scFvs that increased intracellular stability. We used this strategy to isolate anti-Abl-SH3 scFvs. Transient expression of scFvs in K562 cells indicated that two anti-Abl-SH3 scFv decreased viability.

ACKNOWLEDGEMENTS

I would first like to start by thanking my supervisor, Dr. Geyer, for his guidance and support throughout my project. I am grateful for his confidence in my ability to learn and perform the variety of techniques required for this project. His incredible knowledge of the literature and techniques combined with his ability to think of the big picture is inspiring.

I would like to thank current and past members of my committee, Dr. Stanley Moore, Dr. Yu Luo, Dr. Bill Roesler, and Dr. Ramji Khandelwal for their feedback and suggestions over the years of my studies.

I would like to thank all members of the Geyer lab. In particular, I must thank Dr. Landon Pastushok. Beginning when I first started my project and continuing every day since, he not only tolerated the torrent of questions I had, but always responded calmly with helpful answers and insight. The completion of many projects would not have been possible without his help.

The cell biological portion of this project was made possible with the support and facilities of Dr. John DeCoteau. During those experiments, Karen Mochoruk spent many hours and days from her already busy schedule helping and teaching me. I am thankful for the time she devoted.

Finally, I owe my wife, Marie-Paule Hill, great thanks for her love and support during my studies. There were many long nights and weekends where she was left to take care of our energetic first daughter. Then halfway though my studies, our second daughter was born. For your encouragement, understanding, and sacrifice, I will always be grateful.

TABLE OF CONTENTS

LIST OF TABLES

LIST OF FIGURES

LIST OF ABBREVIATIONS

2YT	2x Yeast extract and Tryptone Broth
Abl	Abelson tyrosine kinase
Amp	Ampicillin
ATP	Adenosine triphosphate
Bcr	Breakpoint cluster region
bp	Base pairs
Carb	Carbenicillin
CCC-dsDNA	Covalently Closed Circular dsDNA
Cdk	Cyclin dependent kinase
CDRs	Complementarily determining regions
C_H	Constant heavy domain
CHO	Chinese hamster ovary
C_L	Constant light domain
CML	Chronic myeloid leukemia
Cap	Chloramphenicol
CSM	Complete synthetic media
ddH_2O	Sterile double distilled water
DMSO	Dimethyl sulfoxide
DNA	Deoxyribonucleic acid
DSF	Differential scanning fluorimetry
DTT	1,4-dithiothreitol
dU-ssDNA	Uracil-containing ssDNA
E. coli	*Escherichia coli*
ELISA	Enzyme-linked immunosorbent assay
f1 ori	Filamentous phage origin of replication
Fab	Antigen binding fragment
Fc	Crystallisable fragment
FCC	Frozen competent cell solution
FDA	Food and Drug Administration
FR	Framework region
Fv	Variable fragments
HA	Hemagglutinin tag
I_C	Intein C-terminal domain
IgG	Immunoglobulin G
IMDM	Iscove's modified dulbecco's media
I_N	Intein N-terminal domain
IPTG	Isopropyl β-D-1-thiogalactopyranoside
Kan	Kanamycin
kDa	Kilo dalton
LacZ	Beta-galactosidase
LB	Lysogeny broth
mAb	Monoclonal antibody
MBP	Maltose binding protein
MCS	Multiple cloning site

MSCV	Murine stem cell virus
NEB	New England Biolabs
NLS	Nuclear localization sequence
PBS	Phosphate buffered saline
PBT	Phosphate buffered saline with tween 20
PCR	Polymerase chain reaction
pFv	Permutated Fv
PGK	Phosphoglycerate kinase
Protein-3, P3	M13 bacteriophage gene-3 minor coat protein
PrP	Prion protein
S. cerevisiae	*Saccharomyces cerevisiae*
scFv	Single chain variable fragment
SD	Synthetic dextrose
SD H-	Synthetic dextrose His- media
SD H-W-	Synthetic dextrose His- Trp- media
SD H-W-L- A- Xgal+	Synthetic dextrose His- Trp- Leu- Ade- Xgal+ media
SD W-	Synthetic dextrose Trp- media
SDS-PAGE	Sodium dodecyl sulfate polyacrylamide gel electrophoresis
SGR H-W-L- A- Xgal+	Synthetic galactose raffinose His- Trp- Leu- Ade- Xgal+ media
SH2/3	Src Homology 2/3 domains
SOC	Super Optimal Broth with Catabolic repressor medium
Ssp	*Synechocystis species*
Taq	*Thermus aquaticus*
Tet	Tetracycline
T_m	Melting temperature
Tris	Tris(hydroxymethyl)aminomethane
Tween 20	Polyoxyethylene (20) sorbitan monolaurate
V_H	Variable heavy domain
V_L	Variable light domain
Xgal	5-bromo-4-chloro-3-indolyl-β-D- galactopyranoside
YFP	Yellow fluorescent protein
YPDA	Yeast peptone dextrose adenine
ΔG_u	Gibbs free energy change of unfolding

1 Introduction

Understanding the function and therapeutic potential of proteins has been greatly enhanced due to advances in genomic analysis. However, directed experimentation is still necessary to form a comprehensive understanding of protein function. Strategies for performing reverse analysis on protein function, such as gene deletion or loss of function mutations, are informative but such techniques are difficult to perform rapidly and on a variety of organisms. Technologies that inhibit protein function in a dominant, manner such as antisense RNA, ribozymes, dominant negative proteins, and antibodies, do not alter the genetic material that encodes the protein. These technologies have the advantage of being easier to use in diploid and polypoid organisms. Further, antibodies and dominant-negative proteins inhibit protein function by directly interacting with the protein target. Therefore, they can block specific interaction while leave others unperturbed. This makes them useful for evaluating the therapeutic potential of a protein target.

Antibodies are highly specific for their targets and have the potential to interact with proteins *in vivo* (Antman and Livingston, 1980). However, expression of antibodies inside cells is problematic (Fellouse and Sidhu, 2007). Fortunately, antigen-binding regions of an antibody exist solely on two variable fragments (Fvs); the variable light (V_L) and variable heavy (V_H) domains. Although V_L and V_H are the minimum required elements for antigen binding, when separated from each other, they tend to unfold and aggregate (Jäger and Plückthun, 1999). These fragments can be stablized by joining them together with a short peptide linker. The peptide-linked V_L and V_H fusion is defined as a single chain variable fragment (scFv).

Bacterial expression of scFvs has been problematic as many scFvs are insufficiently stable for intracellular expression. Multiple strategies have been employed to increase scFv stability, including framework mutations (Barthelemy *et al.*, 2008; Jespers *et al.*, 2004; Kügler *et al.*, 2009; Wörn and Plückthun, 2001) and the addition of extra peptide linkers (Brinkmann *et al.*, 1997) or disulphide-bonds (Young *et al.*, 1995; Glockshuber *et al.*, 1992) that join V_L and V_H domains. Attempts have been made to abandon the V_L chain and focus on stabilizing only the V_H chain (Dolk *et al.*, 2005; Jespers *et al.*, 2004). All of these attempts have been met with varying levels of success and a highly stable scFv that can accommodate a wide range of complementarity determining regions (CDRs) has not yet been obtained.

2 Literature Review

2.1 Therapeutic Target Discovery

2.1.1 Drug Discovery

Advances in genomic and proteomic methods have revolutionized our understanding of roles that genes and their encoded proteins play in living cells. Novel techniques for molecular cloning and cultured cell transfection have provided relatively rapid and efficient ways to determine consequences of overexpression or deletion of specific proteins. Combined with the knowledge obtained from the completion of the human genome project, many therapeutic targets for various cancers have been identified.

Until recently, most cancer treatments were chemotherapeutic agents discovered by high-throughput ligand binding assays, biochemical assays, or cell-based assays (Liu *et al.*, 2004). These approaches led to several target-specific anti-cancer agents being approved for treatment of cancer patients. These agents include small molecules such as: all-trans-retinoic acid or ATRA for promyelocytic leukemia, EGF-receptor protein tyrosine kinase inhibitor (Irresa®) for the treatment of non-small cell lung cancer, and Bcr-Abl tyrosine kinase and c-kit tyrosine kinase inhibitor (Gleevec®) used for the treatment of chronic myeloid leukemia (CML) and for gastric intestinal stromal tumor (Atkins and Gershell, 2002). Using similar techniques, a number of antibodies have been approved for treatment. They include anti-HER2 monoclonal antibody (Herceptin®) used for HER-2 positive breast cancer treatment, anti-CD34 monoclonal antibody (Myelotarg®) for acute myelocytic leukemia treatment, and anti-CD20 antibody (Rituxan®, Zevalin®, and Bexxar®) used for treatment of low grade B-cell lymphoma (Liu *et al.*, 2004).

Many therapeutics have been developed by screening large collections of complex natural products or chemical compounds for their cytotoxic activity on cancer cell lines. Most of these drugs are relatively non-specific, toxic, and cause significant side effects on cancer patients. Further, their targets may not be validated with an absolute level of certainty, as the opportunity costs of delaying new treatments must be considered. In fact, the FDA and other regulatory bodies do not require the target of the drug to be known (Hardy and Peet, 2004). Still, their development is very cost prohibitive, such that only large pharmaceutical companies can afford the extensive collections of natural products and compounds required.

The pace of identifying new potential drug targets now far exceeds the development of new therapeutics. Faster methods of drug discovery are needed if we are to fully exploit this flood of information. Indeed, with recent developments in combinatorial chemistry methods (Kennedy *et al.*, 2008); Ng *et al.*, 2012; Messeguer and Cortés, 2007) and biologically-driven library creation (Marasco, 1995; Rimmele, 2003; Sidhu and Koide, 2007), libraries can now be generated by smaller start-up companies and academic laboratories.

With our ever-increasing understanding of oncogenesis combined with the availability of cost-effective high throughput screening assays, more potent, specific, and less toxic anti-cancer agents will be developed. It is anticipated that antibodies and their fragments will be at the forefront of these advances.

2.1.2 Antibodies

Antibodies provide a key portion of our defense against pathogenic organisms and toxins. They are able to bind antigens with high specificity and affinity. Therapeutic antibodies are almost exclusively generated from the main serum antibody, immunoglobulin G (IgG). As shown in Figure 2.1, the intact form of an antibody is a Y-shaped multi-domain protein composed of two light chains and two heavy chains. The heavy chain is comprised of one variable heavy (V_H) domain, and three constant heavy (C_H) domains, identified as C_{H1}, C_{H2}, and C_{H3}. The smaller light chain consists of one variable light (V_L) domain and one constant light region (C_L). The antigen-binding fragment (Fab) is comprised of the C_{H1}, C_L, V_H, and V_L domains, where the antigen-binding site is located on V_H, and V_L domains. Variable domains each contain three hyper-variable loops or CDRs, which are responsible for antigen binding. Recruitment of effector functions are mediated by the stem crystallisable fragment (Fc) domain comprised of constant heavy domains, C_{H2} and C_{H3}.

In research and therapeutic applications, antibodies can be used in reverse genetics approaches. Although requiring injection into cells, antibodies have been shown to block the function of intracellular targets (Antman and Livingston, 1980). Through binding to the target, they have been shown to promote the activation of specific biochemical steps (Hori, 1991; Kim *et al.*, 1993) or couple their natural effector functions (Dyer *et al.*, 1989; Reff *et al.*, 1994). Additionally, through conjugation to secondary proteins or molecules, they can provide even further functions (Hinman *et al.*, 1993; Liu *et al.*, 1996).

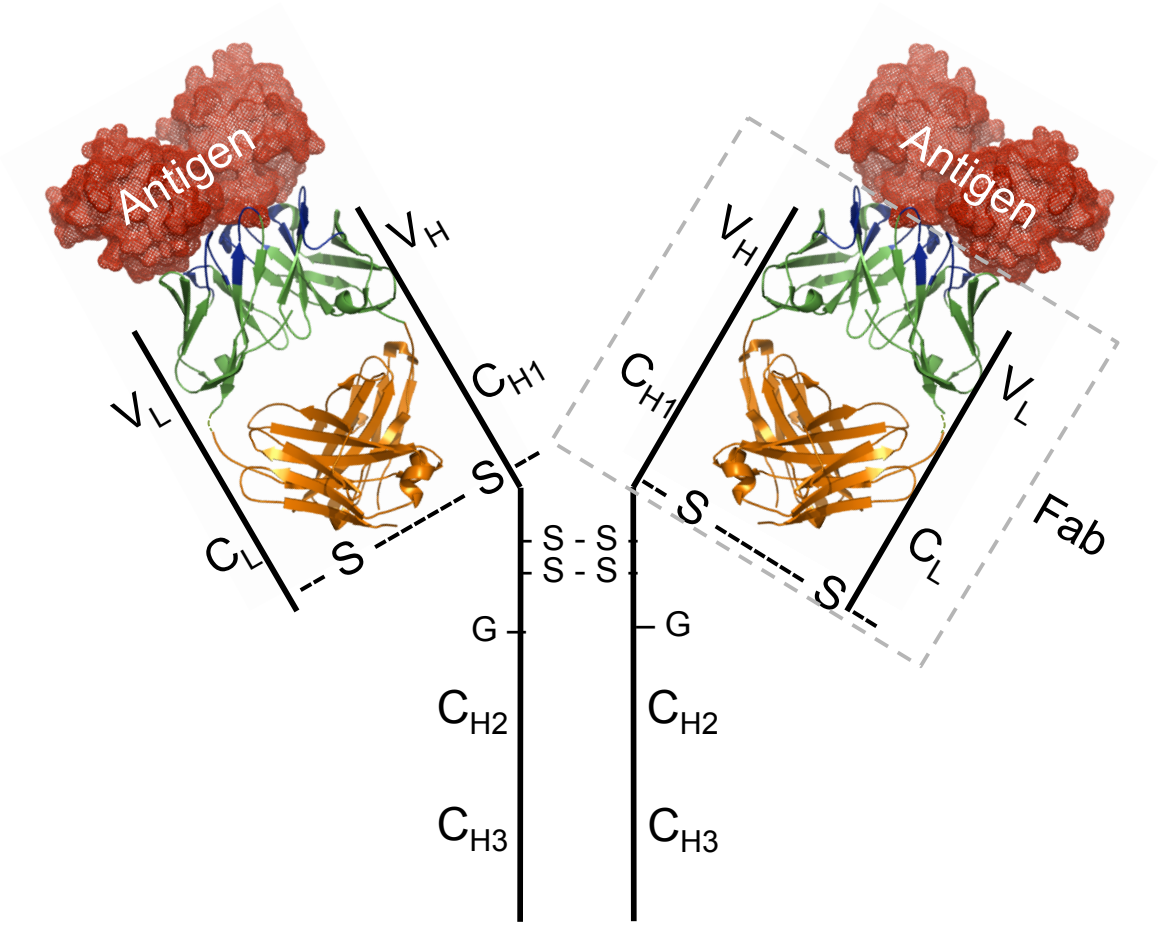

Figure 2.1. Structure of the Immunoglobulin G Antibody
A schematic view of the heterotetramer Immunoglobulin G (IgG) molecule composed of two light chains and two heavy chains. The heavy chain is comprised of one variable heavy (VH) domain, and three constant heavy (CH) domains. The smaller light chain consists of one variable light (VL) domain, and only one constant light region (CL). The antigen-binding fragment (Fab) is comprised of the CH1, CL, VH, and VL domains and is depicted as a cartoon (PDB ID: 3DVG (Newton *et al.*, 2008)). Variable light (VL) and variable heavy (VH) domains each contain three hyper-variable loops known as CDRs, which are shown in blue and bound to the antigen. Interchain disulphide-bonds are shown as (- S - S -) and the glycosylation site on the CH2 domain is shown as (- G). A missing attachment between the VL and CL domain was manually inserted and shown as a dashed green line.

Therapeutic monoclonal antibodies (mAbs) entered clinical study in the early 1980s. However, these antibodies were produced by fusing mouse lymphocytes and myeloma cells to produce murine hybridomas. Problems arose due to patients' production of human anti-mouse antibodies. This immune reaction causes anaphylaxis and serum sickness. Moreover, subsequent administration of the antibody would be ineffective as the immune system would be prepared to destroy them (Shawler and Bartholomew, 1985). To improve the potential of therapeutic mAbs, attempts were made to decrease mAb immunogenicity by reducing the number of murine sequences. This was accomplished through development of mAb chimeras derived from both human and mouse DNA (Morrison *et al.*, 1984), and production of fully human mAbs through CDR grafting onto a human framework or obtained from mice genetically engineered to produce human antibodies (Roque *et al.*, 2004)(Cole *et al.*, 1984). However, removing the murine component was not sufficient to make the immunogenicity problem disappear. Most of the FDA-approved mAbs report that some patients have developed detectable antibodies to the therapeutic (Reichert *et al.*, 2005). Indeed, any protein therapeutic has the potential to cause the human immune system to produce antibodies.

Another problem is the difficulty in producing antibodies in sufficient quantity and quality for therapeutic and commercial applications. Currently, mammalian cells such as Chinese hamster ovary (CHO) and NS0 cells remain the most prominent cell lines of choice for the production of therapeutic antibodies. However, large doses (in some cases over one gram per patient per year) are often required for therapeutic purposes (Andersen and Reilly, 2004). This need has driven the development of alternative systems that can produce antibodies efficiently and cost-effectively.

Ideally, antibody expression would occur in a bacterial host where rapid growth of expression cultures is possible and efficient mutagenesis and DNA manipulation have been established. However, expression of antibodies inside bacterial cells is problematic for a number of reasons: First, antibodies, such as IgGs, contain two heavy chains and two light chains. Folding and assembly of the heterotetramer occurs after translocation through the endoplasmic reticulum membrane and assisted by several molecular chaperones such as BiP and PDI (Gonzalez *et al.*, 2001). This mechanism is not possible using a bacterial expression system. Second, these chains are linked together by several disulphide-bonds. In the cytoplasm of *E. coli*, formation of stable disulphide-bonds does not occur. Indeed, in early antibody-

engineering experiments, antibodies expressed in the cytoplasm of bacteria showed low levels of antigen-binding activity (Boss *et al.*, 1984). Third, a post-translational modification, glycosylation of the heavy chain, is required for biological specific activities of antibodies (Andersen and Reilly, 2004). Gylcosylation is not possible in bacterial since they lack the appropriate glycosylation machinery. Further, antibodies lacking glycosylation can be improperly folded or degraded by the cell (Gonzalez *et al.*, 2001).

The desire for efficient antibody production has led to the recent development of transgenic plant and fungal antibody production systems (Roque *et al.*, 2004) and producing full-length glycosylated antibodies in *E. coli* (Simmons *et al.*, 2002). Nevertheless, mammalian cells are still the dominant system used to produce antibodies.

2.2 Single Chain Variable Fragments

2.2.1 ScFv Development

Since the entire antibody is not required for antigen binding, other development paths have been taken to circumvent many of the issues facing antibody production. The antigen-binding regions of antibodies exist solely on V_L and V_H domains. Each variable domain contains three CDRs that are responsible for binding. These CDRs are hyper-variable loops held together by a moderately conserved framework region (FR) (Kabat *et al.*, 1987). However, when separated from each other, V_L and V_H domains tend to unfold and aggregate. Thus, interaction between the two domains is required for maximum stabilization. In a complete antibody, the V_H-V_L interface is stabilized by fusion to constant regions, which are linked by a disulphide-bond. However, it is possible to stabilize variable domains by joining them together with a short peptide linker (Jäger and Plückthun, 1999). The fusion of a V_L and a V_H together by a peptide linker is defined as a single chain variable fragment (scFv) (Figure 2.2).

Natural antibodies contain intra-molecular and inter-molecular disulphide-bonds. With the construction of an scFv, the inter-molecular disulphide-bonds are no longer of concern as they are removed with the constant regions. However, many scFvs expressed in the cytoplasm of bacteria show low levels of antigen binding. This is a result of improper folding due, in part, from a failure to form stable intra-molecular disulphide-bonds (Morino *et al.*, 2001). Attempts to create an scFv without disulphide-bonds have been unsuccessful (Wörn and Plückthun,

1998). Introducing a signal sequence, such as pelB or ompA, onto the N terminus of the Fv facilitated the transport of the scFv to the periplasm, where conditions are more conducive for the formation of disulphide-bonds. This resulted in the successful production of Fv with "adequate" antigen-binding capabilities (Skerra and Plückthun, 1988).

2.2.2 ScFvs in Research Applications

With the ability to produce antibody fragments on a relatively large scale, techniques evolved to exploit their benefits. For example, antibody microarrays using individually addressable electrodes are able to run thousands of assay in tandem; this is compared to a conventional immunoassay, which is limited to just a couple of hundred assays per day. Moving towards antibody fragment biosensors provides a small, stable and highly specific reagent against the target antigen. This has allowed the movement away from immobilization onto glass-surface microarrays towards more protein friendly surfaces (Hamelinck *et al.*, 2005). As a result, companies such as Biosite, Zyomyx, PerkinElmer, and Pointilliste, have released microarray platforms, incorporating this new technology (Holliger and Hudson, 2005).

Effector functions such as antibody-dependent cell-mediated cytotoxicity are mediated though interaction of the Fc domain with various Fcγ receptor. Successful antibody interaction with its activating receptor is often critical for effective antibody therapeutics (Dyer *et al.*, 1989). Due to the removal of the Fc domain, scFvs lack effector functions. Although effector functions are desirable in many therapeutic treatments, there are some conditions where their removal may have a positive effect on treatment (Simmons *et al.*, 2002). For example, removal of the effector function can be advantageous for imaging applications, where a long serum half-life results in poor contrast (Holliger and Hudson, 2005). Even so, if effector functions are desirable, such as killing the target cell, techniques such as coupling the scFv to a chemical toxin are possible.

Indeed, through conjugation, possibilities of using scFv in diagnostics are only limited by one's imagination. For example, Markiv *et al.* (2011) have created a chimeric scFv for use in screening by bridging the V_L and V_H chains with a red fluorescent protein. Since the monomeric β-barrel fluorophore architecture is essentially the same as other colour variants, the modular nature of this chimeric scFv enables the creation of a palette of fluorescent scFvs for simultaneous multi-analyte detection. Another modification, the addition of cysteine or histidine to the peptide linker, enabled the scFv to self-assemble onto gold nanoparticles. This

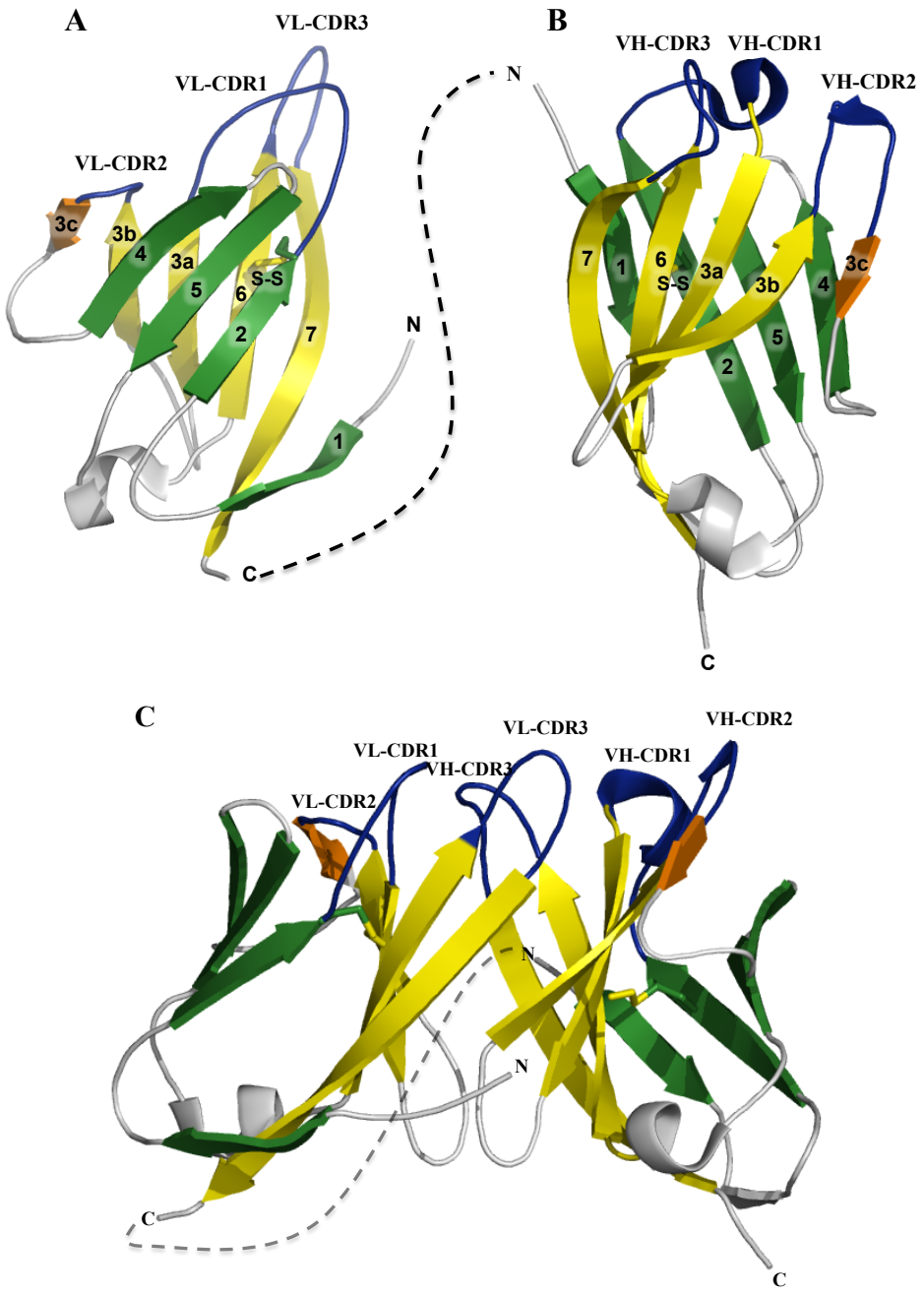

Figure 2.2. ScFv Structure
Crystal structure of anti-ubiquitin single chain variable fragment (scFv) (PDB ID code 3DVG) depicted in cartoon format (Newton *et al.*, 2008). This scFv contains the same framework as the anti-MBP scFv used in this thesis. (**A**) Variable light (V_L) and (**B**) variable heavy (V_H) domains consist of a pair of β sheets with a single disulphide bond (S-S) bridging the two sheets. When the V_L and V_H are fused together by a short peptide linker (manually inserted and shown as dashed line), it is defined as an scFv. Each variable domain contains three hyper-variable loops called complementarity determining regions (CDRs) (shown in blue) that are responsible for binding. (**C**) The variable domains associate through the five strand β sheets (yellow) although strand 3c (orange) does not participate in the packing.

allowed for the development of a highly sensitive colorimetric immunosensor (Liu and Mernaugh, 2009). Even more exotic applications have been developed such as the recent conjugating of scFvs to quantum dots. Using this technology, scFv can potentially be used for targeted imaging and early diagnosis of cancer (Lu *et al.*, 2011).

2.2.3 ScFvs as Therapeutics

Beyond the use of antibody fragments in diagnostics, recent developments have shown their use as therapeutic agents. New display and selection technologies, such as phage display, are improving the speed at which binders can be generated or improved. With the creation of large synthetic *in vitro* repertoires of antibody fragments, library-screening technologies have now superseded hybridoma technology. ScFvs are also commonly used in high throughput screening methods such as phage display (Prins *et al.*, 2005; Sidhu and Koide, 2007) and yeast display (Boder and Wittrup, 1997). Recently, Ho *et al.* (2006) showed that mammalian cells can be engineered for cell surface display of functional scFvs. This was accomplished by fusing the anti-CD22 scFv to the trans-membrane domain of human platelet-derived growth factor receptor (PDGFR) displayed on human embryonic kidney (HEK) 293T cells. Using a combinatorial library created by randomizing the CDR3 of the V_L chain, they showed that an scFv with an increased binding affinity for CD22 could be obtained after a single round of selection (Ho *et al.*, 2006).

As a result of these high throughput selection methods, antibody fragments are joining mAbs as powerful therapeutic agents. In particular, scFvs show promise targeting cancer, inflammatory, autoimmune, and viral diseases. Recently a number of scFv therapeutics been entered into clinical trials. Pexelzumab, a humanized scFv used to block the complement activation following heart bypass surgery, is now in phase III clinical trials (Smith *et al.*, 2011; Testa *et al.*, 2008). Another scFv, SNG-17, used for treating melanoma by targeting the P97 antigen, is now in preclinical trails (Pucca *et al.*, 2011). The breast cancer therapy named F5cys-MP-PEG(2000)-DSPE is an anti-HER2 scFv-lipopolymer conjugate in the preclinical stage (Nellis *et al.*, 2005). Other antibody fragments have entered the preclinical or clinical phase, such as bispecific scFvs and scFvs diabodies, where the V_L and V_H of one scFv bind the V_H and V_L, respectively, of another scFv (Pucca *et al.*, 2011; Holliger and Hudson, 2005).

To highlight the rapid pace of scFv development, a patent search using the free worldwide patent site *espacenet* (http://ep.espacenet.com) showed a total of 757 scFv patents

have been published since 1996. In comparison, a paper looking at the same search parameters in 2009 found 315 scFv published patents (Pucca *et al.*, 2011). Technologies with the ability to improve both pharmacokinetics and functionality of engineered mAb fragments should lead to further increasing the approval and use of scFvs in diagnosis and therapy.

2.2.4 Strategies for ScFv Drug Delivery

In vivo studies have confirmed that molecular size is an important parameter for tissue penetration and retention (Holliger and Hudson, 2005). Proteins, peptides, or small molecules can be directed at extracellular targets. However, if an intracellular target is of interest, then the drug must cross the cell membrane. Traditionally, this has been accomplished with small molecules or peptidomimetic compounds (Liu *et al.*, 2004). Large IgG molecules that have been developed for tumor specific targets, with a size of 150 kDa, have slow solid tumor penetration and high serum levels. Conversely, small scFv fragments with a size of 28 kDa are able to penetrate the tumor rapidly (Holliger & Hudson, 2005). Recently, scFvs targeting the hepatocyte growth factor receptor c-Met, selectively bound to several lung cancer cell lines expressing c-Met and became internalized. Additionally, conjugation of the anti-c-Met scFv with PEGylated liposomes enabled the efficient delivery of doxorubicin into cancer cells (Lu *et al.*, 2011). These results suggest that scFv-mediated drug delivery systems show promise in tumor-targeted therapy.

Unfortunately, although these smaller fragments rapidly penetrate tumors, they are just as rapidly cleared from the blood. This is common to most small molecules, which has fostered the movement towards larger constructs, such as scFv-C_{H3} dimers (75 kDa) called minibodies. Minibodies have shown higher tumor uptake and retention than their IgG counterparts. Combined with their substantially faster clearance, minibodies may be ideal for tumor therapy (Olafsen *et al.*, 2004). However, the rapid clearance of scFvs may be due in part to their monovalent binding properties. Faced with the necessity of frequent delivery of antibody fragments, research has also moved towards the creation of bivalent diabodies (55 kDa). Due to their relatively small size, they retain rapid tissue penetration and blood clearance and have high avidity. These attributes make them ideal for intracellular therapeutic and imaging applications (Robinson *et al.*, 2005).

To circumvent problems with rapid blood clearance and difficulties with large-scale production of scFvs, another strategy for delivery is being developed. *In situ* methods of gene

delivery allow for localized and sustained expression of the scFv. This can be accomplished by transforming cells *ex vivo* and then reintroducing them into the patient. By allowing the synthesis of proteins of interest directly in the host, difficulties with large-scale production are overcome. *In situ* experiments performed with an anti-vascular endothelial growth factor (VEGF) scFv reduced the tumor growth in mice by 50%. When injections of recombinant adenovirus encoding the scFv are administered systemically, substantial tumor inhibition is observed (Afanasieva *et al.*, 2003). Additionally, by administering multiple virus injections the results were improved even further.

2.3 Strategies to Stabilize scFvs

2.3.1 Introduction

Due to the enormous potential of antibody fragments in diagnostics and therapeutics, there has been considerable interest in overcoming the inherit instability of these fragments. Techniques to create a tighter integration between V_L and V_H domains, such as the addition of disulphide-bonds (Young *et al.*, 1995; Glockshuber *et al.*, 1992), V_L and V_H interface point mutations (Tan *et al.*, 1998), or introduction of additional linkers (Brinkmann *et al.*, 1997) have shown moderate success. Other techniques that focus on the framework region have varied levels of success. For example, the introduction of point mutations in the framework (Barthelemy *et al.*, 2008; Jespers *et al.*, 2004; Kügler *et al.*, 2009; Wörn and Plückthun, 2001) or complete transfer of the CDRs to another framework (Jung and Plückthun, 1997) have increased scFv stability.

Another strategy in development to overcome the scFv stability problem is the use of even smaller antibody fragments. Nanobodies, such as the VhH in camelids and V-NAR in sharks, are single V_H-like domains. These domains have four amino acid substitutions in their framework region. This renders the surface more hydrophilic and can explain the observed increase in solubility. VhH also has improved penetration against immuno-evasive target antigens (Stijlemans *et al.*, 2004). However, humanization may be crucial to reduce immunogenicity for *in vivo* administration. Although studies of llama VhH domains have shown to be only minimally immunogenic (Cortez-Retamozo, 2004), for therapeutic applications, human domains would be preferable, provided that problems of poor stability and solubility can be solved.

2.3.2 ScFv Peptide Linkers with Improved Stability

Creating a scFv by fusing V_L and V_H domains together with a linker causes a unique problem; there is a potential for these linkers to cause the formation of dimers and multimers, where the V_L domain of one chain binds to the V_H domain of another chain. Although, formation of multimeric scFvs may be beneficial in some circumstances (Holliger *et al.*, 1993), these multimers result in reduced stability. Therefore, linkers that favour the formation of a monomer over a dimer may increase scFv stability. The length of the peptide linker largely determines the oligomer formation preference. As linker length increases, the proportion of dimer decreases. Linkers that are 0, 5, or 10 amino acids in length mainly form dimers (Arndt *et al.*, 1998). However, as the linker becomes longer, the antigen-binding activity of the scFv is decreased (Desplancq *et al.*, 1994) and the linker may be more susceptible to proteolytic degradation (Alfthan *et al.*, 1995). Therefore, the linker length must be a compromise between antigen-binding potential and degradation resistance of short linkers, and the monomer formation potential of longer linkers.

Using this information, Robinson and Sauer determined that linkers 19 amino acid long have the greatest equilibrium stability to thermal denaturation (Robinson and Sauer, 1998). They further refined the linker composition and created a linker with seven Ser and nine Gly framed by three Gly on either side. This linker provides preference for monomer formation and has suitable antigen-binding activity. The interpretation of these experiments has led to the use of the peptide linker $(G_3S)_4$ as the most common scFv linker. However, currently unpublished data from the Geyer lab identified eleven potential linkers using phage display that may further increase the stability of the scFvs. Thermal stability testing on these linkers has shown that four linkers (C1, C3, E3, E5) (Table 2.1) provide increased thermal stability with one in particular (C3) being the most stable. However, their intracellular stability has yet to be determined.

Table 2.1. Novel ScFv Linkers

Linker	Amino Acid Sequence
Traditional	GGGSGGGSGGGSGGGS
C1	AGSSSSGGSTTGGSTT
C3	GTTAASGSSGGSSSGA
E3	SSATATAGTGSSTGST
E5	TSGSTGTAASSTSTST

2.3.3 ScFv Permutation

In 1997, Brinkmann *et al.* developed a novel method to stabilize scFvs. Typically, the C-terminal end of the V_L chain is joined to the N-terminal end of the V_H chain with the peptide linker $(G_3S)_4$. Brinkmann *et al.* (1997) joined V_L and V_H domains together at the base-loop position (Figure 2.3b). By linking the C-terminus of the V_H domain back to the N-terminus of the same domain they created a permutated scFv. They termed this new scFv, a permutated Fv (pFv). When compared to the non-permutated scFv, the pFv retained its affinity and specificity. The pFv is relatively stable; after 24 hours of incubation at 37˚C, both the unpermutated scFv and the pFv retained similar levels of activity (Brinkmann *et al.*, 1997).

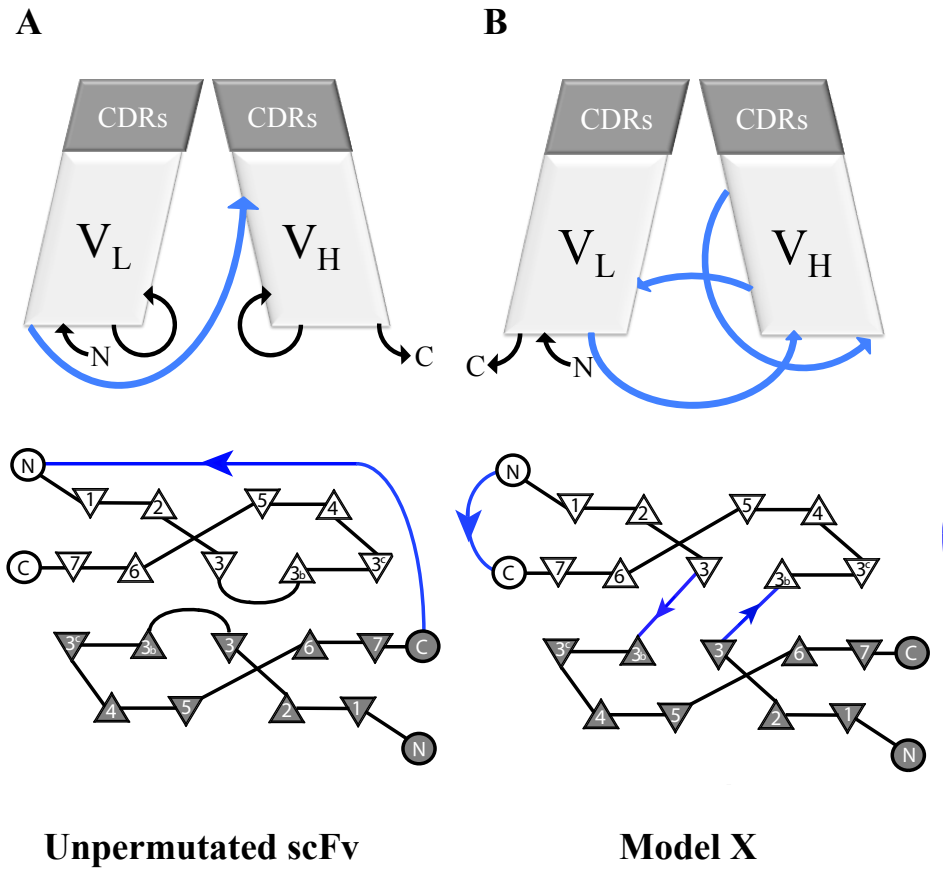

Figure 2.3. Schematic of the Permutated ScFv.
The standard unpermutated scFv (A) is included for reference. Arrows indicate the direction of synthesis from the N- to C-terminis. Peptide linkers are shown in blue. In the top row of images, base-loops are depicted as circular loops located at the bottom of the variable regions. Schematic representations are included in the bottom row. The numbered triangles represent the orientation of strands in β sheets. Model X pFv (B) connects the V_L and V_H though the base-loop regions.

2.3.4 Lariat Peptide Technology

In an attempt to overcome difficulties associated with displaying peptides, such as degradation by proteases, an intein-mediated method has been developed to produce cyclic peptides and proteins *in vivo* (Scott *et al.*, 1999). These naturally occurring intein proteins catalyze a self-splicing reaction, which involves the removal of the intein from a precursor protein to produce a mature protein (Figure 2.4A). A permutated form of the precursor protein where the order of intein domains are changed results is a cyclic protein with no free N or C terminus (Figure 2.4B). Although the elimination of free ends confers increased resistance to protease degradation, it also excludes the potential to fuse additional protein/peptide moieties. Thus, the cyclic technology is not useful for high throughput screen techniques such as the yeast two-hybrid assay. In an attempt to overcome this limitation for use in reverse analysis experiments, a lariat peptide was developed (Barreto *et al.*, 2009) (Figure 2.4C). The lariat peptide is produced by blocking the cyclic peptide reaction at an intermediate step, which produces a lariat peptide fused to a transcription activation domain that is required for the yeast two-hybrid. This lariat peptide strategy has been used to generate combinatorial libraries of lariat scFvs. Lariat scFv libraries performed better in the yeast two-hybrid assay relative to a linear scFv (Bernhard, 2008).

2.3.5 Variable Domain Framework Mutations

Structural studies on the V_H domain showed that a single mutation has dramatic effects of the stability of variable domains. For example, stabilizing experiments performed on the camelid VhH domain showed that mutation of a single amino acid, Gln44 to Arg, significantly increased its affinity for the target (Dolk *et al.*, 2005). Further, using structural knowledge about the camelid VhH domain, the stability of a V_H domain derived from a human framework has been improved by mutating Ser35 of the heavy chain to Gly (Jespers *et al.*, 2004). These results indicate that a single mutation can have a significant stabilizing effect on antibody fragments. However, these results may not be applicable to all V_H-like domains.

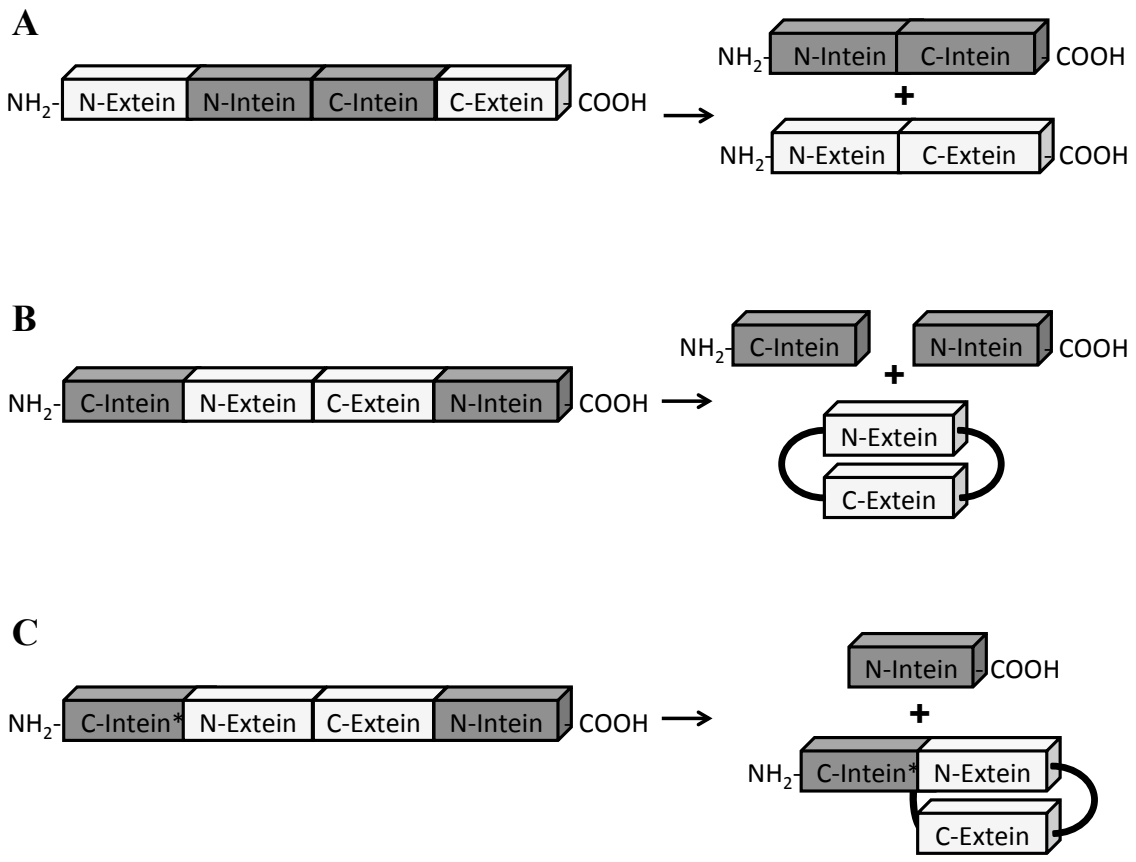

Figure 2.4. Intein-Mediated Protein Splicing
(A) Naturally occurring inteins (grey) catalyze a self-splicing reaction, removing the intein from a precursor protein and joining exteins (white) to produce a mature protein. **(B)** A permutated form of the intein changes the relative order of the intein domains. In this permutated arrangement, the self-splicing reaction produces a head to tail cyclization of the extein. **(C)** A mutation of the C-intein (*) blocks the reaction at an intermediate step where only the N-intein is removed. A lariat protein is produced which retains the C-intein domain. This lariat peptide strategy has been used to generate combinatorial libraries of lariat scFvs.

The stabilizing strategies, involving the mutation of Gly to Ala and any amino acid (Xaa) to Pro, was first described by Matthews *et al.* (1987). This study showed that mutating certain amino acids to Pro or mutating Gly to Ala increased the stability of bacteriophage T4 Lysozyme (Matthews *et al.*, 1987). This is due to the relationship between the stability of proteins and Gibbs free energy of unfolding (ΔG_u). For most proteins, as the temperature increases, the ΔG_u decreases (Schellman, 1997). When the concentrations of folded and unfolded proteins are equal, ΔG_u equals zero. The temperature at which this occurs is the melting temperature (T_m) (Niesen *et al.*, 2007). By reducing the conformational flexibility of the protein, these mutations are able to decrease the entropy of unfolding.

Framework mutations as described by Matthews have been successfully applied to Beta-propeller phytase (Tung *et al.*, 2008), Cold shock protein B, Histidine-containing phosphocarrier protein (HPr), and several ribonucleases (Fu *et al.*, 2009). In 2009, Robert *et al.* successfully prevented aggregation of the WO-2 scFv with a Ser46 to Pro mutation (Robert *et al.*, 2009).

2.3.6 Phage Display

In 1985, George Smith first described the phage display technology for selecting peptides from combinatorial peptide libraries (Smith, 1985). Five years later it was shown that this technique could also be used to display antibody fragments (McCafferty *et al.*, 1990). The strength of this technique is that it provides a physical link between the genotype and phenotype. This is possible due to the use of a specialized vector called a phagemid, which contains the following components: First, the phagemid contains a dsDNA origin of replication as well as an ssDNA filamentous phage origin of replication (f1 ori). The f1 ori allows packaging of the DNA into the phage particles. Second, the phagemid contains a fusion protein consisting of the protein of interest fused to the gene-3 minor coat protein of the filamentous bacteriophage M13 (P3 or pIII) (Lee *et al.*, 2007). The fusion protein is displayed on the outside surface of the bacteriophage with the DNA that encodes the protein encapsulated inside the phage particle (Figure 2.5A).

ScFv libraries that are displayed on phage particles are screened for interactions with a target as shown in Figure 2.5B. Library members that are able to bind to the target are retained. Conversely, library members that do not bind to the target are washed away. The bound phage are eluted and used immediately for infection and amplification in a bacterial host strain. Once

purified, the newly enriched phage library can be used for analysis or another round of enrichment.

The power and utility of the phage display technique cannot be overstated: the development of scFv-cys stabilized gold NPs (Liu and Mernaugh, 2009), the isolation of anti-CEA nanobodies (Cortez-Retamozo, 2004), and the development of scFvs with improved solubility and thermodynamic stability (Jespers *et al.*, 2004), are all accomplished using the phage display technique. Indeed, many of the technologies mentioned in this thesis have also been developed using phage display.

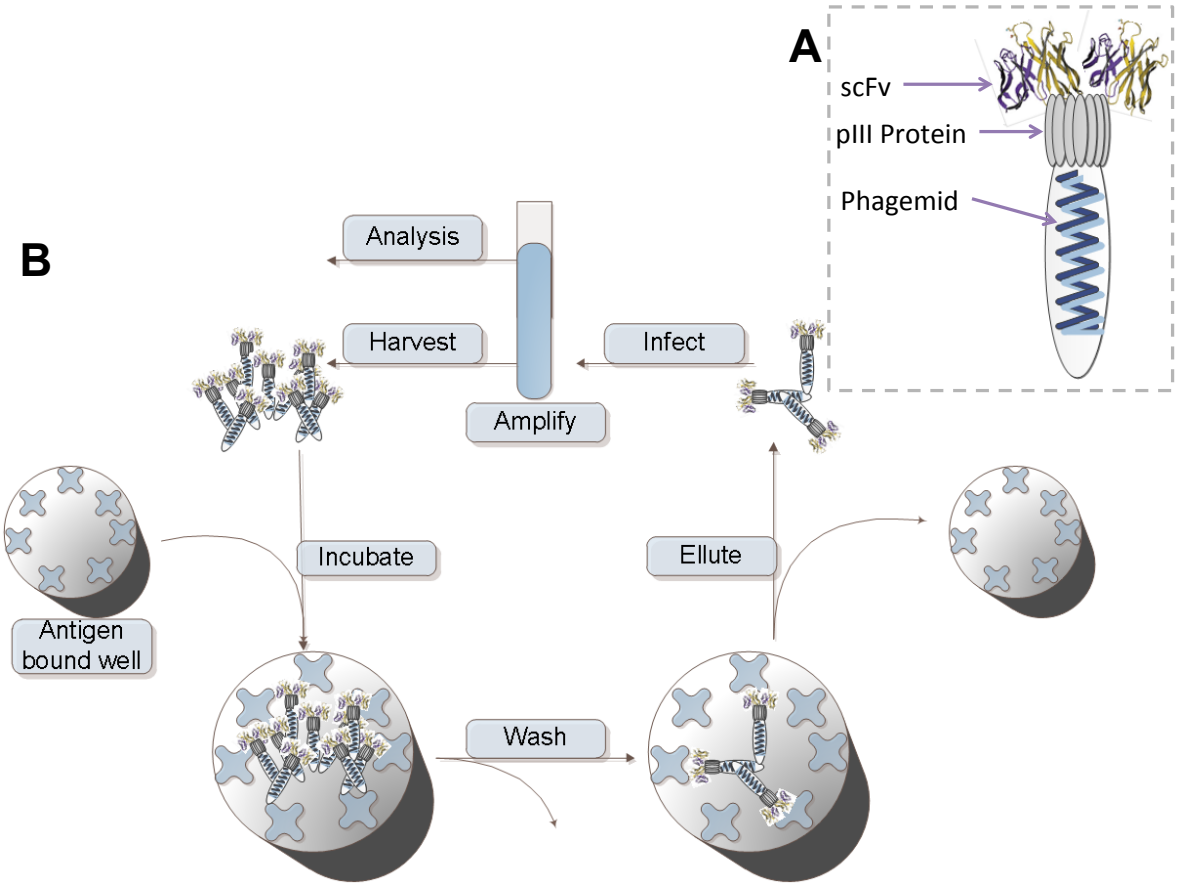

Figure 2.5. Phage Display Selection
(A) Phage structure. ScFvs are fused to the pIII coat protein and displayed on the outside surface of the bacteriophage with the ssDNA that encodes the protein encapsulated inside the phage particle. **(B)** Phage display selection: A library of phage particles are incubated in a well coated with the target protein. The well is washed and phages that bind to the target remain. Bound phage are eluted and amplified by infection into a bacterial host. Phage can be harvested and used for analysis or another round of enrichment.

3 Objectives and Specific Aims

The development of antibody fragments, such as scFvs, circumvents many of the issues faced with full-length antibody production. However, they are not without their own unique set of limitations such as stability. Due to the enormous potential of antibody fragments in diagnostics and therapeutics, there has been considerable interest in overcoming the inherit instability of these fragments. To improve the stability of scFvs the following strategies were pursued: (i) Increasing the number of linkers that join the V_L and V_H domains together. (ii) Introducing stabilizing mutations into the framework region of variable domains. (iii) Designing new genetic selections to isolate scFvs with stable CDRs.

3.1 Specific Aim 1: Increase ScFv Stability Using Novel Linkers

Permutated scFvs will be designed with an increased number of linkers joining the V_H and V_L domains. Purification of permutated scFvs will be attempted using two new plasmids and two *E.coli* expression strains. Following purification, thermal stability assays will be performed to determine the stability of the permutated scFvs as well as cyclic and lariat scFvs.

3.2 Specific Aim 2: Increase ScFv Stability Using Variable Domain Framework Mutations

Amino acids in the framework region of the variable domains that can tolerate a proline mutation or a glycine to alanine mutation will be identified. A phage library containing all possible combinations of mutations will be created by Kunkel mutagenesis. Mutations favouring the antigen binding properties of scFvs will be identified using phage display selection. ScFvs containing favourable mutations will be purified and their thermal stability will be will be tested.

3.3 Specific Aim 3: Increase the Intracellular Stability of ScFvs

A library of scFvs enriched by phage display selection will be panned against their targets using the yeast two-hybrid assay. The yeast two-hybrid assay will be performed using two of our prey vectors (linear and lariat) and compared for their relative efficiency in promoting scFv interaction with its target. CDRs of scFvs isolated by yeast two-hybrid screening will be compared to CDRs isolated by the phage display assay. ScFvs that interact

with their target in the yeast two-hybrid assay and the phage display screening will be identified. The effects of two anti-Abl-SH3 scFvs on chronic myeloid leukemia cell viability will conducted by transient expression in leukemia cells.

4 Materials and Methods

4.1 General Information

4.1.1 Reagents and Suppliers

Table 4.1. Reagents

Reagent	Supplier
Gel Purification Kit	Qiagen
PCR Clean-up Kit	Qiagen
Miniprep Kit	Qiagen
QIAPrep Spin M13 Kit	Qiagen
PCR Purification Kit	Bio Basic Inc.
Plasmid DNA Kit	Bio Basic Inc.
Nitrocellulose	Bio-Rad
Odyssey Blocking Buffer	LI-COR Biosciences
Oligonucleotides	Integrated DNA Technologies (IDT)
Salmon Sperm DNA	Sigma
Fast SYBR® Green Master Mix	Applied Biosystems
EZ-Link Sulfo-NHS-LC-Biotin	Thermo Scientific
Protein Assay Dye Reagent Concentrate	Bio-Rad
SYPRO Orange	Sigma
TMB Liquid Substrate	Sigma
Strep-Tactin Superflow Agarose	Novagen
MicroAmp® Fast Optical 96-Well Reaction Plate, 0.1 ml	Applied Biosystems
MicroAmp® 96- & 384-Well Optical Adhesive Film	Applied Biosystems

Table 4.2. Enzymes

Enzyme	Supplier
Calf Intestinal Phosphatase (CIP)	New England Biolabs
HotStar Taq	Invitrogen
Platinum Taq DNA Polymerase High Fidelity	Invitrogen
T4 DNA ligase	New England Biolabs
T4 DNA ligase High Concentration	Invitrogen
*EcoR*I	New England Biolabs
*Xho*I	New England Biolabs
*Sal*I	New England Biolabs
*Nru*I	New England Biolabs
T7 DNA Polymerase	New England Biolabs
T4 Polynucleotide Kinase (PNK)	New England Biolabs

Table 4.3. Antibodies

Antibody	Supplier
Goat Anti-Mouse LI-COR IRDye 800CW	LI-COR Biosciences
Mouse Anti-SBP antibody	LI-COR Biosciences
Horseradish peroxidase/anti-M13 antibody conjugate	GE Healthcare

Table 4.4. Oligonucleotides

Oligonucleotides were obtained from IDT. Restriction enzyme cut sites are italicized and linkers are underlined.

S.No	Name	Sequence (5' -> 3')
1	P1 scFv/pET-LP2 5'	GCG GAA TTC GAT ATC CAG ATG ACC CAG TCC
2	P2 scFv/pET-LP2 3'	GCG GTC GAC CGA GGA GAC GGT GAC CAG
3	ProAla Sub p1	ATG ACC CAG TCC CCG YTC TCC CTG TCC GCC TC
4	ProAla Sub p2	AGC TCC CTG TCC GCC YCT SYG GGC GAT CSG GTC ACC ATC ACC TG
5	ProAla Sub p3	ATC AAC AGA AAC CAG SAA AAS CGC CGA AGC TTC TGA TT
6	ProAla Sub p4	GAA AAG CTC CGA AGC YGC TGA TTT ACT CGG C
7	ProAla Sub p5	TAC TCT GGA GTC CCT YCA CGC TTC TCT GGT A
8	ProAla Sub p6	CTT CTC GCT TCT CTG SAA GCC GTT CCG SGA CGG ATT TCA CTC T
9	ProAla Sub p7	TTC ACT CTG ACC ATC YCC YCC CTG CAG CCG GAA G
10	ProAla Sub p8	TCA CGT TCG GAC AGG SAA CCA AGG TGG AGA TC
11	ProAla Sub p9	AGC TGG TGG AGT CTG SCS SAG GCC TGG TGC AGC CAG
12	ProAla Sub p10	TGG TGC AGC CAG GGG SAT CAC TCC GTT TGT C
13	ProAla Sub p11	CAC TGG GTG CGT CAG SCG CCG GGT AAG GGC C
14	ProAla Sub p12	GTG CGT CAG GCC CCG GSA AAG GSC CTG GAA TGG GTT GC
15	ProAla Sub p13	ACT ATA AGC GCA GAC MCG YCC AAA AAC ACA GCC T
16	ProAla Sub p14	GCC TAC CTA CAA ATG MMC AGC CYA AGA GCT GAG GAC AC
17	ProAla Sub p15	GGG GTC AAG GAA CCC YAG TCM CCG TCT CCT CGG TCG
18	P1 VL G41A	CCT GGT ATC AAC AGA AAC CAG CAA AAG CTC CGA AGC TTC TGA TTT AC
19	P2 VL G64A	CCT TCT CGC TTC TCT GCT AGC CGT TCC GGG ACG
20	P3 S76/77P	GAT TTC ACT CTG ACC ATC CCC CCT CTG CAG CCG GAA GAC TTC
21	P4 VH G9R	CTG GTG GAG TCT GGC CGT GGC CTG GTG CAG C
22	P5 VH G16A	CTG GTG CAG CCA GGG GCC TCA CTC CGT TTG TCC
23	P6 VH G42A	GTG CGT CAG GCC CCG GCT AAG GGC CTG GAA TG
24	3BP2-SH2 5' /pEG202	CTG GCG GTT GGG GTT ATT CGC AAC GGC GAC TGG CTG *GAA TTC* ACG ACA GAG TCC TGC GAG
25	3BP2-SH2 3' /pEG202	AAT TCG CCC GGA ATT AGC TTG GCT GCA GGT CGA *CTC GAG* TTA AGC GTA GCC GTA TGG GTG
26	ABL1-SH3 5' /pEG202	GCG GTT GGG GTT ATT CGC AAC GGC GAC TGG CTG *GAA TTC* GGA CCC AGT GAA AAT GAC CCC
27	ABL1-SH3 3'	AAT TCG CCC GGA ATT AGC TTG GCT GCA GGT CGA *CTC GAG*

	/pEG202	TTA AAT TCC CCC TCG AGG GAC
28	SRC-SH3 5' /pEG202	CTG GCG GTT GGG GTT ATT CGC AAC GGC GAC TGG CTG *GAA TTC* GGG GCA CTG GCT GGC GGC
29	SRC-SH3 3' /pEG202	TCG CCC GGA ATT AGC TTG GCT GCA GGT CGA *CTC GAG* TTA TTC AGC CTG GAT GGA GTC TGA
30	scFv/pJG4-5 5'	TAT GAT GTG CCA GAT TAT GCC TCT CCC *GAA TTC* GGA TCC GAT ATC CAG ATG ACC CAG TCC
31	scFv/pJG4-5 3'	AAC CTC TGG CGA AGA AGT CCA AAG CTT *CTC GAG* TTA CGA GGA GAC GGT GAC CAG GGT TCC
32	scFv/pIN01 5'	CAC AAC TTC TTG TTG GCT AAC GGT GCT ATT GCT CAC GCT TCG GGA TCC GAT ATC CAG ATG
33	scFv/pIN01 3'	CAA AAT TTC AGT ACC GAA AGA CAA ACA AGA GCC GCC GCC TTT TTC GAA CTG CGG GTG AGA CCA AGA ACC ACC ACC CGA GGA GAC GGT GAC
34	pEG202 near 5'	TCG AGT CGA CCT GCA GCC AA
35	pEG202 near 3'	GAG TCA CTT TAA AAT TTG TAT ACA C
36	pJG4-5 near 5'	GAG TGG AGA TGC CTC CTA CC
37	pJG4-5 near 3'	AAC CTT GAT TGG AGA CTT GAC C
38	KB41 near 5'	GCC ACA AGA TCA CAA CTT CTT G
39	KB41 near 3'	GGC AAT GGA CCG TAT TCA ACA G
40	P1 scFv/pMSCV 5'	GCG *GAA TTC* ATG TAC CCT TAT GAT GTG CCA GAT TAT GCC GAT ATC CAG ATG ACC CAG TCC
41	P2 scFv/pMSCV 3'	GCG *CTC GAG* TTA CTT ATC ATC ATC ATC CTT GTA ATC CGA GGA GAC GGT GAC CAG
42	pMSCV Seq P1	CCC TTG AAC CTC CTC GTT CGA CC

4.1.2 Strains

Table 4.5. *S. cerevisiae* Strains and Genotypes

Strain	Genotype	Reference
EY93	MATa *ura2 his3 trp1 leu2 ade2::URA3*	(Barreto *et al.*, 2009)
EY111	MATα *his3 trp1 ura3::LexA8op-LacZ ade2::URA3-LexA8op-ADE2 leu2::LexA6op-LEU2*	(Barreto *et al.*, 2009)

Table 4.6. *E. coli* Strains and Genotypes

Strain	Genotype	Reference
MC1061	*F– araD139 Δ(araA-leu)7697 galE15 galK16 Δ(lac)X74 rpsL (Strr) hsdR2 (rK-mK+) mcrA mcrB1*	(Wertman *et al.*, 1986)
XL1-Blue	*recA1 endA1 gyrA96 thi-1 hsdR17 supE44 relA1 lac (F′ proAB lacIqZΔM15 Tn10 (Tetr))*	Stratagene
CJ236	FΔ*(HindIII)::cat* (Tra^+ Pil^+ Cam^R)/ *ung-1 relA1 dut-1 thi-1 spoT1 mcrA*	New England Biolabs
BL21 (DE3)	F– *omp*T *hsd*SB(r_B^-, m_B^-) *gal dcm* (*DE3[lacI lacUV5-T7 gene 1 ind1 sam7 nin5]*)	Novagen
SS320	*hsdR mcrB araD139 Δ(araABC-leu)*7679 Δ*lac*X74 *galUgalK rpsL thi*	Lucigen

SHuffle™	F′ *lac pro lacI^q / Δ(ara-leu)7697 araD13 fhuA2 Δ(lac)X74 Δ(phoA)PvuII phoR ahpC* galE (or U) galK Δλatt::pNEB3-r1-cDsbC (Spec^R, lacI^q) ΔtrxB rpsL150(Str^R) Δgor Δ(malF)3*	New England Biolabs (C3028H)

Table 4.7. Mammalian Cell Lines

Strain	Disease	Description	Reference
K562	Chronic myelogenous leukemia (CML)	Erythrocytic cell type, triploid, multiple t(9;22) translocations, b3-a2 Bcr -Abl fusion	American Type Culture Collection (ATCC) (CCL243)

4.1.3 Plasmids

The following plasmid maps were created using the free online web source PlasMapper (http://wishart.biology.ualberta.ca/PlasMapper/) (Dong *et al.*, 2004)

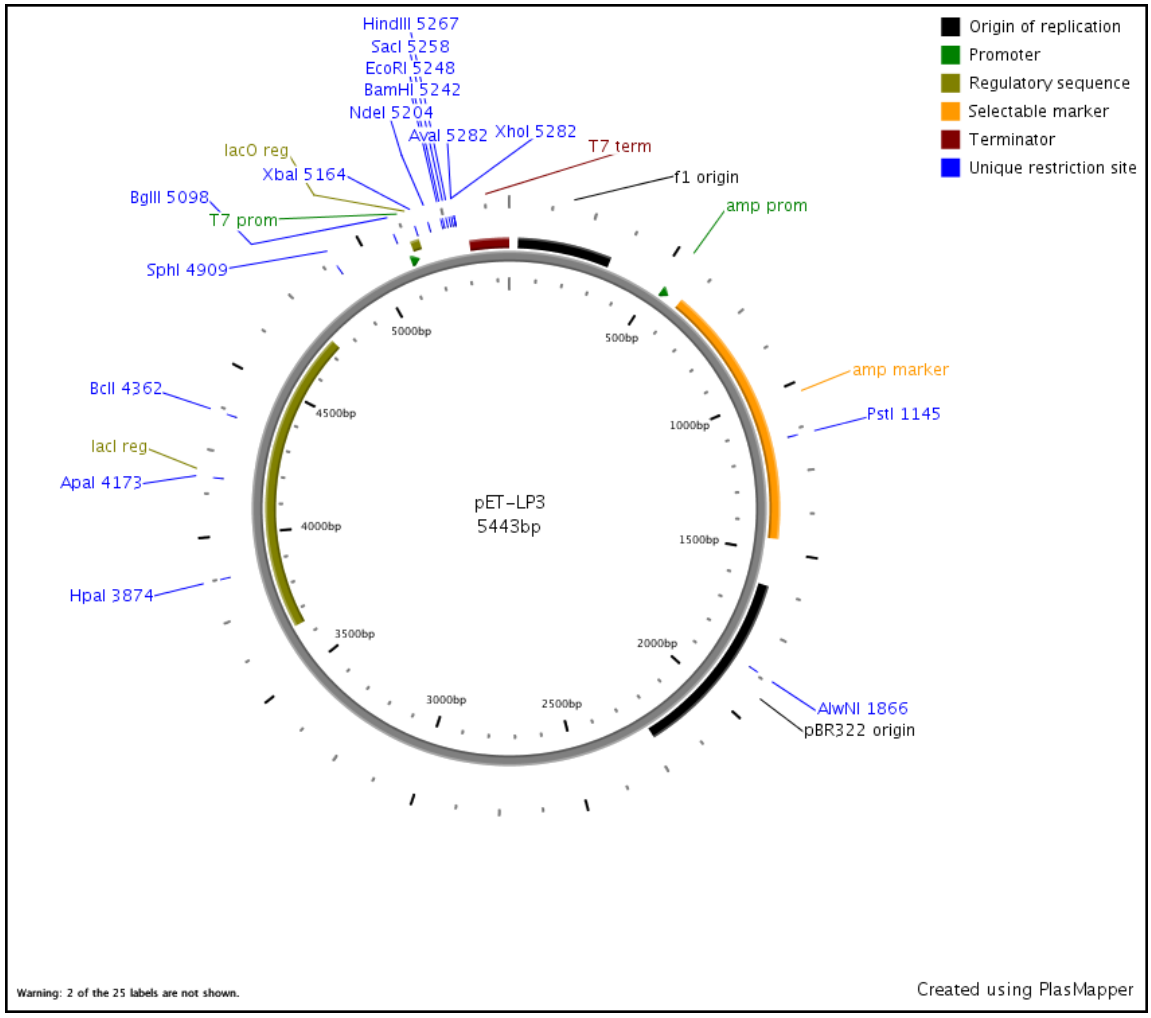

Figure 4.1. pET-LP3 Plasmid

pET-LP3 was used to express proteins in *E. coli*. Protein genes were cloned between *Eco*RI and *Sal*I sites using restriction enzyme cloning. Proteins were expressed with a C -terminal six-histidine sequence tag (6xHis), and an N-terminal Strep-tag II. Expression and termination were controlled by the IPTG inducible T7 promoter (T7 prom) and the T7 terminator sequence, respectively. When required the F1 origin of replication (F1 ori) was used for single -stranded DNA (ssDNA) production. The pBR322 origin was used to maintain a high copy plasmid number in *E. coli*. The ampicillin-resistance gene (amp marker) was used to select for the plasmid in *E. coli*.

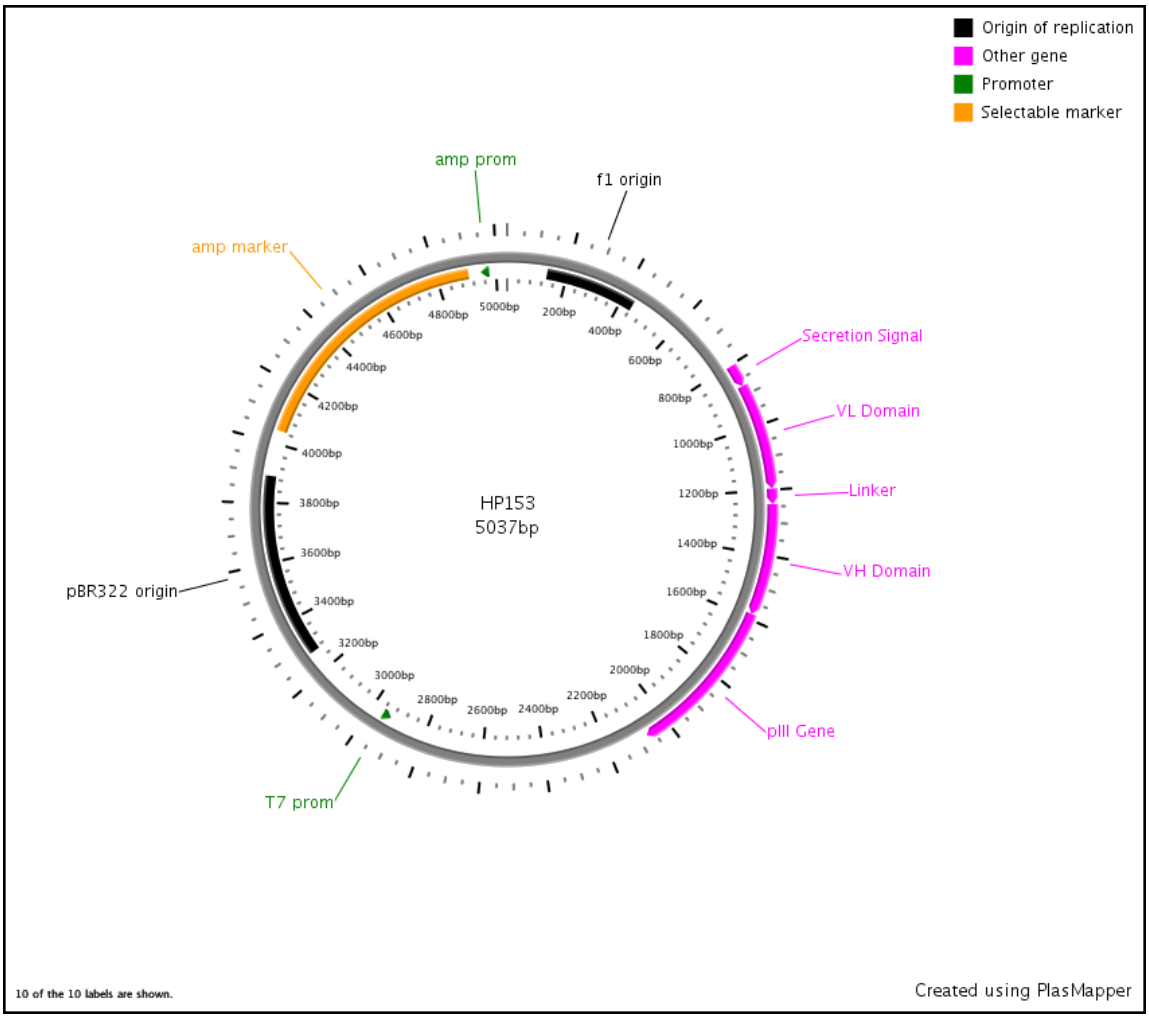

Figure 4.2. HP153/ scFv Phagemid

The HP153 phagemid was designed for scFv display. The phagemid contained a double-stranded DNA origin of replication (pBR322 ori) for replication in *E. coli* and a single-stranded DNA filamentous phage origin of replication (f1 ori) to allow packaging into phage particles. To maintain the plasmid in *E. coli*, the ampicillin-resistance gene (amp marker) was used. For scFv display, the phagemid also contained a cassette, consisting of a promoter that controlled transcription of the scFv, which was fused to an N-terminal secretion signal (Signal peptide) and a C-terminal phage coat protein (pIII gene). Following infection with the helper phage M13K07, ssDNA replication was initiated. The scFv fusion protein was incorporated onto phage particles, whereas the phagemid ssDNA was packaged inside.

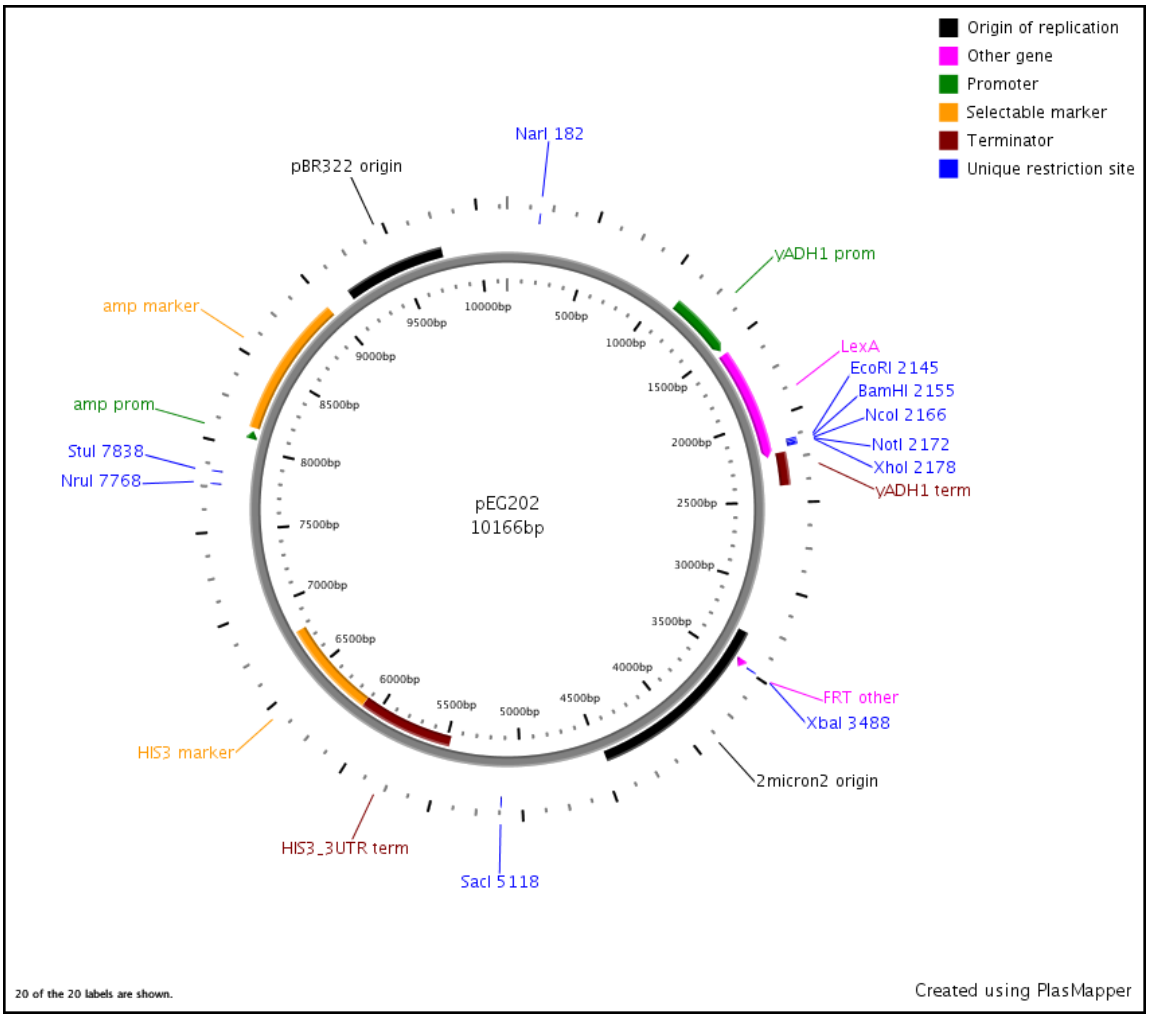

Figure 4.3. pEG202 Yeast Two-hybrid Bait Plasmid.
pEG202 (GenBank accession U89960) was used as the bait plasmid for the yeast two-hybrid assay. Bait protein expression and termination were controlled by the alcohol dehydrogenase promoter (yADH1 prom) and the yeast alcohol dehydrogenase terminator (yADH1 term), respectively. Targets were cloned between *EcoR*I and *Xho*I sites using homologous recombination, which allowed genes to be cloned as C-terminus fusions to the DNA binding domain LexA. The 2 µm origin of replication was used to maintain a high copy number of the plasmid in yeast, whereas the pBR322 was used to maintain the high copy number in *E. coli*. The *HIS3* gene is an auxotrophic marker used to maintain the plasmid in yeast. To maintain the plasmid in *E. coli*, the ampicillin-resistance gene (amp marker) was used.

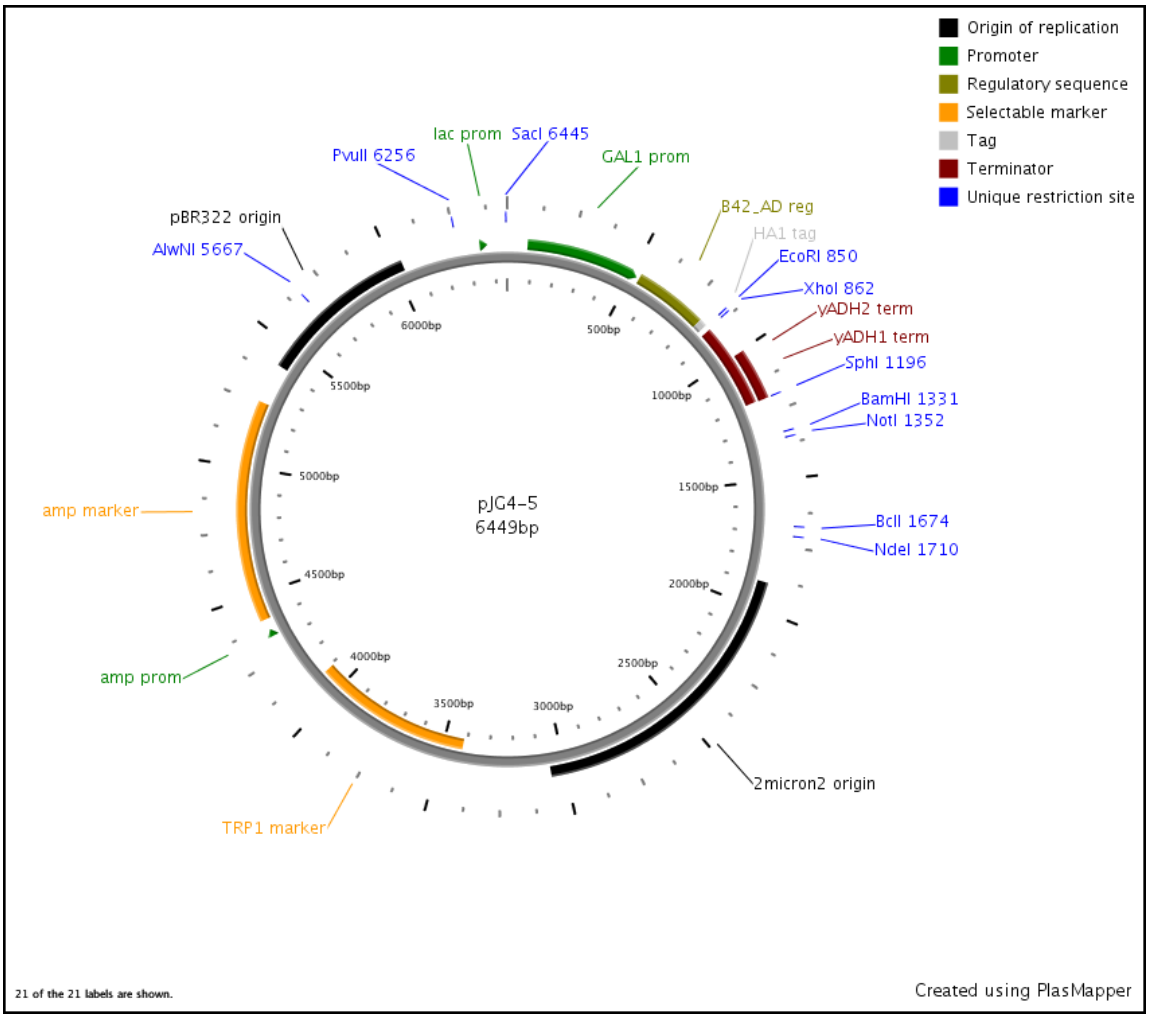

Figure 4.4. pJG4-5 Yeast Two-hybrid Prey Plasmid.
pJG4-5 (GenBank accession U89961) was used as the prey plasmid for the yeast two-hybrid assay. Prey scFv expression and termination were controlled by the galactose promoter (GAL1 Prom) and the yeast alcohol dehydrogenase terminator (yADH1 term), respectively. Prey genes were cloned between *EcoR*I and *Xho*I sites using homologous recombination, which allowed genes to be cloned as C-terminus fusions to the fusion tag consisting of the hemagglutinin tag (HA), nuclear localization sequence (NLS), and B42 activation domain (B42_AD). The 2 µm origin of replication was used to maintain a high copy number of the plasmid in yeast, whereas the pBR322 was used to maintain the high copy number in *E. coli*. The *TRP1* gene auxotrophic marker was used to maintain the plasmid in yeast. To maintain the plasmid in *E. coli*, the ampicillin-resistance gene (amp marker) was used.

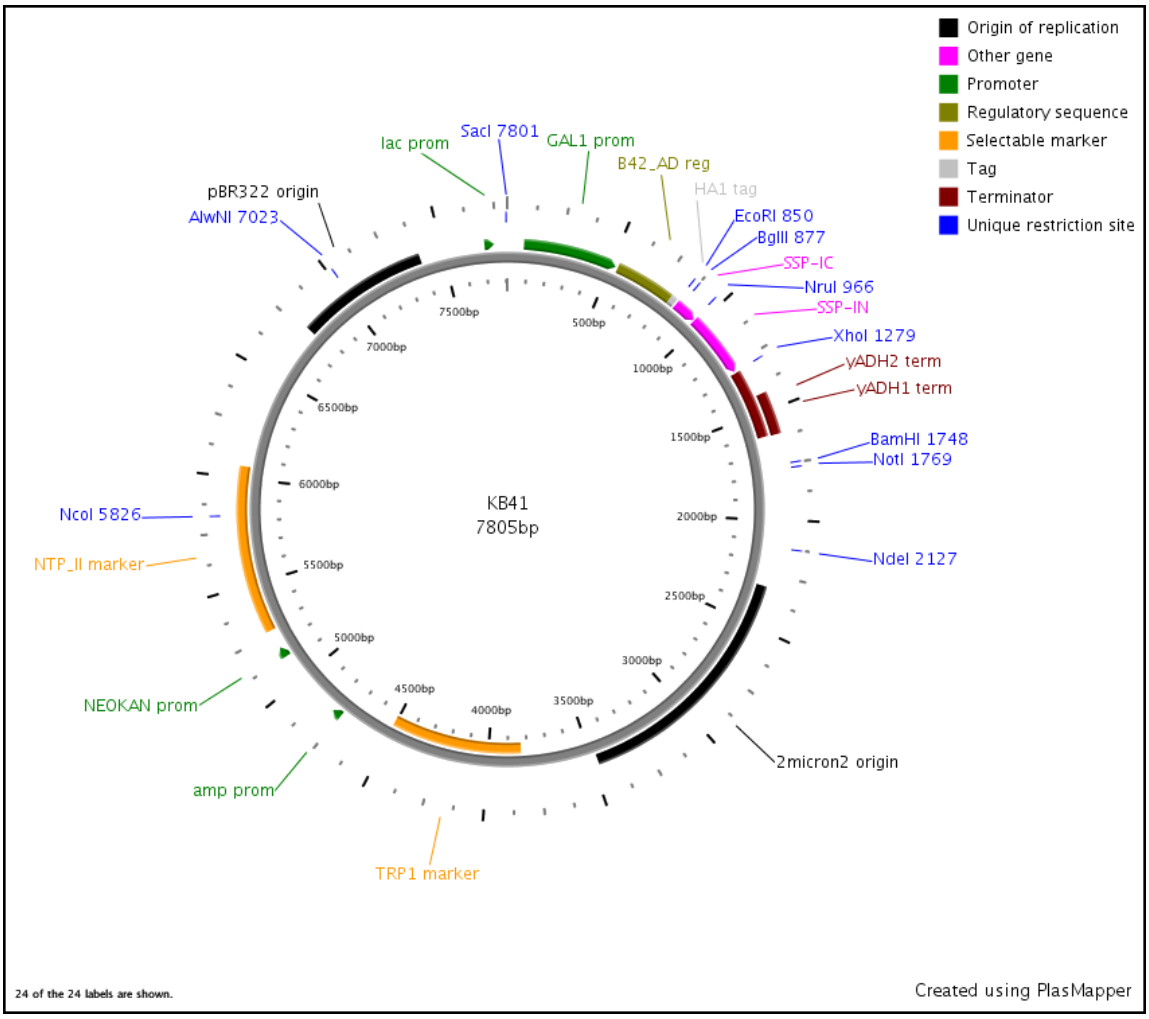

Figure 4.5. KB41 Lariat Yeast Two-hybrid Prey Plasmid.
KB41 was used as the lariat prey plasmid for the Y2H assay. Prey scFv expression and termination were controlled by the galactose promoter (GAL1 Prom) and the yeast alcohol dehydrogenase terminator (yADH1 term), respectively. Genes were cloned at the *Nru*I site using homologous recombination, which allowed genes to be cloned as a fusion to the Ssp-I_C and Ssp-I_N domains for intein processing. Following processing, targets would remain as C-terminus fusions to the fusion tag consisting of the haemagglutinin tag (HA), nuclear localization sequence (NLS), and B42 activation domain (B42_AD). The 2 µm origin of replication was used to maintain a high copy number of the plasmid in yeast, whereas the pBR322 was used to maintain the high copy number in *E. coli*. The *TRP1* gene auxotrophic marker was used to maintain the plasmid in yeast. To maintain the plasmid in *E. coli*, the kanamycin-resistance gene (kan marker) was used.

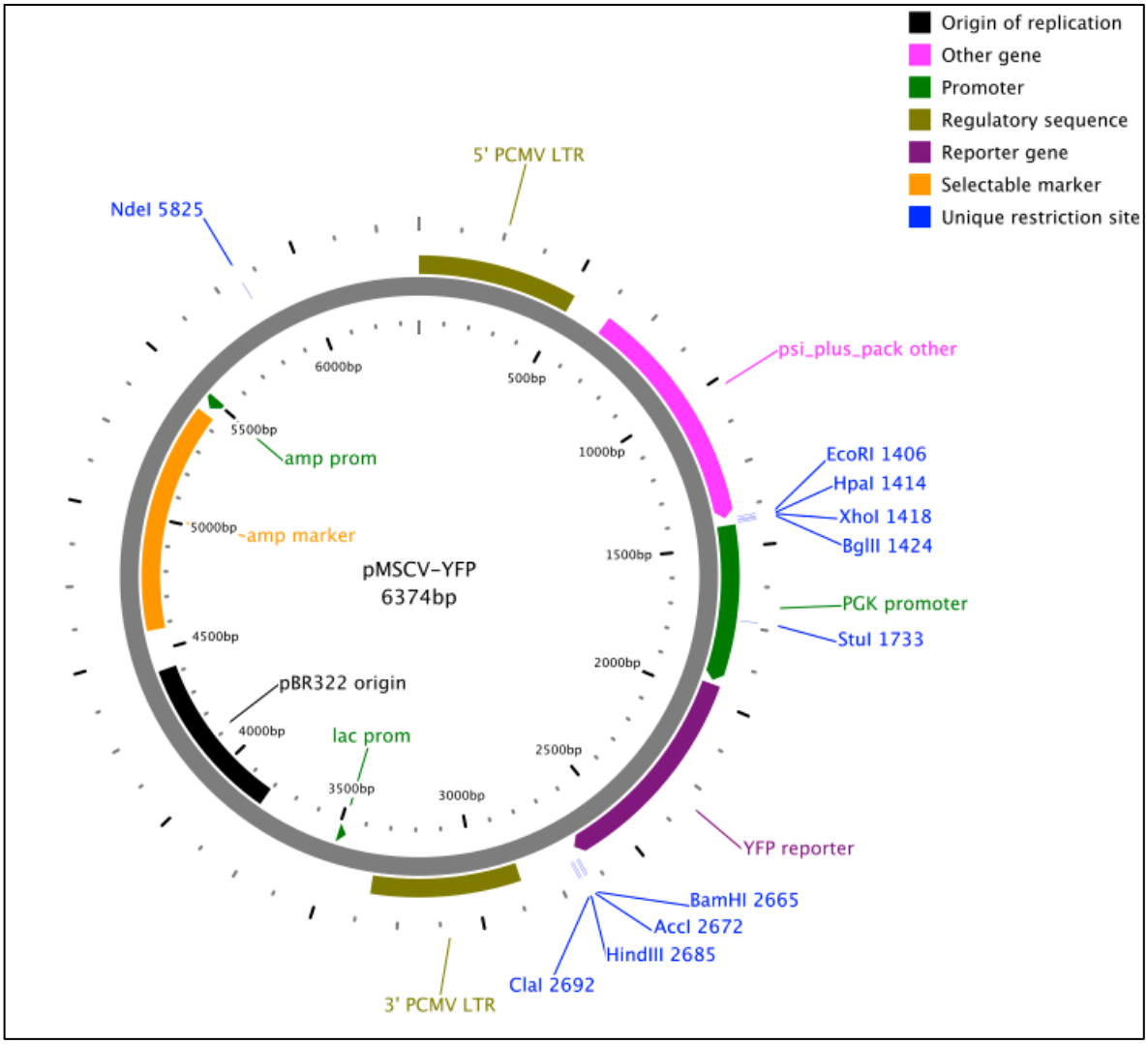

Figure 4.6. pMSCV-YFP Plasmid
pMSCV-YFP is a murine stem cell virus (MSCV) retroviral expression plasmid. This plasmid contained a specially designed 5' long terminal repeat (5' PCMV LTR) that controlled high level, constitutive expression of the target in mammalian cell lines, including stem cells. A separate promoter, the murine phosphoglycerate kinase (PGK) promoter, controlled the expression of the YFP marker gene. In packaging cell lines, the pMSCV plasmid produced replication incompetent, infectious retrovirus particles that can infect the target and transmit genes of interest to them. The plasmid contains a double-stranded DNA origin of replication (pBR322 ori) to enable replication in *E. coli.* To maintain the plasmid in *E. coli*, the ampicillin-resistance gene (amp marker) was used. ScFvs were subcloned into the plasmid at restriction sites *EcoR*I and *Xho*I. This plasmid was provided to our lab by Dr. Craig Jordan.

4.2 General Protocols

4.2.1 Sodium Dodecyl Sulphate Polyacrylamide Gel Electrophoresis (SDS-PAGE)

Protein samples were prepared by suspending proteins in 4x SDS loading dye (240 mM Tris-HCl pH 6.8, 20% (v/v) glycerol, 8% (w/v) SDS, 16% (v/v) 2- mercaptoethanol, 0.01% (w/v) bromophenol blue) for a final concentration of 1x. *E. coli* samples were resuspended in 4x SDS loading dye for a final concentration of 3x. Samples were boiled for 5 minutes and cooled before loading.

SDS-PAGE was performed using a Mini-Protean 3 electrophoresis unit (Bio-Rad) as described by Laemmli (Laemmli, 1970). Sample fractions were resolved on a 12% polyacrylamide gel (0.375 M Tris-HCl pH 8.8, 0.1% SDS, 12% degassed acrylamide:bis-acrylamide (37.5:1), 0.05% (v/v) TEMED, and 0.05% (w/v) ammonium persulphate) with a 4% stacking gel (125 mM Tris-HCl pH 6.8, 0.1% SDS, 4% degassed acrylamide:bis-acrylamide (37.5:1), 0.1% (v/v) TEMED, and 0.05% (w/v) ammonium persulphate) in 1x running buffer (25 mM Tris-HCl pH 8.3, 190 mM glycine, 0.1% (w/v) SDS) at 180 V for 55 minutes.

Proteins were visualized by Coomassie-staining or by Western analysis. For Coomassie staining, SDS-PAGE gels were incubated in staining solution (0.12% (w/v) Coomassie Brilliant Blue R-250, 50% methanol, 10% acetic acid) for 1 hour and washed with destaining solution (40% methanol, 10% acetic acid) for 4 hours to overnight. Destained gels were visualized and scanned using an Odyssey infrared imager (LI-COR Biosciences) at 700 nm.

For Western analysis, proteins were transferred from SDS-PAGE gels to nitrocellulose membranes using a semi-dry electrophoretic transfer cell (Trans-Blot) at 15 V for 20 minutes in the presence of transblot buffer (48 mM Tris-HCl pH 8.3, 39 mM glycine, 20% (v/v) methanol, 0.04% (w/v) SDS). Membranes were blocked with Odyssey blocking buffer (LI-COR Biosciences) for 1 hour at room temperature, then incubated 45 minutes with primary antibody (diluted in Odyssey blocking buffer, 0.2% Tween-20) at 4°C. Membranes were washed three times with PBT (PBS with 0.1% Tween-20) and incubated with a fluorescently labeled secondary antibody (diluted in Odyssey blocking buffer, 0.2% Tween-20) for 30 minutes at 4°C. Membranes were washed three times with PBT, and two times with PBS. Blots were visualized and scanned using an Odyssey infrared imager (LI-COR Biosciences).

4.2.2 Agarose Gel Electrophoresis

PCR products and plasmids were visualized using agarose gel electrophoresis. Samples were mixed with 6x loading dye (50% (v/v) glycerol, 0.2 M EDTA pH 8.3, 0.05% (w/v) bromophenol blue) for a final dye concentration of 1x. Samples were resolved in an agarose gel consisting of 0.8 to 1% (w/v) ultrapure agarose in 1x TAE Buffer (40 mM Tris- acetate, 1 mM EDTA, pH 8.0) and 0.5 µg/mL ethidium bromide. Gels were run at 100 to 120 V for 30 to 60 minutes in 1x TAE Buffer and photographed using a UV light transilluminator (Bio-Rad).

4.2.3 Purification and Extraction of DNA

PCR products were purified using a PCR cleanup kit (Qiagen/Bio-Basic) according to manufacturer's instructions. Restriction enzyme-digested plasmids were purified using a gel purification kit (Qiagen/Bio-Basic), according to manufacturer's instructions.

4.2.4 DNA Sequencing

DNA samples were diluted to a concentration of 50 µg/mL. DNA was sequenced at the Plant Biotechnology Institute, National Research Council of Canada.

4.3 Polymerase Chain Reactions

4.3.1 High Fidelity PCR

High fidelity PCR reactions were used for gene amplification and library creation. Reactions (50 - 100 µL), contained 60 mM Tris-SO_4 (pH 8.9), 180 mM $(NH_4)_2SO_4$, 1.5 mM $MgSO_4$, 200 µM dNTPs, 1 µM of forward and reverse primers, 50 - 200 ng template DNA, and 1 Unit/50 µL of Platinum® Taq DNA Polymerase High Fidelity. PCR products were amplified with a 2 minutes initial denaturation step at 95°C followed by 25 cycles of amplification. Each cycle contained denaturation step of 94°C for 30 seconds, 55°C for 30 seconds, 68°C for 1 minute per kilobase pair. A final extension step of 10 minutes at 68°C was included.

4.3.2 Low Fidelity PCR

Low fidelity PCR was used to check plasmids for the product after cloning. A standard PCR reaction was performed in a 50 µL reaction containing 1x Taq Buffer (10 mM Tris-HCl pH 8.3, 50 mM KCl, 1.5 mM MgCl2), 200 µM dNTP, 1 µM Primers, 10 - 300 ng template, and 1 µL of Taq DNA Polymerase. The DNA template was denatured with a 15 minutes denaturation step at 95°C, followed by 25 cycles of amplification. Each amplification cycle

contained a denaturation step at 94°C for 30 seconds, an annealing step at 55°C for 30 seconds, and an extension step at 72°C for 1 minute per kilobase pair of DNA. A final extension step of 7 minutes at 72°C was included.

4.3.3 *E.coli* Colony PCR

Colony PCR was performed to verify the construction of an insert before subsequent plasmid purification. A single colony was picked from an LB agar plate, containing the appropriate antibiotic. The colony was resuspended in 150 µL of LB broth, containing the appropriate antibiotic. One microlitre of the LB broth was used as the template for the PCR reaction using the low fidelity PCR protocol. The remaining media was incubated at 37°C until the completion of the colony PCR. If the PCR result was positive, then the sample was used to inoculate 5 mL of LB broth, containing the appropriate antibiotic for subsequent plasmid purification.

4.3.4 Yeast Colony PCR

Yeast colony PCR was performed to verify the homologous recombination of a DNA insert into a plasmid before subsequent plasmid purification and sequencing. A single yeast colony was picked, resuspended in 20 µL of 0.02 N NaOH, heated at 95°C for 5 minutes, and centrifuged at 13,000 X g for 5 minutes. Three microliters of the mixture was used as a template for the PCR reaction using the low fidelity PCR protocol (4.3.2) or high fidelity PCR protocol (4.3.1).

4.4 General *E.coli* Protocols

4.4.1 Bacterial Media

Lysogeny Broth (LB): LB media was prepared with 1% (w/v) tryptone, 0.5% (w/v) yeast extract, 85.6 mM NaCl, and 1 mM NaOH in ddH_2O. Solid media contained 1.5% (w/v) agar.

2x Yeast Extract and Tryptone Broth (2YT): 2YT media was prepared with 1.6% (w/v) tryptone, 1.0% (w/v) yeast extract, 85.6 mM NaCl, and 1 mM NaOH in ddH_2O. Solid media contained 1.5% (w/v) agar.

Super Optimal Broth with Catabolic Repressor Medium (SOC): SOC media was prepared with 2% (w/v) peptone, 0.5% (w/v) Yeast extract, 10 mM NaCl, 2.5 mM KCl, 10 mM $MgCl_2$, 10 mM $MgSO_4$, 20 mM Glucose.

Antibiotics: Antibiotics were prepared at a 1000x stock in ddH_2O (or methanol for Chloramphenicol) and stored at -20°C. The appropriate antibiotics were added at concentrations listed on Table 4.8 after the media had cooled to 55°C.

Table 4.8. Antibiotic Concentrations

Antibiotic	Concentration (µg/mL)
Ampicillin (amp)	75
Carbenicillin (carb)	50
Chloramphenicol (cap)	5
Kanamycin (kan)	25
Tetracycline (tet)	5

4.4.2 Strain Propagation

Standard techniques were used to culture and propagate *E. coli* (Elbing and Brent, 2001). Unless otherwise noted, liquid cultures were grown at 37°C with shaking at 200 rpm. Cultures on solid media were grown overnight at 37°C.

4.4.3 Plasmid DNA Preparation

Plasmid DNA was prepared by inoculating 5 - 10 mL of media, containing the appropriate antibiotic with a single colony and grown to saturation. Cells were collected by centrifugation at 4000 X g for 5 minutes and the supernatant was removed. Plasmid DNA was purified using both Qiagen and Biobasic mini-preparation kits (modified Alkaline Lysis) as described by the manufacturer. DNA concentration was determined using the NanoDrop 2000c spectrophotometer (Thermo Scientific)

4.4.4 *E. coli* Transformation

Bacterial cells were transformed using electroporation. One microlitre of plasmid DNA at a concentration of 50 - 150 ng/µL was mixed with 50 µL of competent cells. The mixture was transferred to an ice-cold electroporation cuvette. Cells were then electroporated using a field strength of 12.5 kV/cm (Ec2 on Bio-Rad Micro Pulser). Electroporated cells were rescued

with 500 µL of SOC media and incubated for 30 to 60 minutes at 37°C. Cells were then plated onto agar plates, containing the appropriate antibiotic.

4.5 General Yeast Protocols

4.5.1 Yeast Media

Synthetic Plates and Liquid Media: Synthetic media was prepared with 0.67% (w/v) yeast nitrogen base without amino acids and was supplemented with complete supplemental media (CSM) lacking the appropriate amino acid(s). 2% (w/v) dextrose or 2% (w/v) galactose supplemented with 1% (w/v) raffinose or sucrose was used as the carbon source. Solid media contained 1.5% (w/v) agar.

Synthetic media was defined by an S, followed by the type of sugar and any modifications to the media. A negative sign indicates the removal of an amino acid or nucleotide. A plus sign indicates a media supplement. For example, a typical bait selection plate was SD H-, meaning the synthetic media was supplemented with dextrose (D) and lacked Histidine (H-).

X-Gal Plates: X-Gal plates were prepared similar to the synthetic plates except they were supplemented with BU salts and 80 mg/L of 5-bromo-4-chloro-3-indolyl-β-D-galactopyranoside (X-gal). 10x BU salts were prepared by dissolving 70 g of $Na_2HPO_4 \cdot 7H_2O$, 30 g of NaH_2PO_4 in 900 mL of ddH_2O, and pH adjusted to 7.0. The X-Gal solution was prepared by dissolving X-Gal in dimethyl formamide to a final concentration of 80 µg/mL.

Yeast Peptone Dextrose Adenine (YPDA) Plates and Liquid Media: YPDA media was prepared with 1% (w/v) yeast extract, 2% (w/v) peptone, 80 mg/L adenine, and 2% (w/v) dextrose in ddH_2O. Solid media contained 1.5% (w/v) agar.

4.5.2 Yeast Strain Propagation

Standard techniques were used to culture and propagate *S. cerevisiae* (Geyer and Brent, 2000). Liquid cultures were grown at 30°C with shaking at 200 rpm. Cultures on solid media were inverted and grown at 30°C.

4.5.3 Plasmid DNA Preparation from Yeast

Plasmids were isolated according to the "smash and grab" protocols previously described (Hoffman and Winston, 1987);(Geyer and Brent, 2000). A single yeast colony was

used to inoculate 1.5 mL of appropriate synthetic amino acid dropout media and grown overnight at 30°C and 200 rpm. Cells were pelleted by centrifugation at 10,000 X g for 2 minutes. The cell pellet was resuspended in 200 µL of yeast breaking buffer (2% (v/v) Triton X-100, 1% (v/v) SDS, 100 mM NaCl, 10 mM Tris -HCl pH 8.0, 1 mM EDTA). Next, 300 µg of glass beads and 200 µL of phenol-chloroform-isoamyl alcohol (25:24:1, v/v/v) were added to the solution. Yeast cell walls were disrupted by vortexing the mixture for 5 minutes. The mixture was centrifuged for 5 minutes at 18,000 X g. Approximately 50 to 100 µL of the DNA containing aqueous layer was removed. Between 2 and 5 µL were used for transforming bacterial cells by electroporation. The remaining samples were stored at -20°C.

4.5.4 Yeast Lithium Acetate Transformation

The high efficiency method previously described (Gietz and Schiestl, 2007) was used for library generation and for routine cloning. Lithium acetate competent yeast cells were prepared by inoculating 25 mL 2x YPDA media and grown overnight at 30°C and 200 rpm. The cell density was measure spectrophotometry and using the conversion factor of 1.0×10^7 CFU/mL at OD_{600} of 1.0. 2.5×10^9 cells were added to 500 mL of pre-warmed 2x YPDA for a concentration of 5×10^6 cells/mL. The cells were grown at 30°C and 200 rpm to an OD_{600} of 0.6 - 0.8. Cells were collected by centrifuging 5 minutes at 3,000 X g and washed once in 250 mL sterile water. The supernatant was removed and the pellet was resuspended in 5 mL of sterile water. The sample was centrifuged 5 minutes at 3,000 X g and resuspended in 5 mL of sterile frozen competent cell (FCC) solution (5% v/v glycerol, 10% v/v DMSO). The competent cells were divided into 50 µL aliquots. The cells were stored at -80°C or used immediately for transformation.

A supermix was prepared for the number of transformants plus one extra for a control. The supermix consisted of 260 µL polyethylene glycol (50% (w/v) PEG -3350), 36 µL of 1 M LiAc, 50 µL of 2 mg/mL single-stranded carrier DNA, 14 µL plasmid DNA (1 µg). The plasmid DNA was prepared by restriction digestion followed by gel purification. When performing this protocol for homologous recombination a 30 µL PCR insert was included. This PCR insert was amplified using the high fidelity PCR protocol mentioned in 4.3.1 followed by PCR purification. Aliquots containing 50 µL of competent cells were centrifuged at 13,000 X g for 2 minutes. After the supernatant was removed, the cell pellet was resuspended in 360 µL of the supermix. The mixture was incubated for 45 minutes at 42°C, centrifuged for 30 seconds at

13,000 X g, and the supernatant was removed. The pellet was resuspended in 200 µL sterile water and 150 µL was plated on the appropriate media. The plates were incubated for 1 - 3 days at 30°C. Plates containing libraries were scraped and resuspended in FCC solution and stored at -80°C. Individual colonies were isolated from plates containing a single transformant and prepared for sequencing according to section 4.5.3.

4.5.5 Yeast Two-Hybrid Interaction Mating Assay

Yeast interaction mating (Kolonin *et al.*, 2000) was used to test interactions between the scFv library and the corresponding bait.

Bait genes were cloned into the pEG202 bait plasmid (Figure 4.3) using the lithium acetate transformation protocol (section 4.5.4) into the bait strain, EY111. Cells were plated on SD H^- plates as the bait plasmid has the histidine auxotrophic selection marker. Proper clones were confirmed first by colony PCR (section 4.3.4) followed by sequencing (section 4.2.4).

Prey genes were cloned into pJG4-5 (Figure 4.4) and KB41 (Figure 4.5) bait plasmids using the lithium acetate transformation protocol (section 4.5.4) into the prey strain EY93. Serial dilutions were plated on SD W- plates (prey plasmids have the tryptophan auxotrophic selection marker) to determine the library diversity. The remaining cells were plated on a large SD W- plate and incubated 2 days at 30°C. Cells were scraped off the plates and resuspended in FCC solution and stored at -80°C.

The bait strain was prepared for mating by inoculating 10 mL of SD H- and incubating overnight at 30°C and 200 rpm. The cells were pelted by centrifugation at 4000 X g for 10 minutes. The pellet was resuspended in 1 mL of sterile water and the number of bait and prey cells were calculated by the optical density using the conversion factor where OD_{600} of 1.0 is equal to 1.0×10^7 CFU/mL. Prey and bait strains were combined in a 1:2.5 ratio respectively. In a total volume of 300 µL, 1.0×10^7 prey cells were mixed with 2.5×10^7 bait cells. The entire 300 µL yeast mixture was plated on a large YPDA plate and incubated overnight at 30°C.

The following day, plates were scraped and cells resuspended in 1 mL of FCC solution. Serial dilutions were made and plated in triplicate on: YPDA plates (to determine the total number of cells), SD H-W- plates (to determine the concentration of diploids per mL of media), and SGR H-W-L-A- Xgal+ plates (to estimate the number of interactions per mL of media). The remaining cells were stored at -80°C. Mating efficiency was calculated by dividing the number of colonies on the YPDA plates by the number of diploids on the SD H-W- plates. The

positive (blue) colonies on SGR H-W-L-A- Xgal+ were mixed with FCC solution and stored at –80°C for further analysis.

For each variable, sixteen blue colonies from the SGR H-W-L-A- Xgal+ plates were used to inoculate 100 µL of SD W- in a 96-well plate. The media was incubated for 48 hours at 30°C. The culture was transferred using the 96-pin replicator to a SD H-W- plate to confirm they contained both bait and prey plasmids. The culture was also transferred to a SGR H-W-L- plate and SD H-W-L- plate to confirm the cells dependence on galactose as a sugar source, and a SGR H-W-A- Xgal+ plates to observe the strength of the interactions. The 96-pin replicator was washed between replicating in 10% bleach for 1 minute, rinsed with water by raising and lowering the replicator five times, sterilized in 95% ethanol, and dried using a flame. Plates were incubated for 2 - 7 days at 30°C.

4.6 Phage Display

4.6.1 Kunkel Mutagenesis

4.6.1.1 Template Purification

A single colony of CJ236, containing the HP153/anti-MBP scFv phagemid, was used to inoculate 1 mL of 2YT/carb/cap medium supplemented with M13K07 helper phage and incubated at 200 rpm and 37°C. After 2 hours, kanamycin was added (25 µg/mL) to select for clones that were co-infected with the M13K07 helper phage. Infected cells were shaken at 200 rpm and 37°C for 6 hours and then transferred to 30 mL of 2YT/carb/kan/uridine medium. The medium was then incubated overnight at 200 rpm and 37°C. Phage were purified from the overnight medium and described in section 4.6.3.

Purification of the uracil-containing ssDNA (dU-ssDNA) was performed at room temperature using a modified version of the Qiagen QIAprep Spin M13 kit protocol. Following phage purification, 7 µL of buffer MP (Qiagen) was added to 500 µL of the phage solution and incubated for 2 minutes. The sample was then added to a QIAprep spin column (Qiagen) and centrifuged for 30 seconds a 10,000 X g. The flow-through was discarded as the phage remained bound to the column. To separate the DNA from the phage protein coat, the column was washed twice by the addition of 0.7 mL of buffer MBL (Qiagen) and centrifuged 30 seconds at 10,000 X g. The DNA remained bound to the column matrix and the protein coat

containing flow-through was discarded. The column was washed an additional two times by the addition of 0.7 mL of buffer PE (Qiagen) and centrifuged 30 seconds at 10,000 X g to remove additional salts and proteins. The column was centrifuged for an additional 30 seconds to remove any residual buffer PE. The dU-ssDNA was then eluted from the column by the addition of 100 µL of buffer EB (Qiagen) to the center of the membrane, incubated for 10 minutes, and then centrifuged at 10,000 X g for 1 minute into a clean microcentrifuge tube.

4.6.1.2 Synthesis of Covalently Closed Circular dsDNA (CCC-dsDNA)

Although the library size used in this thesis is less than 10^5 members, the procedure described below is sufficient for the construction of a library of up to 10^{10} members.

First, mutagenic oligonucleotides were phosphorylated using 0.6 µg of the oligonucleotide, 2.0 µL 10x TM buffer, 2.0 µL 10 mM ATP, 1.0 µL 100 mM DTT, and ddH_2O for a final volume of 20 µL. After the addition of 20 units of T4 polynucleotide kinase, the reaction was incubated for 1 hour at 37°C. After the phosphorylation reaction was complete, oligonucleotides were immediately annealed to the dU-ssDNA template under the following conditions: 20 µg of dU-ssDNA, 20 µL 10x TM buffer, 20 µL of each of the phosphorylated oligonucleotides, and ddH_2O to a final volume of 250 µL. The reaction was then incubated at 90 °C for 3 minutes, 50°C for 3 minutes, and then 20°C for 5 minutes.

The CCC-dsDNA was synthesised from the annealed oligonucleotide/template mixture by the addition of 10 µL of 10 mM ATP, 10 µL 25mM dNTP mix, 15 µL 100 mM DTT, 30 units of T4 DNA ligase, and 30 units of T7 DNA polymerase. The reaction was incubated overnight at 20°C. The DNA was then purified and desalted using the Qiagen QIAquick DNA purification kit protocol with the following changes: First, 1 mL of buffer QG (Qiagen) was added to the annealed oligonucleotide/template mixture. This mixture was separated and applied to two columns. Second, the CCC-dsDNA was eluted from each column membrane using 35 µL of ultrapure irrigation USP water following 2 minutes incubation.

4.6.2 Phage Display Library Creation

Following the creation of the CCC-dsDNA library, the phage display library was created and amplified in a bacterial host. The *E. coli* SS320 strain (*E. coli* MC1061 strain with the F' episome from XL1-blue) was used as it has both a high electroporation efficiency of

MC1061 with the ability to be infected by M13 helper phage conferred by the F' episome (Tonikian *et al.*, 2007).

First, 5 µg of CCC-dsDNA, 80 µL of electrocompetent SS320 cells, and ultrapure water for a final volume of 350 µL, were added to a chilled electroporation cuvette. Cells were electroporated with a Bio-Rad Gene Pulser with the following settings: 2.5 kV field strength, 200 ohms resistance, and 25 µF capacitance. Cells were immediately rescued with 1 mL of SOC medium and transferred to a baffled flask containing 22 mL of pre warmed SOC. The cuvette was then wash twice more with SOC and transferred to the flask for a final volume of 25 mL. The cells were incubated for 30 minutes at 200 rpm and 37°C. To determine the library diversity, serial dilution were plated on 2YT/carb plates and incubated overnight at 37°C. The liquid culture was transferred to a 2 L baffled flask containing 500 mL of 2YT/carb/kan medium and incubated overnight at 200 rpm and 37°C. The following morning the phage library was purified using the following protocol (4.6.3).

4.6.3 Phage Purification

An overnight culture of phage infected *E. coli* were centrifuged for 10 minutes at 16,000 X g and 4°C. The supernatant was transferred to a tube containing 1/5 volume of PEG/NaCl and incubated for 30 minutes on ice to precipitate the phage. The mixture was centrifuged for 10 minutes at 12,000 X g and 4°C. The supernatant was discarded and then was centrifuged for an additional 2 minutes at 2,000 X g and 4°C. The remaining supernatant was removed with a pipette. The phage pellet was resuspended in 1:25 of the overnight culture volume in PBS. To pellet the remaining insoluble matter, the sample was centrifuged for 5 minutes at 27,000 X g and 4°C. The purified phage was then transferred to a clean tube and used immediately for selection experiments, stored at 4°C or at -80°C in 10% glycerol.

4.6.4 Selection of Phage against Adsorbed Antigen

Maxisorp immunoplate wells were coated with 100 µL of 5 µg/mL Protein A in coating buffer (50 mM NA_2CO_3, adjusted to pH 9.6 using concentrated HCl) and incubated at room temperature for 2 hours. The coating solution was removed and the wells were blocked with 200 µL of PBS with 0.2% BSA. After incubation for 1 hour, wells were washed four times with PT buffer. 100 µL of the phage library was added to each of the coated wells in a concentration of 1 x 10^{12} phage/mL in PBT buffer. The solution was incubated at room

temperature for 2 hours. The phage solution was removed and the wells were washed ten times with PT buffer. The bound phage were eluted by the addition of 100 µL of 100 M HCl and incubated for 5 minutes at room temperature. The solution was neutralized by the addition of 27 µL of 1.0 M Tris-HCl (pH 8.0). The eluted phages were amplified as described in section 4.6.5.

4.6.5 Phage Amplification

Phage amplification was performed by the addition of 60 µL of eluted phages to 600 µL of actively growing *E. coli* XL1-Blue and incubated for 20 minutes at 37°C and 200 rpm. To determine the enrichment, ten-fold serial dilutions of the infected *E. coli* culture was plated on 2YT/carb plate and incubated overnight at 37°C. The culture was then infected with M13K07 helper phage for a final concentration of 10^{10} phage/mL and incubated for 45 minutes at 37°C and 200 rpm. The culture was transferred to a baffled flask containing 16.7 mL of 2YT/carb/kan medium and incubated overnight at 200 rpm and 37°C. The following morning, the phage library was purified using the protocol 4.6.3.

4.6.6 Protein Biotinylation

To allow non-specific immobilization of maltose binding protein (MBP) to Maxisorp plate wells, MBP was biotinylated using EZ-Link NHS-SS-biotin. First, MBP was expressed in BL21 using the pHFT2-MBP plasmid obtained from Dr. Koide's lab at the University of Chicago (Koide *et al.*, 2007) and purified using a 6x-His column. The protein was then diluted to 2 mg/mL using MOPS buffer (50 mM MOPS, 250 mM NaCl, pH 6.5). It was dialyzed in 200 mL of the same buffer overnight, replacing the buffer 3 times. The protein was diluted with the MOPS buffer for a final concentration of 1 mg/mL. EZ-Link NHS-SS-biotin was dissolved in ddH_2O for a final concentration of 1 mg/mL. The biotinylation reagent solution was then mixed with the MBP solution with a 1:19 ratio, respectively. The mixture was incubated at room temperature for 60 minutes with occasional gentle mixing. 1/10 volume of 1M Tris-CL buffer (pH 7.5) was added to quench the reaction. To remove the unreacted biotin, the solution was dialyzed in PBS buffer (pH 7.5) overnight, replacing the buffer three times. Protein concentration was determined using the Bradford assay and aliquots were stored at 4°C for short-term storage or -80°C in 10% glycerol for long-term storage.

4.6.7 Selection of Phage against Neutravidin-Immobilized Antigen

A modified version of the phage display technique described in section 4.6.4 was used when MBP was the immobilized antigen. First, MBP was biotinlyated as described in section 4.6.6. Library phage was combined with the biotinylated MBP for a final concentration of 1 x 10^{12} phage/mL and 10 nM MBP. The solution was incubated at room temperature for 2 hours. Maxisorp immunoplate wells were coated with 100 µL of 5 µg/mL Neutravidin solution in coating buffer (50 mM Na_2CO_3 pH 9.6) and incubated at room temperature for 2 hours. The coating solution was removed and the wells were blocked with 200 µL of PBS with 0.2% BSA. Wells were washed four times with PT buffer followed by the addition of 100 µL of the phage/antigen mixture to the Neutravidin-coated wells. After incubating 15 minutes at room temperature, the phage solution was removed and wells were washed 10 times with PT buffer. Bound phages were eluted by the addition of 100 µL of 100 M HCl and incubated for 5 minutes at room temperature. The solution was neutralized by the addition of 27 µL of 1.0 M Tris-HCl (pH 8.0). Eluted phages were amplified as described in section 4.6.5.

4.6.8 Quantification of Phage-Antigen Interaction Using Enzyme-Linked Immunosorbent Assay (ELISA)

To determine relative affinities of individual anti-MBP scFv clones, direct binding ELISAs were performed. First, purified library phage was combined with the biotinylated MBP for a final concentration of 1 x 10^{12} phage/mL and 10 nM MBP. The solution was incubated at room temperature for 2 hours. Maxisorp immunoplate wells were coated with 100 µL of 5 µg/mL Neutravidin solution in coating buffer (50 mM Na_2CO_3, pH 9.6) and incubated at room temperature for 2 hours. The coating solution was removed and the wells were blocked with 200 µL of PBS with 0.2% BSA. Wells were washed four times with PT buffer followed by the addition of 100 µL of the phage/antigen mixture to each of the Neutravidin-coated wells and incubated for 15 minutes. The phage solution was removed and wells were washed eight times with PT buffer. Next, 100 µL of horseradish peroxidase/anti-M13 antibody conjugate diluted 1:3000 with PBT was added to wells and incubated for 30 minutes at room temperature. The antibody solution was removed and wells were washed six times with PT buffer and two times with PBS. Next, 100 µL of TMB substrate (Sigma) was added to the wells and incubated for 2 - 10 minutes until colour had developed. The reaction was stopped using 100 µL of 1.0 M

H_3PO_4. Absorbance was measured at 450 nm using SpectraMax M5 microplate reader (Molecular Devices).

4.7 Thermal Stability Assay

4.7.1 ScFv Expression

The SHuffle *E. coli* strain (NEB) was transformed with the pET-LP3 protein expression plasmid containing the desired scFv gene according to section 4.4.4. A colony from the freshly transformed *E. coli* was used to inoculate 10 mL of 2YT/carb and grown overnight at 30°C and 200 rpm. The overnight culture was then used to inoculate 250 mL to 1 L of 2YT/carb in a baffled flask. The culture was incubated at 30°C and 200 rpm until mid-log phase (OD_{600} 0.500 to 0.800). Protein expression was induced with 100 mM Isopropyl β-D-1-thiogalactopyranoside (IPTG) for a final concentration of 0.1 mM. The culture was incubated overnight at room temperature and 200 rpm. Cells were centrifuged 30 minutes at 4°C and 6000 X g and the supernatant was removed. The pellet was used immediately for protein purification as described in section 4.7.2 or stored at -80°C until needed.

4.7.2 ScFv Strep-Tactin Purification

The cell pellet containing cells expressing scFvs of interest was resuspended in 1/10 of the overnight volume in 1x Strep-Tactin Wash Buffer (150 mM NaCl, 100 mM Tris-HCl, 1 mM EDTA, pH 8.0). Cells were lysed at 4°C using a cell disruptor (Constant Systems LTD) with 10,000 PSI. The insoluble fraction was pelleted by centrifugation for 45 minutes at 27,000 X g and 4°C. The scFv containing supernatant was removed and filter purified using a 0.8 µm syringe-driven filter (Millipore). The solution was then added to a 250 µL bed volume of prewashed Strep-tactin, a strepavidin derivative, Superflow Agarose (Novagen) which has the theoretical capacity to yield up to 0.7 mg of purified scFvs. The entire sample was allowed to pass though the column using gravity flow. The column was then washed five times with 500 µL of 1x Strep-tactin wash buffer. Samples were collected at each step for further analysis if needed. The bound protein was then eluted by the addition of 250 µL of 1x Strep-Tactin Elution Buffer (150 mM NaCl, 100 mM Tris-HCl, 1 mM EDTA, 2.5 mM desthiobiotin, pH 8.0). The elution step was repeated five times with each elution fraction collected separately. Success of the purification was determined by analysis on SDS-PAGE gel (section 4.2.1) and protein concentrations of the eluted fractions were determined by the Bradford assay.

4.7.3 Thermal Stability Assay

ScFv melt curves were generated using a modified version of the high-throughput thermal scanning method as described by Laviner *et al.* (2009). After protein purification, the scFv concentration was determined using the Bradford assay. ScFvs were diluted to a concentration of 10 µM in Strep-tactin Elution Buffer. One µL of 300x SYPRO Orange (provided at 5000x stock concentration) was added to 19 µL of scFv solution. A sample used for background correction was created by loading a well with 1 µL of 300x SYPRO Orange to 19 µL of Strep-tactin Elution Buffer without any protein. Samples were loaded in triplicate into a 0.1 mL MicroAmp Fast Optical 96-well reaction plate (Applied Biosystems) and sealed with MicroAmp optical adhesive film (Applied Biosystems). Samples were centrifuged for 5 minutes at 3700 X g to ensure the samples were at the bottom of the well and bubble free. Thermal denaturation was performed using a StepOnePlus Real-time PCR system (Applied Biosystems) with 0.2°C per 12 seconds steps. A melting curve was generated by measuring the fluorescence intensities after each step using a 490 nm excitation filter and a 575 nm emission filter.

Calculations of the scFv T_ms and visualization of the melt curves were performed using a Differential Scanning Fluorimetry (DSF) tool (Niesen *et al.*, 2007). This Excel program is freely provided by the Frank Niesen lab (ftp://ftp.sgc.ox.ac.uk/pub/biophysics). This worksheet calculates the T_m values using the first derivative curve but to achieve a more accurate fitting to the Boltzmann equation, GraphPad Prizm was used. Detailed descriptions of the method are also available (Niesen *et al.*, 2007).

4.8 Mammalian Cell Studies

The effect of anti-Abl1-SH3 scFvs on chronic myelogenous leukemia cells were conducted with the K562 cell line obtained from ATCC. Cells were cultured in Iscove's Modified Dulbecco's Media (IMDM) supplemented with 10% fetal bovine serum, 100 IU/mL penicillin and 100 mg/mL streptomycin. Cells were grown at 37°C with 5% CO_2.

K562 cells were transiently transfected with pMSCV plasmids using the Nucleofector II system (Amaxa Biosystems) according to manufacturer's instruction. First, 1 x 10^6 cells were suspended in 100 µL of nucleofector solution. 5 µg of plasmid DNA was added to the solution. Nucleofection was performed using program T-016. The cells were immediately rescued by

the addition of 500 μL of pre-warmed culture media (IMDM supplemented with 10% fetal bovine serum, 100 IU/mL penicillin and 100 mg/mL streptomycin). Cells were grown at 37°C with 5% CO_2.

Cell viability was assessed by staining the cells with trypan blue and counting cells using a hemocytometer. The transfection efficiency was determined by measuring the YFP expression using Coulter's Epics XL flow cytometer.

5 Results

5.1 Specific Aim 1: Increase ScFv Stability Using Novel Linkers

5.1.1 Introduction

Permutation of V_L and V_H domains by joining them together using multiple linkers was first shown to be possible by Brinkmann *et al.* (1997) with their permutated scFv (pFvs) design. Their pFv (referred to as Model X) retained specificity and affinity for its antigen. Although the thermal stability of this permutated scFv did not show an improvement over the "standard" unpermutated scFv, it still retained 25% of its binding activity after 24 hours incubation at 37ºC. We hypothesised that permutating an scFv to increase the number of peptide linkers joining V_L and V_H domains would increase scFv stability. We designed two new permutated scFvs (Table 5.1), named Model 1 (Figure 5.1C) and Model 3 (Figure 5.1D). These permutated scFvs had an increased number of peptide linkers that joined V_H and V_L domains relative to the unpermutated scFv.

Previous attempts by the Geyer lab to purify Model X, 1, and 3 using a modified pET expression plasmid, pET-LP1, were unsuccessful. This plasmid expressed scFvs using a T7 inducible promoter with an C-terminal His-Tag followed by a pelB leader sequence. In previous studies, Models 1 and 3 were successfully expressed in the periplasm of *E. coli* strain BL-21 and after isolation of Models by osmotic shock, pFvs remained in the soluble fraction. However, pFvs could not be purified further since they did not bind to the Ni^{2+}- NTA column. These results, combined with our inability to purify other scFvs using C-terminal His tags (unpublished), suggested that this affinity tag was not suitable for purifying scFvs.

Following these experiments, we developed new expression plasmids, pET-LP2 and pET-LP3 (Figure 4.1), to express scFvs. pET-LP2 was a modified pET-LP1 plasmid that included a N-terminal Strep-tag. The pET-LP3 plasmid was modified to include a N-terminal Strep-tag and to remove the pelB leader sequence.

Table 5.1. pFv's Permutated Sequences

pFv	Permutated Sequence
Model X	V_L(1-42)/GSSAGG/V_H(43-END)/$(G_3S)_3$/V_H(1-42)/SSAGG/V_L(43-END)
Model 1	V_L(1-42)/$(G_3S)_3$/V_H/$(SG_3)_3$/V_L(43-END)
Model 3	V_L(1-42)/$(G_3S)_3$/V_H(1-42)/$(G_3S)_2$/V_L(43-END)/$(SG_3)_3$/V_H(43-END)

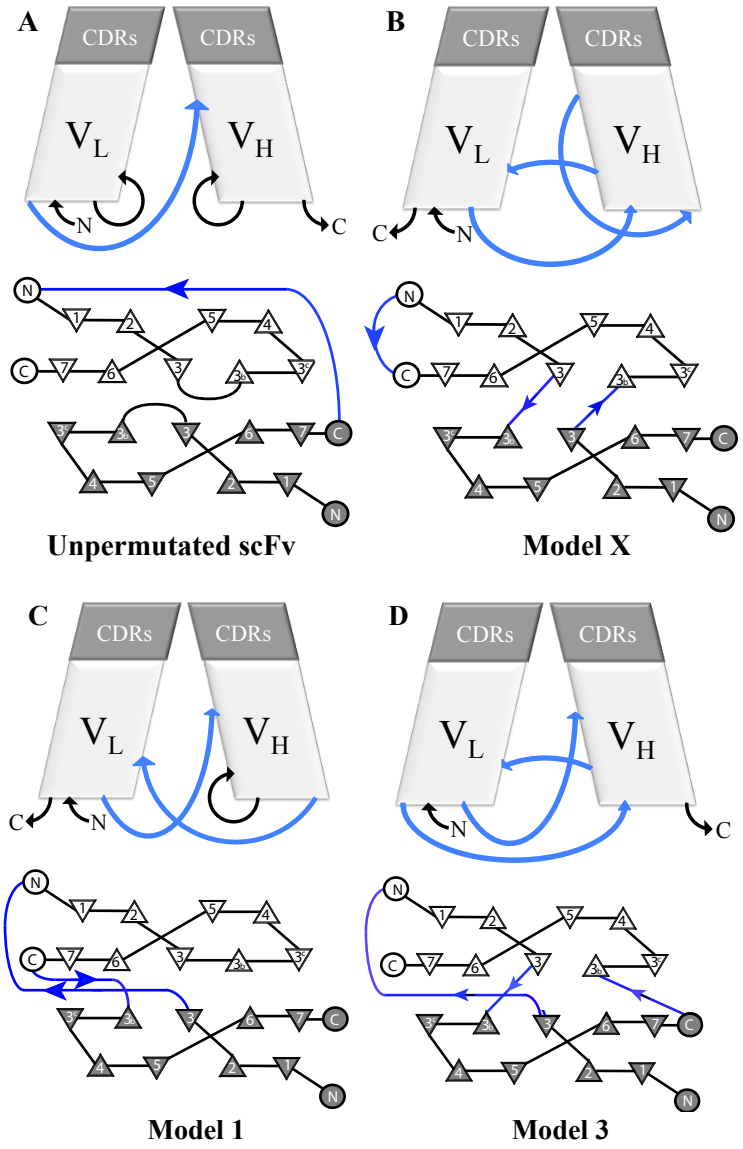

Figure 5.1. Schematics of Permutated ScFvs.
The standard unpermutated scFv **(A)** is included for reference. Arrows indicate the direction of synthesis from the N- to C-terminis. Peptide Linkers are shown in blue. In the top row of images, base-loops are depicted as circular loops located at the bottom of the variable regions. Schematic representations are included in the bottom row. Numbered triangles represent the orientation of strands in β sheets. Model X pFv **(B)** connects the V_L and V_H though the base-loop regions. Model 1 **(C)** connects two fragments together using the base-loop of the V_L domain. The N-terminal end of the V_L base loop is attached to the C-terminal of the V_H chain. The C-terminal of the V_H is attached to the C-terminal end of the V_L base loop, thus completing the formation of a single chain protein. Similar to Model 1, in Model 3 **(D)** the N-terminal end of the V_L base loop is attached to the C-terminal of the V_H chain. In this model, the N-terminal end of V_H base-loop is connected back to the V_L chain at the C-terminal end of the base-loop. The single chain is completed with the C-terminal of the V_L connected to the C-terminal end of the V_H base-loop.

Further, we obtained a protein expression strain, SHuffle (NEB), which was engineered to allow the formation of disulphide-bonds in the cytoplasm. This modifications in the SHuffle strain, such as the expression of disulfide bond isomerase DsbC in the cytoplasm and the lacking two reductases (*trxB* and *gor*), were thought to favour the expression of proteins that rely on disulphide-bonds for stability, such as scFvs (de Marco, 2009).

We performed experiments to determine if scFvs could be expressed and purified using these new expression plasmids and Shuffle strain. Upon successful purification, thermal stability assays on the permutated scFvs were performed.

5.1.2 Optimization of ScFv Expression

pET-LP1 plasmids encoding standard and permutated scFvs were used to transform *E. coli* XL1-Blue. Plasmids were amplified and purified as per section 4.4.3. Genes encoding scFvs were isolated by digesting plasmids with *EcoR*I and *Sal*I and gel purifying DNA fragments (Section 4.2.3). Purified genes were cloned into pET-LP2 and pET-LP3 using restriction cloning. Following sequence verification, scFvs were expressed under a variety of conditions to optimize expression by varying Isopropyl β-D-1-thiogalactopyranoside (IPTG) concentration, induction time, and incubation temperature. There was no noticeable increase in scFv expression using the pET-LP2 expression plasmid with the pelB leader sequence over pET-LP3 plasmid. Following expression using pET-LP2, the Strep-tactin purified scFvs showed multiple bands on a Coomassie-stained SDS-PAGE gel. Further, there was no noticeable increase in expression when IPTG concentration was increased above 0.1 mM. However, after IPTG induction, incubating the scFv expression culture at room temperature increased pFv levels in the soluble fraction compared to levels observed when the culture was incubated at 30ºC or 37ºC. Further, we observed that 4 hours incubation following induction was insufficient for high levels of scFv expression, whereas 24 hours after induction, high levels of scFvs were detected.

We also compared scFv expression in the SHuffle strain to the BL21 expression strain. Expression levels were higher for pFvs expressed in the SHuffle strain (Figure 5.2). As a result, we expressed scFvs in pET-LP3 plasmids in the SHuffle strain at room temperature with using 0.1 mM IPTG for induction.

5.1.3 Purification of Permutated ScFvs

After optimization, pFvs were expressed according to Section 4.7.1, followed by Strep-tactin purification according to Section 4.7.2 (Figure 5.3). Due to the appearance of multiple bands, Western analysis was performed to identify the correct location of the pFv (Figure 5.3B).

5.1.4 Thermal Stability of Permutated ScFvs

Thermal stability testing of the unpermutated scFv and pFvs was performed according to Section 4.7.3 with one exception; proteins were diluted to 9 μM (Figure 5.4). The unpermutated scFv had a calculated T_m of 55.0 ± 0.1ºC. Model X had a T_m calculated at 44.5 ± 0.2ºC. Both Model 1 and Model 3 showed improved stability with calculated T_ms of 64.0 ± 0.8ºC and 67.1 ± 0.4ºC, respectively.

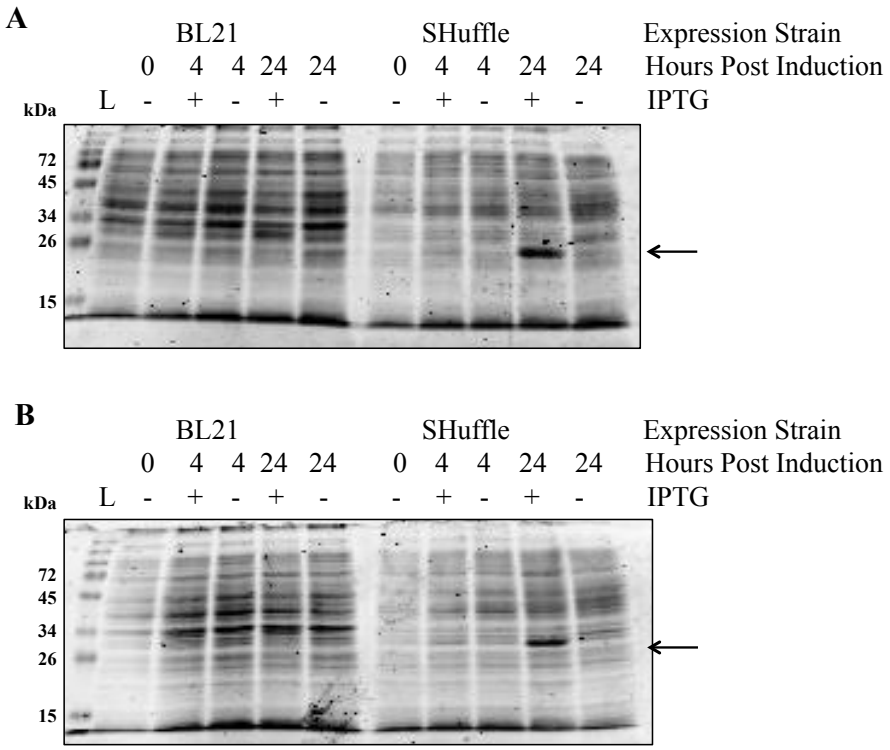

Figure 5.2. Comparison of ScFv and pFv Expression Levels Using BL21 and SHuffle Strains.
Unpermutated scFv **(A)** and the Model X permutated scFv **(B)** were expressed using pET-LP3 in BL21 and SHuffle expression bacteria strains. IPTG induction is indicated by a + sign, whereas a – sign indicates that no IPTG was added to the media. Following induction, cells were incubated at room temperature and samples were removed at 0, 4, and 24 hours post IPTG induction. The whole bacterial lysate was resolved on a SDS-PAGE gel. Proteins were visualized by Coomassie staining. Arrows indicate the expected location of the scFv or pFv.

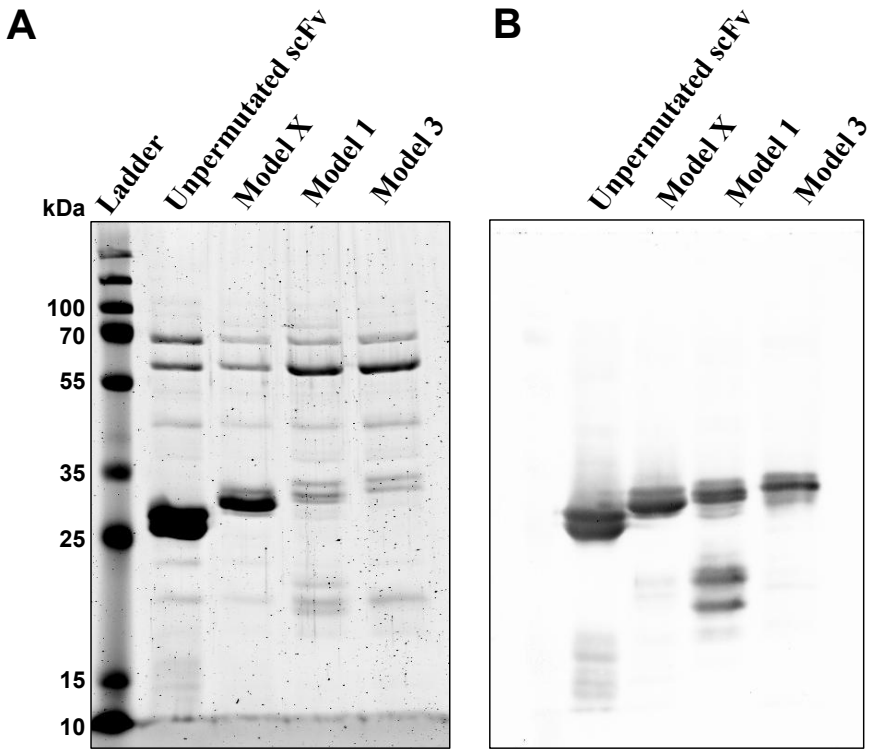

Figure 5.3. Strep-tactin Purification of pFvs.
pFvs were expressed in the SHuffle expression strain using the pET-LP3 plasmid. At 24 hours post-IPTG induction, scFvs were purified using strep-tactin purification (4.7.2). The lane labeled with "Ladder" refers to molecular weight marker ladder. Following purification, pFvs were detected by Coomassie staining **(A)** and by Western analysis using an anti-SBP antibody **(B)**.

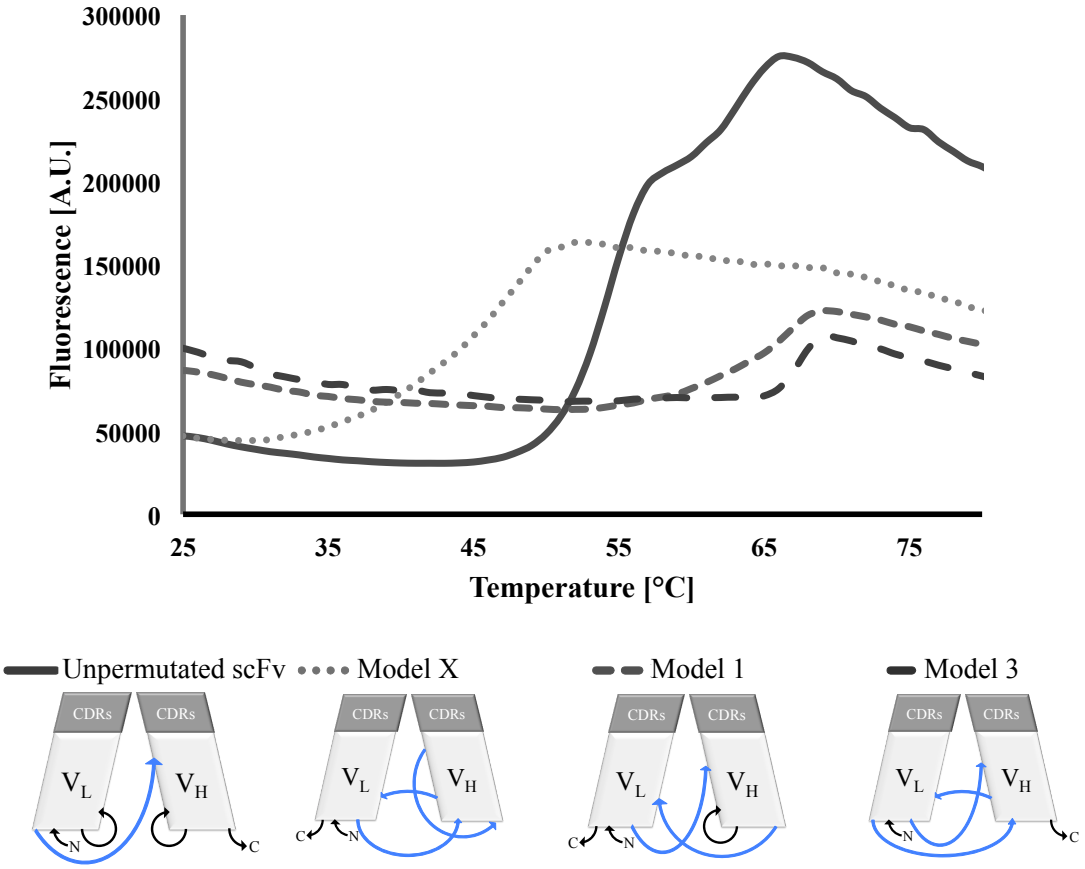

Figure 5.4. Melting Temperatures of Permutated ScFvs
The thermal stability assay was performed on permutated and unpermutated scFvs as per Section 4.7.3. Briefly, scFvs were diluted to a concentration of 9 µM in Strep-tactin elution buffer. Samples were loaded in triplicate into a 96-well plate. Thermal denaturation was performed using the Step One Plus Real-time PCR system (Applied Biosystems) with 0.2°C per 12 seconds steps. Calculations of the scFv T_ms and visualization of melting curves were performed using a Differential Scanning Fluorimetry (DSF) tool. A melting curve of all pFvs compared to the unpermutated scFv is shown. Assays were repeated three times with a standard deviation of ± 0.1ºC for the unpermutated scFv, ± 0.2ºC for Model X, ± 0.8ºC for Model 1, and ± 0.4ºC for Model 3.

5.1.5 Purification of Cyclic and Lariat ScFvs

Following optimization of scFv expression and purification, attempts were made to determine the thermal stability of cyclic and lariat scFvs. Cyclic and lariat scFvs were created using a permutated design of the intein-mediated protein splicing reaction (Scott *et al.*, 1999). The scFv was synthesised with the C-intein domain fused to the N-Terminal of the scFv and the N-intein domain fused to the C-Terminal with a short peptide linker (Figure 5.5A). The linker was included to provide sufficient length for the N-intein and C-intein domains to interact. Catalysis of the intein processing reaction releases the N-intein domain. However, a mutation of an asparagine to alanine in the C-intein domain stops the reaction at this intermediate step producing a lariat scFv (Barreto *et al.*, 2009) (Figure 5.5C). If the C-intein domain is not mutated, the intein processing reaction will continue producing the cyclic scFv (Figure 5.5D).

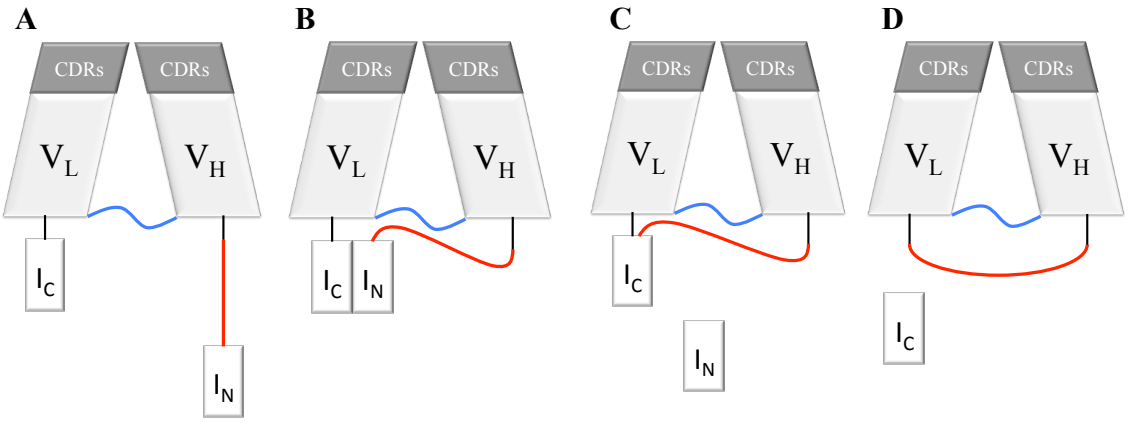

Figure 5.5. Creation of Lariat and Cyclic ScFvs
I_N and I_C represents the N-terminal and C-terminal domains of the intein, respectively. The standard peptide linker joining the V_L and V_H domains is shown in blue. **(A)** The protein is synthesised with the I_C fused to the N-Terminal of the scFv and the I_N fused to the C-Terminal with a short peptide linker (red). **(B)** The linker allows the I_N and the I_C domains to come into contact. **(C)** Catalysis of the intein processing reaction releases the I_N domain. Mutation of an asparagine in the I_C domain to alanine stops the reaction at this lariat intermediate. **(D)** If the I_C domain is not mutated, the intein processing reaction will continue producing the cyclic scFv.

pET-LP1 plasmids encoding cyclic and lariat scFvs were used to transform the *E. coli* strain XL1-Blue. Plasmids were amplified and purified as per Section 4.4.3. Plasmids were digested with *EcoR*I and *Sal*I followed by gel purification (4.2.3) Genes were cloned into pET-LP3 using restriction cloning and plasmids with the correct inserts were verified by DNA sequencing (4.2.4). Cyclic and lariat scFvs were expressed according to Section 4.7.1 and purification was performed according to Section 4.7.2. We were unable to purify samples to homogeneity as indicated by multiple bands on the Coomassie-stained gel (Figure 5.6). One band in particular, the unprocessed form of the lariat scFv, has been previously identified (Bernhard, 2008). However, there are still multiple bands that have not been identified.

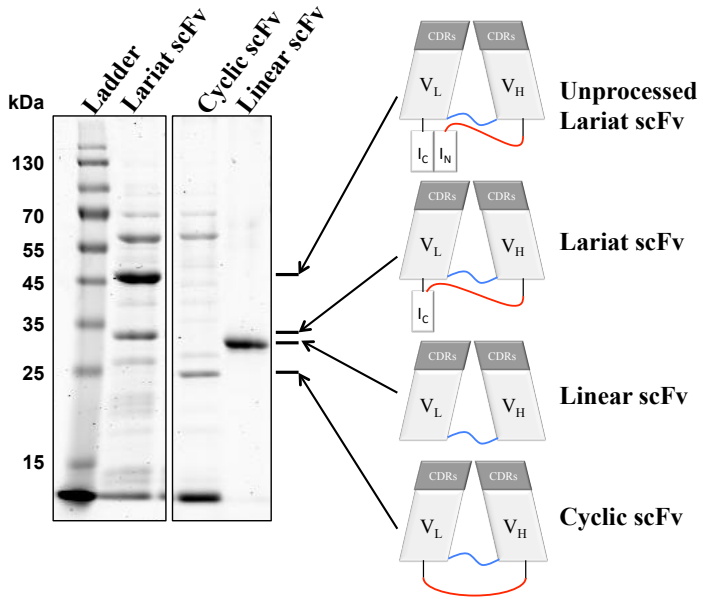

Figure 5.6. Strep-tactin Purification of Cyclic and Lariat ScFvs
Cyclic and lariat scFvs were expressed in the SHuffle expression strain using the pET-LP3 plasmid. At 24 hours post-IPTG induction, scFvs were purified using strep-tactin purification (4.7.2). Following purification, samples were resolved on a 1% SDS-PAGE gel and scFvs were detected with Coomassie stain. Arrows indicate the expected location of the corresponding scFv.

5.1.6 Thermal Stability of Cyclic and Lariat ScFvs

Although we were unable to purify cyclic and lariat scFvs to homogeneity, we assayed the thermal stability of the mixture. Protein levels were quantitated using a Bradford assay and were diluted to a concentration of 10 µM for thermal stability testing. Thermal stability testing of cyclic and lariat scFvs was performed according to Section 4.7.3 and results are shown in Figure 5.7. T_ms of cyclic and lariat scFvs were 43.2 ± 0.1ºC and 44.2 ± 0.2ºC, respectively. Both of these were lower than the linear scFv, which has a T_m of 46.0 ± 0.1ºC.

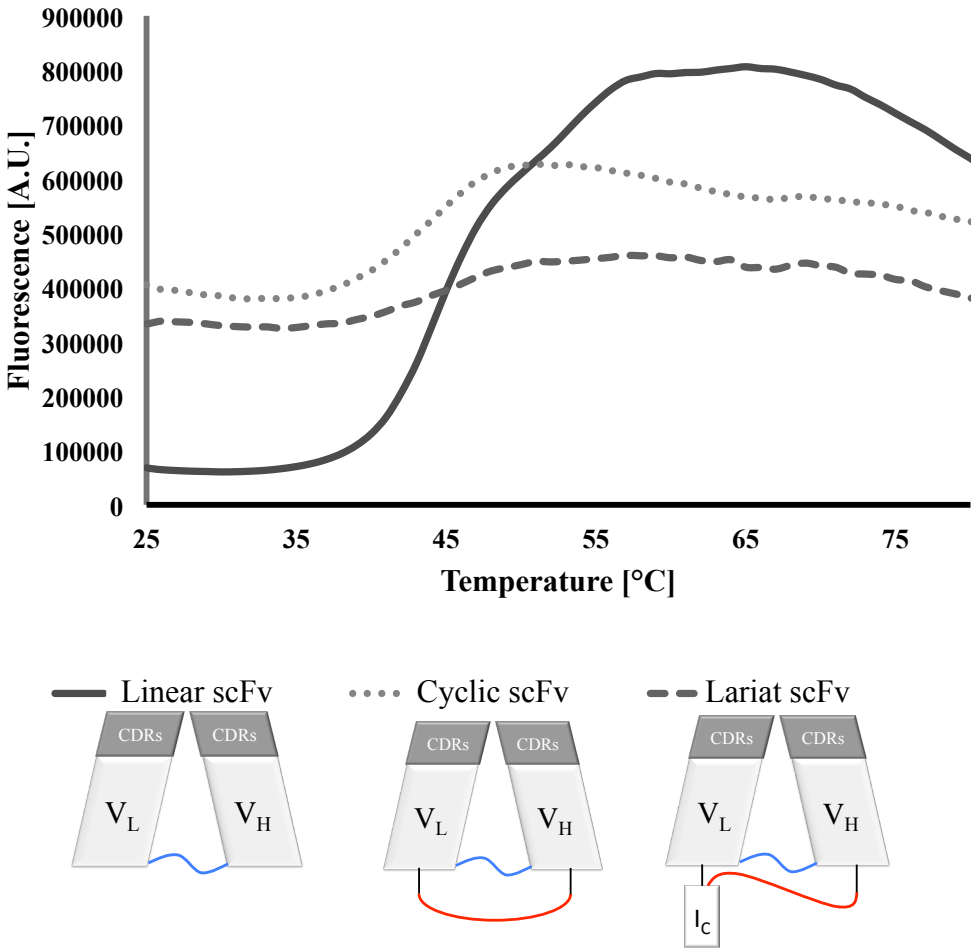

Figure 5.7. Cyclic and Lariat ScFv Melting Curves
The thermal stability assay was performed on cyclic and lariat scFvs as per Section 4.7.3. Briefly, scFvs were diluted to a concentration of 10 µM in Strep-tactin elution buffer. Thermal denaturation was performed using the Step One Plus Real-time PCR system (Applied Biosystems) with 0.2°C per 12 seconds steps. Calculations of the scFv T_ms and visualization of melting curves were performed using a Differential Scanning Fluorimetry (DSF) tool. A melting curve of the linear scFv is included for comparison.

5.2 Specific Aim 2: Increase ScFv Stability Using Variable Domain Framework Mutations

5.2.1 Introduction

We hypothesised that by reducing the conformational flexibility of the scFv through framework mutations, we would be able to decrease the entropy of unfolding. This would result in an scFv with increased stability.

We used phage display to screen a library of mutant anti-maltose-binding protein (MBP) scFvs for their ability to bind MBP. We selected sites in framework regions of the scFv in a semi-rational manner using the proline mutation and glycine to alanine mutation strategy as first shown by Brinkman *et al.* (1987) and recently shown to work with scFvs (Robert *et al.*, 2009). Framework mutations were performed on an anti-MBP scFv using Kunkel mutagenesis. We used phage display to identify mutations that did not affect the ability of the scFv to bind MBP. We hypothesized that these mutations would have enhanced thermostability.

5.2.2 Designing Mutations to Stabilize ScFvs

To determine locations that could tolerate a proline or alanine substitution, the frequency of these amino acids at specific locations were determined using a multiple sequence alignment obtained using data from PDB blast (Appendix 2). The reference sequences used were V_L and V_H domains of the anti-ubiquitin Fab (PBI reference: 3DVG) (Newton *et al.*, 2008). Although 3DVG was a Fab, V_L and V_H domains were used as the blast reference since our anti-MBP scFv framework was identical to 3DVG. We focused on identifying loops that could tolerate a proline substitution and glycine positions that could tolerate an alanine mutation. We hypothesized that if these substitutions exist in nature, that they would be tolerated in the anti-MBP scFv. CDR regions were not mutated, as they were responsible for antigen-binding. Three amino acids on each side of the CDRs were also not mutated as to avoid interfering with antigen binding. Glycine positions that contained at least one alanine, as determined by Blast results, were selected for mutation. The secondary structure of the scFv was used to determine possible sites for proline substitutions. Only loop regions were considered for proline substitution. Positions where an scFv contained at least one proline in PDB Blast results were selected for mutation. A total of twenty-six positions were identified as mutation candidates (Table 5.2, Figure 5.8).

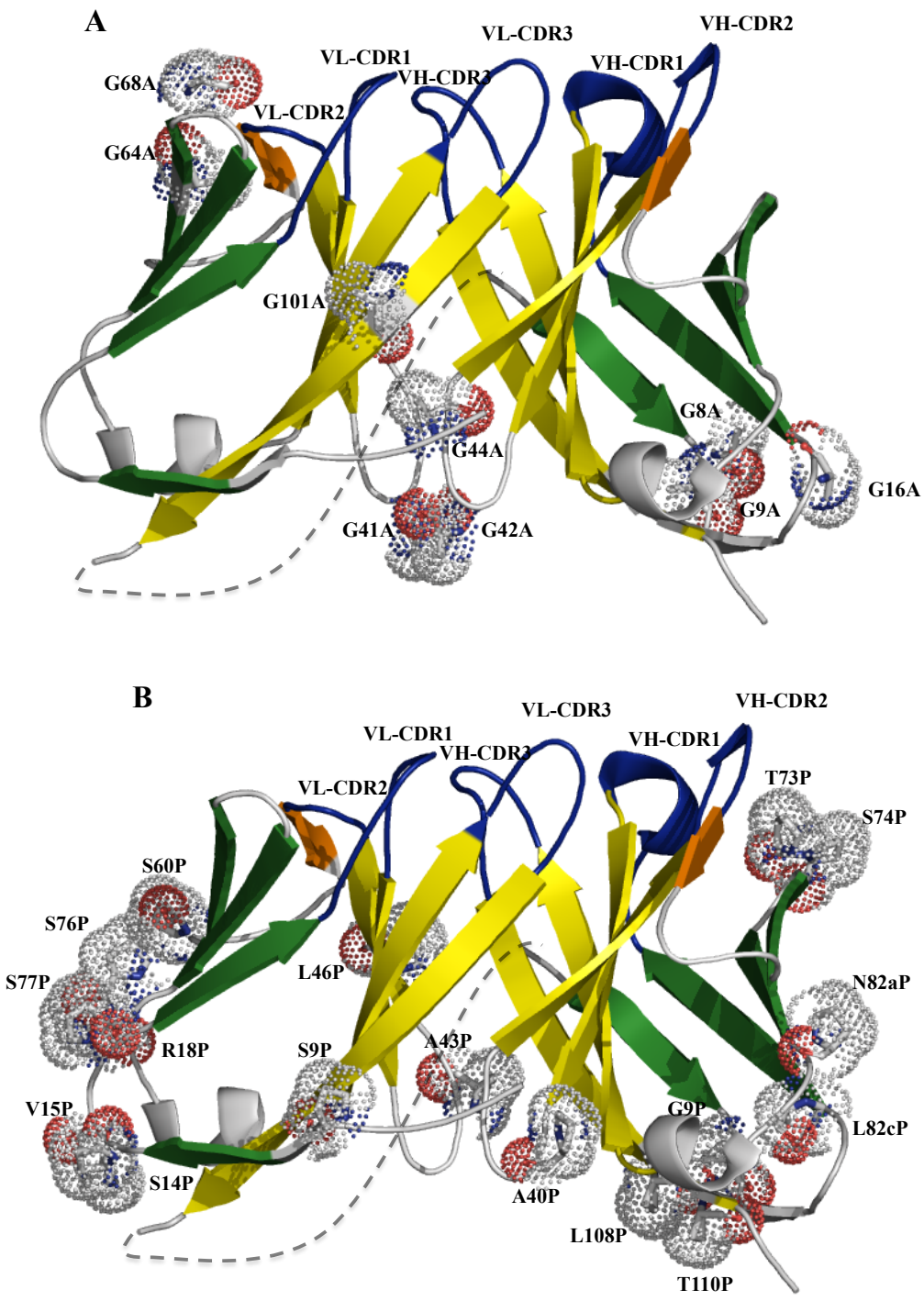

Figure 5.8. Location of Alanine and Proline Mutations in Anti-MBP ScFv.
A modified ribbon diagram of VL (left) and VH (right) domains (PBI ID: 3DVG (Newton *et al.*, 2008)) with mutation sites shown. The short peptide linker has been manually inserted and shown as dashed line. Complementarity determining regions (CDRs) are shown in blue. Glycine to alanine mutations sites (**A**), and proline mutations (**B**), are shown in the stick format and highlighted with a dot radius.

Table 5.2. Mutation Candidates.

Pro Substitutions		Ala Substitutions	
VL	**VH**	**VL**	**VH**
S9P	**G9P**	**G41A**	**G8A**
S14P	**A40P**	**G64A**	**G9A**
V15P	**T73P**	**G68A**	**G16A**
R18P	**S74P**	**G101A**	**G42A**
A43P	**N82aP**		**G44A**
L46P	**L82cP**		
S60P	**L108P**		
S76P	**T110P**		
S77P			

5.2.3 Construction of Anti-MBP Framework Mutation ScFv Libraries

Anti-MBP scFv libraries containing different combinations of mutations were created by performing multiple Kunkel mutagenesis reactions in tandem using pools of primers. Primers were designed with relatively similar lengths and annealing temperatures. Further, silent mutations were incorporated into every primer to allow us to distinguish between failed and successful Kunkel mutagenesis reactions. Further, following phage display selection, we could determine if original amino acids were preferred by observing silent mutations in the sequence. Oligonucleotides and locations of silent mutations are shown in Appendix 3A.

To increase the Kunkel mutagenesis efficiency, multiple Kunkel reactions were performed using a sub-set of primers. Pools were determined by grouping primers that had similar T_ms in the same pool with the requirement that there was no overlap in primer annealing positions. The phagemid library was created by performing Kunkel mutagenesis on each pool as described in section 4.6.1. The mutagenesis efficiency was calculated by sequencing twenty clones from each reaction and counting the number of silent mutations. If the calculated mutagenesis efficiency was sufficiently high, then pools were combined to create a complete library for use in phage display selections.

5.2.4 Phage Display Enrichment of Mutant ScFv Libraries A and B.

Our first library, Library A, was created using five separate Kunkel reactions with three primers per pool. Oligonucleotides used for each pool are shown in Appendix 3B. After

creation of Library A, phage display screening was performed as per Section 4.6.4. Previous attempts to use MBP as the target were unsuccessful. Although it has not been confirmed, we speculated that the MBP preferentially binds to wells in a specific orientation, which blocked the scFv-binding site. Therefore, our phage display work used Protein A as the scFv target, since it is known to bind the scFv framework region. Following two rounds of selection, twenty colonies were isolated from plates used for calculating enrichment and sequenced. Unfortunately, only five mutations were observed (Table 5.3, Mutants 9 - 13). Further, only the G64A mutation was observed in multiple sequences. To determine which amino acid substitutions are potentially favourable, higher mutagenesis efficiency would be needed.

To improve phage display selection, we first needed to optimize the Kunkel mutagenesis procedure to make libraries that are more comprehensive. We analyzed the effect of primer to template ratios and the number of primers per Kunkel reaction on library diversity. During optimization, a library was created that had a sufficient mutagenesis efficiency. This library was called Library B and was created using only two pools of primers, with eight and seven primers per pool. Oligonucleotides used for each pool are shown in Appendix 3B and consisted of primer pools PA11 and PA12 (Appendix 3A). Following Kunkel mutagenesis on separate pools, colonies were isolated from plates that were used for calculating library diversity and sequenced to calculate the mutagenesis efficiency. For the PA11 pool, out of 48 maximum potential primer-annealing positions, 21 silent mutations were found (Appendix 4), which reflects a 44% mutagenesis efficiency. For PA12, out of 35 potential primer-annealing positions, 19 silent mutations were found (Appendix 4), which reflects a 54% mutagenesis efficiency. Since the total combinations of scFvs in the mutant library was 6.7×10^7 members (2^{26}) and the calculated library diversity was 9.18×10^{12} members, a 40% efficiency would ensure that each permutation would be covered approximately 55,000 times.

Two rounds of phage display were performed on Library B. Twenty colonies were isolated and sequenced. The sequence analysis of Library B yielded only one mutation out of the twenty clones sequenced. Further, no silent mutation markers were present. This result was surprising considering the 44% and 58% mutation efficiencies of naïve libraries.

Table 5.3. Isolated Mutant ScFvs

Mutant #	VL mutations	VH Mutations
1	L46P	
2	S14P	L108P
3	R18P	
4	S14P	
5	V15L	
6	S76P	N82aT L82cS
7		N82aT
8	S77P	N82cH
9	G64A	
10		G9A G42A
11	G64A	
12	G41A	G16A
13	G64A	G9R
14	V15P	
15	R18P	
16	R18P L46P	N82aT
17	S14P V15A G68A G101A	G42A L82cP
18	L46P	N82aT L82cP
19	S9F A43P S60P S76P S77P	G9R
20	S76P S77P	
21	S9F A43P	
22	S9F	
23	**Wild-Type**	
24		T73P S74P V109L

There were two possible explanations for this: first, no mutations were beneficial and very few mutations were tolerated. Therefore, they were removed from the library during phage display selections. The second explanation was that the Kunkel mutagenesis was not efficient and very few phagemids were successfully mutated. This would result in a starting library with almost all wild-type scFvs. Analysis of silent mutations provided insight; if the first explanation is correct and the Kunkel mutagenesis was effective, but no mutations were favourable, we would still expect to see silent mutations in sequences. However, this is not the case; with only a few exceptions, all sequences contained wild-type codons and no silent mutations.

There was a contradiction; the naïve Library B contained almost 50% mutated library members. This indicated that the Kunkel reaction was successful. Nevertheless, after only two

rounds of panning, the lack of any silent mutation makers indicates a failed Kunkel reaction. To avoid additional troubleshooting, we abandoned the scFv library selection strategy and focused on characterizing specific framework mutations.

5.2.5 Analysis of Anti-MBP scFv Mutants Using ELISA

Previously, the strength of interaction between the anti-MBP scFv and MBP could not be quantified using ELISA. Since we were using protein A as the target, the Horseradish peroxidase/anti-M13 antibody conjugate that is required for ELISA quantitation would also bind to Protein A and a signal would be detected. To overcome this problem, we obtained a MBP protein expression plasmid and an optimized MBP biotinylation protocol from Dr. Koide's Lab at the University of Chicago. In this protocol, anti-MBP scFv mutants expressed on phage were incubated with biotinylated MBP. Following incubation, the mixture was added to a well that has been coated with NeutrAvidin. The biotinylated MBP binds to the NeutrAvidin coating the well and consequently any scFvs that were bound to the MBP also remained in the well throughout the subsequent washing steps.

Using biotinylated MBP, allowed us to quantitate the strength of the scFv interaction with MBP. At the same time, a relatively large number of phagemids with known scFv mutations had been identified (Table 5.3) as a result of troubleshooting and optimization of the Kunkel mutagenesis reaction.

Each mutant scFv was amplified as per Section 4.6.5. The relative strength of their interaction with MBP was quantified by ELISA as described in Section 4.6.8 and compared to the non-mutated anti-MBP scFv. Several isolated mutants showed a larger signal than the anti-MBP scFv (Figure 5.9). All anti-MBP scFv mutants isolated from the Library A phage display selection (Mutants 9-13) had a higher signal. This indicated that the phage display assay was successful in selecting and enriching for mutations that did not affect MBP binding. In particular the G64A mutant showed up in three of the five mutants and showed an approximately 100% increase in ELISA signal over the standard scFv. Mutant 20, which contained a Ser76Pro and Ser77Pro mutation showed a significant increase in ELISA signal compared to the anti-MBP scFv. In total, seven mutations showed strong ELISA signals: G41A, G64A, S76P with S77P, G9R, G16A, and G42A (Figure 5.10).

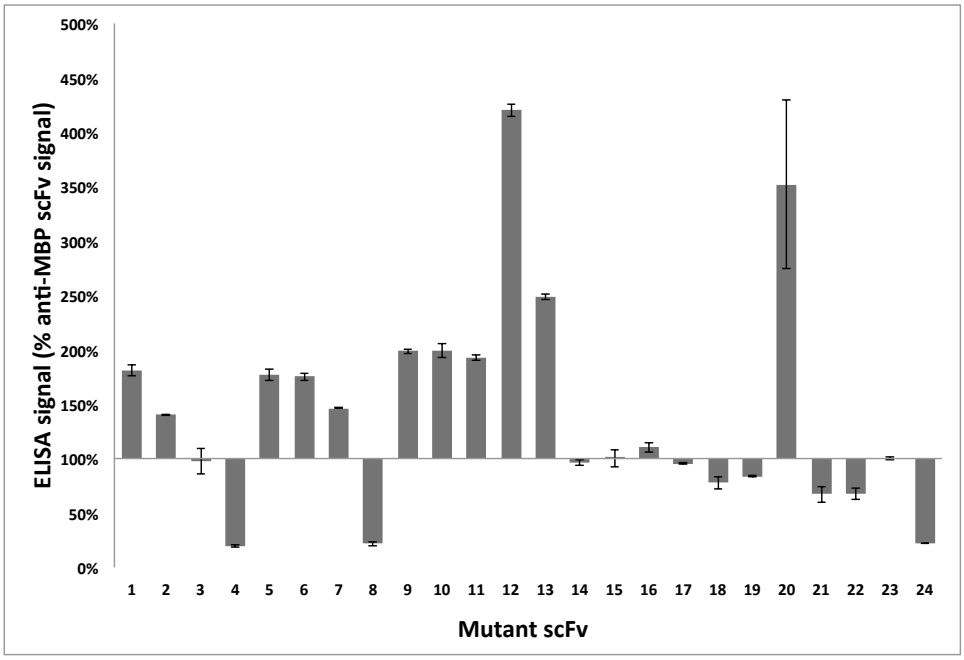

Figure 5.9. ELISA Signal of Isolated Mutants Relative to Anti-MBP ScFv
Relative binding strength of mutant scFvs were determined by ELISA. The strength of interaction was calculated as the ELISA signal divided by the negative control for the corresponding mutant. Quantitation was standardized to the anti-MBP scFv signal, which was set at 100%. Mutations contained in each mutated scFv are listed in Table 5.3.

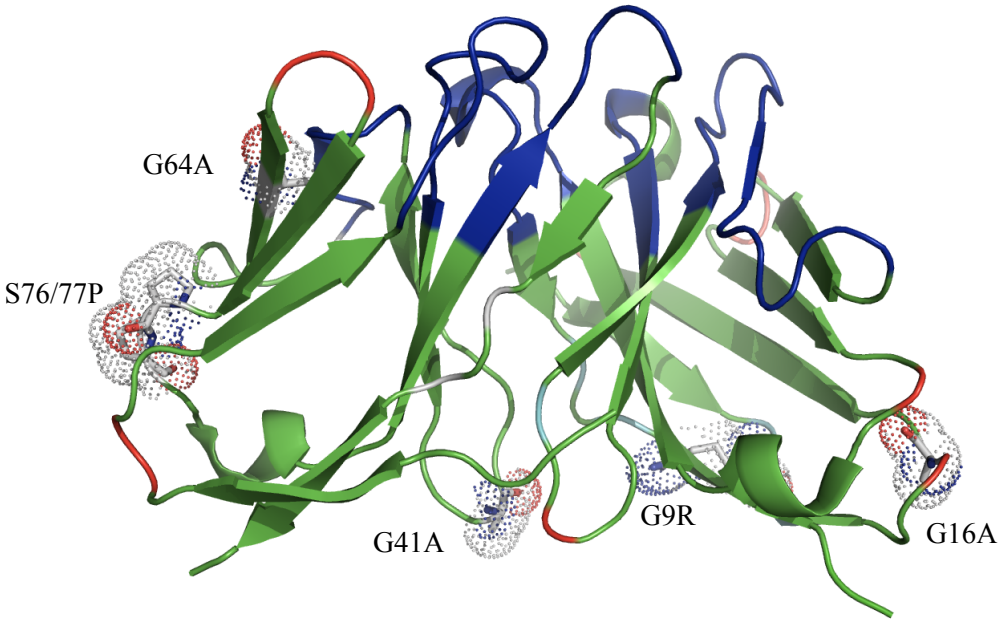

Figure 5.10. Potential ScFv Stabilizing Mutations
A modified ribbon diagram of V_L (left) and V_H (right) domains (PBI ID: 3DVG (Newton *et al.*, 2008)) with mutations showing strong interactions in the phage ELISA. The framework region is green and CDRs are blue. Mutations are shown in stick format and highlighted with a dot radius.

5.2.6 Quantification of Single and Double ScFv Mutants Binding to MBP Using ELISA

Another set of mutant scFvs was created, consisting of combinations of mutants described in Section 5.2.5. Some of single and double mutants had previously been isolated while others were created using Kunkel mutagenesis. The list of mutants along with phagemids and oligonucleotides used to create them are listed on Table 5.4.

Following sequence confirmation, mutant scFvs displayed on the surface of phage were purified and the strength of scFv interactions with MBP were quantified by ELISA. All single and double mutants showed either equal or greater ELISA signals as compared to the anti-MBP scFv (Figure 5.11). In particular, the G64A single mutant showed a very strong ELISA signal. The three highest double mutants all contained the G64A mutation.

Table 5.4. Single and Double Mutant anti-MBP ScFvs

Mutant	Mutations	Previously Isolated	Phagemid Template	Oligonucleotides
M1	G41A		w.t.	18
M2	G64A	PA1		
M3	S76/77P	PA11-2		
M4	G9R		w.t.	21
M5	G16A		w.t.	22
M6	G42A		w.t.	23
M12	G41A + G64A		PA1	18
M13	G41A + S76/77P		PA11-2	18
M14	G41A + G9R		w.t.	18 and 21
M15	G41A + G16A	PA18		
M23	G64A + S76/77P		PA1	20
M24	G64A + G9R	PA20		
M25	G64A + G16A		PA1	22
M34	S76/77P + G9R		PA11-2	21
M35	S76/77P + G16A		PA11-2	22
M45	G9R + G16A		w.t.	21 and 22

The G64A mutation was isolated in three of five mutants from Library A phage display screening and it consistently showed higher ELISA signals than standard scFv. When coupled with the G64A mutation, there were other mutations, such as S76/77P, G41A, and G16A, which had high ELISA signals.

5.2.7 Purification of Single and Double Mutant ScFvs

Since all mutants showed higher ELISA signals than the anti-MBP scFv, four mutants with the highest signals were identified for thermal stability testing. One single mutant, M2 (G64A), and three double mutants, M12 (G64A + G41A), M23 (G64A + S76/77P), and M25 (G64A + G16A) were chosen for further analysis.

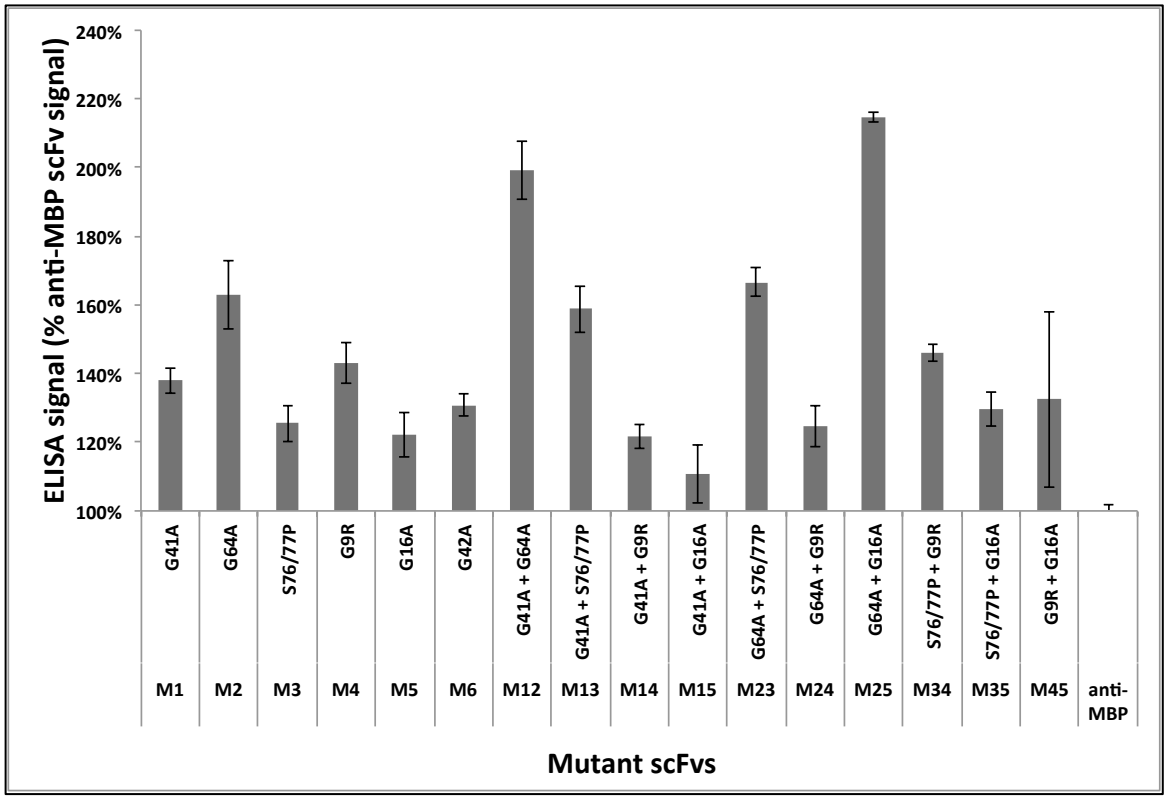

Figure 5.11. ELISA Signal of Single and Double Mutants Relative to anti-MBP ScFv. Quantification of mutant scFvs strength of interaction with MBP was determined using ELISA. The strength of interaction was calculated as the ELISA signal divided by the negative control for the corresponding mutant. Quantitation is standardized to the anti-MBP scFv signal, set at 100%.

We cloned mutant scFvs from the phagemid HP153 to the protein expression plasmid pET-LP3 (Figure 4.1) by restriction cloning. Genes encoding mutated scFvs were amplified from the corresponding phagemids using oligonucleotides 1 and 2 as per Section 4.3.1. Genes were then cloned into the protein expression plasmid pET-LP3 using restriction cloning. Expression of scFvs were performed in the *E. coli* SHuffle strain according to Section 4.7.1. Purification of the control and mutant anti-MBP scFvs were performed according to Section 4.7.2. M2, M12, and M25 were successfully purified as shown in Figure 5.12. Upon difficulty purifying M23, a fifth mutant was chosen, M3 (S77/77P). This mutant was included to ensure that difficulties with M23 purification were due to the S76/77P mutation and not some other anomaly. Indeed, difficulties in purification of the M23 were also observed with the M3 mutant.

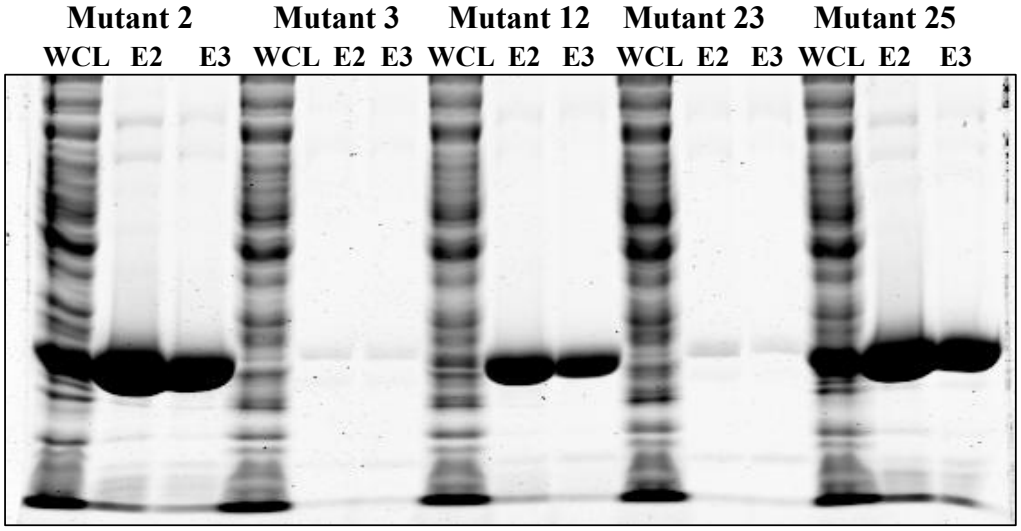

Figure 5.12. Coomassie-stained SDS-PAGE Gel of Purified Mutant scFvs
Mutant scFvs, Mutant 2 (G64A), Mutant 3 (S76/77P), Mutant 12 (G64A + G41A), Mutant 23 (G64A + S76/77P), and Mutant 25 (G64A + G16A) were expressed in the SHuffle strain and purified by a strep-tactin column as per Section 4.7.2. Following purification, the whole cell lysate (WCL), and elution fractions 2 (E2) and 3 (E3) were run on a SDS-PAGE gel and Coomassie-stained as per Section 4.2.1.

5.2.8 Thermal Stability of Single and Double Mutant ScFvs

We tested the thermal stabilities of mutant anti-MBP scFvs, M2, M12, and M25 using the thermal stability assay as described in Section 4.7.3. Melting curves for all samples including the control are shown in Figure 5.13. T_ms were calculated using a Differential Scanning Fluorimetry (DSF) tool, which was provided by the Frank Niesen lab (ftp://ftp.sgc.ox.ac.uk/pub/biophysics) (Niesen *et al.*, 2007). The control anti-MBP scFv had a T_m of 49.3 ± 0.8ºC. The T_m of M2 was 46.7 ± 0.4ºC with a p-value of 0.0073, which indicated that the lower T_m was statistically significant. In fact, all mutants had a statistically significant lower T_m than the control scFv. The T_m of M12 was 47.9 ± 0.1ºC with a p-value of 0.0396 and the T_m of M25 was 46.4 ± 0.4ºC with a p-value of 0.0024.

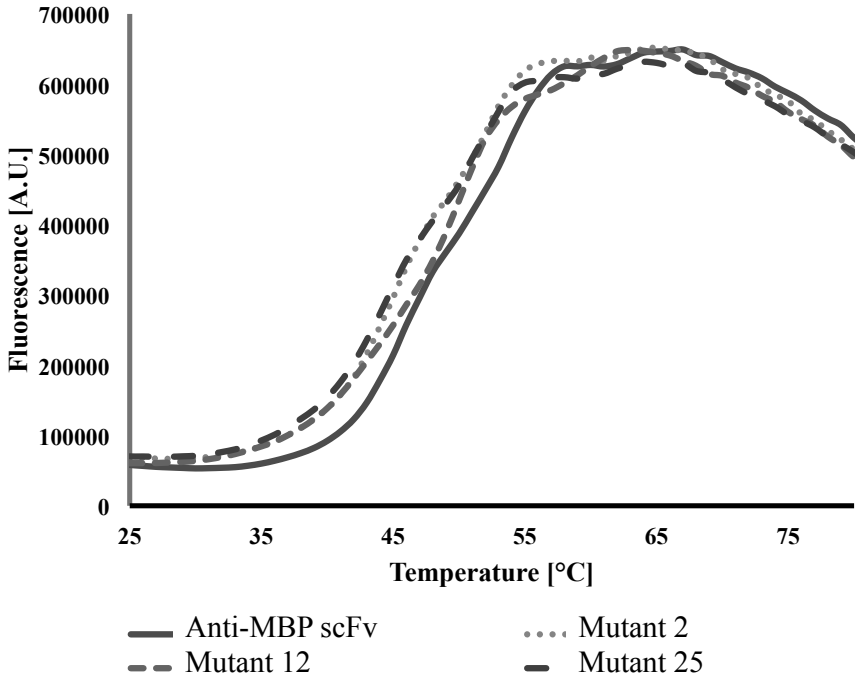

Figure 5.13. Melting Curves of Mutant anti-MBP ScFvs
The thermal stability assay was performed on the mutant scFvs diluted to 10 uM. Thermal denaturation was performed on Step One Plus Real-time PCR system (Applied Biosystems) with 0.2°C per 12 seconds steps. Calculations of scFv T_ms and visualization of melting curves were performed using a Differential Scanning Fluorimetry tool. A melting curve showing all mutant anti-MBP scFvs are shown with the non-mutated scFv.

5.3 Specific Aim 3: Increase the Intracellular Stability of ScFvs

5.3.1 Intracellular ScFv Inhibitors of Bcr-Abl

Chronic myeloid leukaemia (CML) is associated with the chromosomal abnormality called the Philadelphia translocation [t(9;22) (q34;ql l)]. This chromosomal translocation leads to the constitutively activated expression of Bcr-Abl, a fusion of the breakpoint cluster region (BCR) gene and the Abelson tyrosine kinase (ABL1) (Wong and Witte, 2004).

The breakthrough treatment of imatinib (Gleevec) leads to remission in the majority of CML patients in the early chronic phase of the disease. Imatinib functions as a highly specific Bcr-Abl tyrosine kinase inhibitor. However, point mutations in the Bcr-Abl kinase domain can cause imatinib resistance. Since this resistance leads to patient relapse, there is a need for further development of second-generation inhibitors. Two examples of next generation Bcr-Abl inhibitors are nilotinib and dasatinib, which target most imatinib-resistant Bcr-Abl variants (Shah and Sawyers, 2003; Quintás-Cardama *et al.*, 2007). However, all of these approaches are aimed at targeting the ATP-binding pocket of the Bcr-Abl kinase domain and do not target the disease-initiating leukemic stem cells (Perrotti *et al.*, 2010). The result is the development of resistance mutations and reduced responses in advanced disease stages (Jabbour *et al.*, 2010). Therefore, targeting additional sites on Bcr-Abl for use in combination with the commonly targeted ATP-binding pocket may result in improved future therapeutic options.

Substantial research, including work done in our lab (VMaruthachalam, 2011), has been devoted to targeting the Abl-SH2 domain (Grebien *et al.*, 2011; Wong and Witte, 2004). However, studies have also shown the potential for targeting the Abl-SH3 domain (Skorski *et al.*, 1998; Gross *et al.*, 1999). The Abl-SH3 domain has been shown to bind to several different proteins including; 3BP-1, 3BP-2, Abi-1, Abi-2, AAP-1, Ena, SHPTP-1, PAG, and Rin (Gross *et al.*, 1999). Through these binding proteins, the Abl-SH3 domain of Bcr-Abl may play a role in cellular transformation and leukemogenesis. For these reasons, we chose to develop scFv inhibitors of the Abl SH3 domain.

Although phage display is a powerful technique for enriching scFvs against specific targets, the resulting scFvs are not guaranteed to function *in vivo*. Phage display is an *in vitro* technique that uses bacteria to propagate the phage that are fused to a coat protein. Fusion to the coat protein may stabilize the scFv, which may not be as stable when expressed natively. This was possibly what we noticed with M3 and M23 scFvs in Section 5.2.7, where these scFvs

showed high ELISA signals when fused to the pIII protein, but they were unable to be purified for downstream experiments. Further, the objective of these thermal stability assays was to develop scFvs that were sufficiently stable for use as diagnostics and therapeutic reagents. However, there are enormous differences between the controlled *in vitro* conditions used during phage display and the intracellular environment.

Yeast two-hybrid assay is a common technique used to characterize protein interactions. The yeast two-hybrid assay is carried out in the nucleus of yeast cells and is therefore a eukaryotic *in vivo* technique. However, the yeast two-hybrid assay can screen ~10^7 cells (Benatuil *et al.*, 2010), whereas phage display libraries can have a diversity of greater than 10^{10} (Tonikian *et al.*, 2007). Therefore, screening of large libraries, such as a naïve scFv library, is far more cumbersome with yeast two-hybrid screening when compared to phage display. We hypothesised that the yeast two-hybrid assay could be performed on an scFv library already enriched to bind a target by phage display. This strategy may provide further enrichment towards scFvs that are suitable for a eukaryotic cellular environment.

In collaboration with Dr. Sidhu's lab at the University of Toronto, we performed yeast two-hybrid assays using scFv libraries that were enriched for several targets by phage display. In addition, our lab showed the benefit in using a lariat peptide for yeast two-hybrid screening (Barreto *et al.*, 2009). We were interested in determining if scFvs would also benefit from lariat structure when used in this yeast two-hybrid assay.

5.3.2 Construction of Prey Library from Enriched Phage Display ScFv Libraries

Three Src Homology (SH) domains were chosen as scFv targets (baits); 3BP2-SH2, ABL1-SH3, and v-SRC-SH3. Naïve scFv libraries were enriched against each target by members of Dr. Sidhu's lab at the U of T.

Genes encoding SH2 and SH3 domains used for selection by Dr. Sidhu lab were received and amplified by PCR as per Section 4.3.1 using oligonucleotides 24 and 25 for 3BP2-SH2, oligonucleotides 26 and 27 for Abl1-SH3-SH2, and oligonucleotides 28 and 29 for Src-SH3. SH2 and SH3 domains were cloned into the yeast two-hybrid bait plasmid, pEG202 (Figure 4.3), by homologous recombination as per Section 4.5.4.

Following four rounds of phage display, enriched phage libraries were sent to our lab. The scFv library was cloned into the yeast two-hybrid prey plasmid (pJG4-5, Figure 4.4), as well as our yeast two-hybrid lariat prey plasmid (KB41, Figure 4.5). ScFv libraries were

amplified from phagemids by PCR as per Section 4.3.1 using oligonucleotides 30 and 31 for the yeast two-hybrid linear prey plasmid (pJG4-5) and oligonucleotides 32 and 33 for the yeast two-hybrid lariat prey plasmid (KB41). In order for the lariat to properly form, a linker was added to oligonucleotides 33 (underlined in Table 4.4) to provide sufficient length for the N-intein domain to interact with the C-intein domain (Figure 5.5). ScFvs were cloned into the corresponding prey plasmid by homologous recombination as per Section 4.5.4.

5.3.3 Comparison of Lariat and Linear Prey Constructs

Since the Geyer lab showed the benefit in using a lariat structure for yeast two-hybrid screening of peptides (Barreto *et al.*, 2009), we were interested in determining if scFvs would also benefit from lariat structure when used in this yeast two-hybrid assay. Yeast containing prey library plasmids were mated with yeast containing their corresponding bait plasmid using a 1:2.5 prey to bait ratio as per Section 4.5.5. Serial dilutions were plated on SD H-W- to determine the number of diploid yeast cells, and on SGR H-W-A-L- Xgal+ plates to identify scFvs that interacted with the bait. Diploid yeast cells were incubated at 30ºC and colonies were counted after 5 days. Blue colonies were observed on X-gal plates, indicating an interaction between the scFv and the target. This result indicated that scFvs isolated by phage display are sufficiently stable *in vivo* to interact with their target and can be used in yeast two-hybrid assays.

The effectiveness of two different prey plasmids, which expressed the linear and lariat scFvs, were compared by determining the probability of an scFv prey interacting with the bait target. This was done by calculating the ratio of interacting colonies (on SGR H-W-A-L-Xgal+ plates) to the total number of diploids (on SD H-W- plates). **Error! Reference source not found.** shows that for each target, the lariat prey plasmid had less interactions/diploid than the linear plasmid.

5.3.4 Analyzing CDR Preferences for Intracellular scFvs

To determine if there was any enrichment in scFvs after screening for interaction using the yeast two-hybrid assay, colonies were isolated and the prey plasmids prepared for sequencing. Thirty-two yeast colonies showing positive yeast two-hybrid reporter gene outputs (sixteen from the lariat and sixteen from the linear prey libraries) were picked from SGR H-W-

A-L- Xgal+ plates for each target. Each colony was used to inoculate 100 µL of SD H-W- media in a 96 well plate. Cells were incubated overnight at 30ºC. The following day, 5 µL of the media was spotted on SG H-W- plates, SGR H-W-A-L- Xgal+ plates, and SD H-W-A-L- Xgal+ plates to select for diploids, scFvs that interacted with the bait, and galactose-dependent activation, respectively.

SG HW- plates were incubated for one day at 30ºC and prey plasmids from colonies from these plates were used for sequencing. A small portion of cells were picked from colonies on SG H-W- plates and prepared for colony PCR as per Section 4.3.4. Genes encoding scFv library members were amplified from the prey plasmid using high fidelity PCR as per Section 4.3.1 with oligonucleotide 36 and 37 (linear plasmid) or oligonucleotides 38 and 39 (lariat plasmid). Following PCR clean up, amplicons were sequenced using oligonucleotides 36 (linear plasmid) or 38 (lariat plasmid).

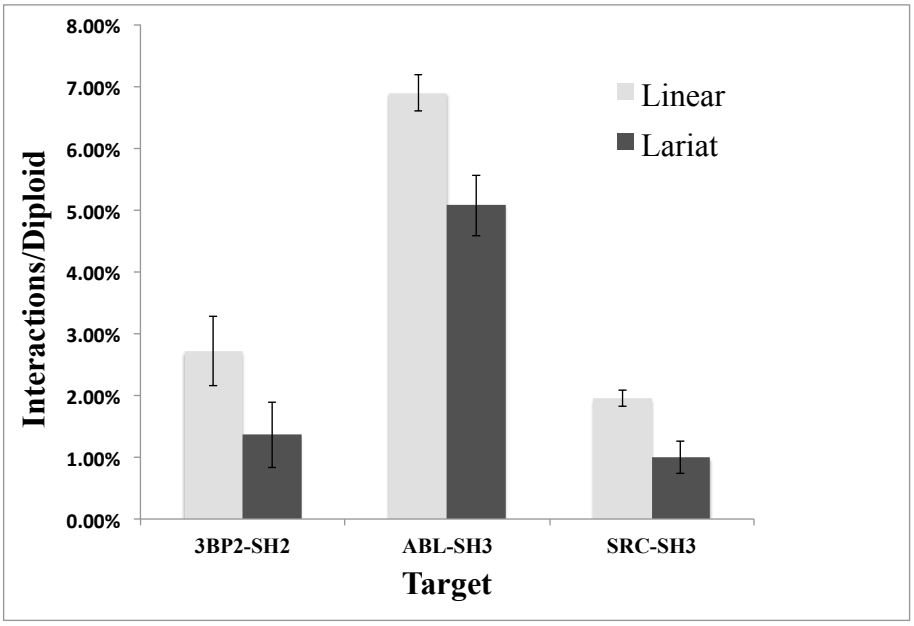

Figure 5.14. Interactions/ Diploid of the Linear and Lariat Prey
Yeast cells containing prey libraries were mated with yeast cells containing their corresponding bait plasmid. The percent of interacting colonies (on SGR H-W-A-L- Xgal+ plates) to the total number of diploids (on SD H-W- plates) is plotted on the y-axis. ScFv interactions from linear plasmid (pJG4-5) and lariat plasmid (KB41) are compared for each target listed on the x-axis.

Sequencing results were aligned using MacVector software and CDRs were identified. The complete list of all CDRs is shown in Appendix 5. Frequency counts of each CDR were compared between lariat and linear scFv preys. No discernible differences between colonies isolated from linear and lariat prey plasmids were found. When comparing scFvs to those isolated by phage display in the Sidhu lab, there was some correlation. First, scFvs that had a frequency greater than one (Table 5.5A) were also isolated at a higher frequency by Dr. Sidhu's lab (Table 5.5B). Further, ELISA experiments performed by Dr. Sidhu's lab showed affinity measurements higher than 70% for scFv that were isolated at the highest frequency by both techniques.

Table 5.5. Highest Frequency CDRs Isolated from Yeast Two-Hybrid Screening

A

ScFv Name	CDR1-VL	CDR2-VL	CDR3-VL	CDR1-VH	CDR2-VH	CDR3-VH
3BP2-A	QYY--SY	GASYLYS	QQSWYAHSGLIT	GFNI--GGGSI	YIYPGYSSTY	ARTVRGSKKPYFSGWAMDY
3BP2-B	QYY--SY	GASYLYS	QQSYYSSGGLIT	GFNI--GGGSI	YIYPGYSSTY	ARTVRGSKKPYFSGWAMDY
3BP2-C	QSY--SY	GASSLYS	QQWYYVSGSPIT	GFNI--GSYGM	YISSYSSGTY	ARTVRGSKKPYFSGWAMDY
ABL-A	QYG-YSS	GASGLYS	QQYGY--GWPIT	GFNL--SYSGM	GIYSSYGYTY	ARYYWSS------YGGGMDY
ABL-B	QYYSYGY	YASYLYS	QQAAG---SPIT	GFNIG-SGSSI	YISPGYSYTS	ARGWW----------WAMDY
SRC-A	Q-YY-GY	GASYLYS	QQYSG---PPIT	GFNLG-YSSYM	SISPYSGYTG	ARSSSFHGWV-HYVGALDY
SRC-B	QGYY-GS	YASYLYS	QQAPS---ALIT	GFNI--YYYYI	SISPYSGYIG	ARGGW----------AIDY
SRC-C	Q-YGYSS	GASGLYS	QQFWG-SHSLIT	GFNLS--YSGM	GIYSSYGYTY	ARYVSSS--------GLDY
SRC-D	Q-YSYGY	GASYLYS	QQPAG-PWHPIT	GFNL--YYGYI	SIYPPYGSTS	ARSVY---------SGLDY
SRC-E	Q-YY-GS	GASGLYS	QQAHG----PIT	GFNIYYGSYGI	YISSYYGYTS	ARTVRGSKKPYFSGWAMDY

B

ScFv Name	Yeast Two-Hybrid Frequency (count/ total sequences)	Phage Display Frequency (count/ total sequences)	Affinity Measurement	
			10 nM	50 nM
3BP2-A	3 / 32	2 /19	71%	77%
3BP2-B	2 / 32	8 / 19	72%	81%
3BP2-C	2 / 32	1 / 19	26%	46%
ABL-A	6 / 27	2 / 20	82%	84%
ABL-B	5 / 27	5 / 20	86%	87%
SRC-A	3 / 29	12 / 22	90%	92%
SRC-B	3 / 29	5 / 22	70%	87%
SRC-C	2 / 29	0 / 22	N/A	N/A
SRC-D	2 / 29	0 / 22	N/A	N/A
SRC-E	2 / 29	0 / 22	N/A	N/A

A galactose-inducible promoter regulates expression of scFv prey libraries. In the presence of glucose the scFv prey is not expressed and no interaction can occur. Therefore, to ensure that the expression of reporter genes was a result of bait and prey protein interaction, colonies were incubated on plates with dextrose. Colonies were incubated on SGR H-W-A-L- Xgal+ plates and SD H-W-A-L- Xgal+ plates for 7 days at 30ºC (Figure 5.15). Several ABL1-SH3 and SRC-SH3 interacting colonies grew on the SD H-W-A-L- Xgal+ plates indicating a lack of galactose-dependent activation. Sequences of non-sugar dependent clones are shown in red in Appendix 5.

5.3.5 Construction of Anti-Abl SH3 ScFv Retroviral Plasmid

Following the identification of CDR preferences, two of the highest occurring scFvs for each target were chosen for biological studies. ScFvs were selected if they were isolated from the phage display library by Dr. Sidhu's lab and showed high affinity in the competition assay performed by Dr. Sidhu's lab (shown under affinity measurements in Table 5.5B). ScFvs labeled as 3BP2-A, 3BP2-B, ABL-A, ABL-B, SRC-A, and SRC-B were identified as containing all the above criteria.

Genes were amplified from amplicons previously used for sequencing using the high fidelity PCR protocol as per Section 4.3.1 with oligonucleotides 40 and 41. Amplified fragments were digested with *EcoR*I and *Xho*I and cloned into the pMSCV-YFP plasmid

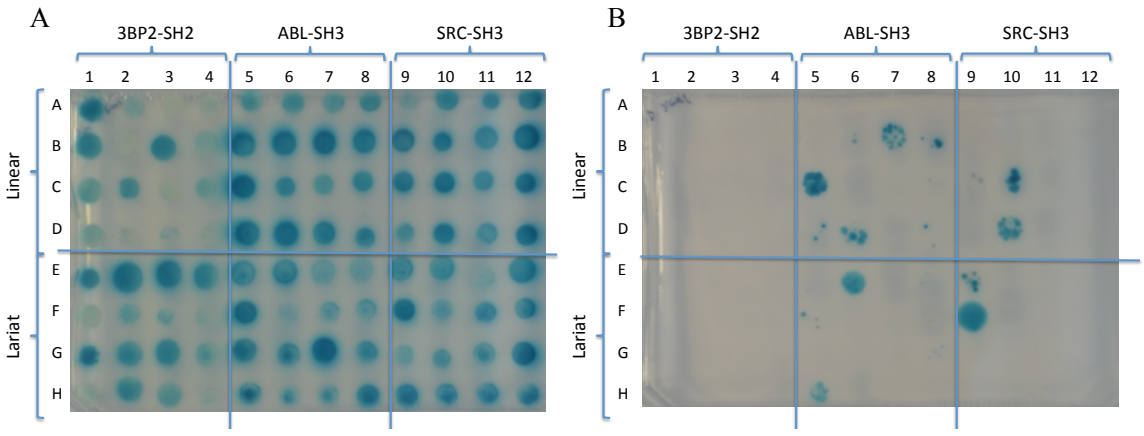

Figure 5.15. Yeast Colonies Isolated From Yeast Two-Hybrid Assay.
EY111 yeast strains containing baits were mated with EY93 yeast strains containing their corresponding bait scFv. Following the yeast two-hybrid screening, sixteen colonies from each condition were isolated and spotted on SGR H-W-A-L- Xgal+ plates **(A)** and SD H-W-A-L-

Xgal+ plates **(B)**. Colonies that grew on the SD H-W-A-L- Xgal+ plates indicate a lack of Galactose dependence for reporter gene activation.
(Figure 4.6) using restriction based cloning procedures. Successful clones were identified using colony PCR as described in Section 4.3.3 followed by sequence confirmation using oligonucleotide 42. Newly constructed retroviral plasmids were sent to the Rottepel Lab at the University of Toronto for further experimentation. As of writing, the results are not yet known.

5.3.6 Inhibitory Activity of anti-ABL1 ScFvs in Chronic Myelogenous Leukemia Cell Lines

We tested whether the anti-Abl SH3 domain scFvs had activity in K562 cells, a CML cell line that express the Bcr-Abl fusion gene. K562 cells are an undifferentiated pluripotent cell line, which was isolated from a CML patient in 1970 (Rodley *et al.*, 1997). Using K562 cells as a model, effects of our anti-Abl1-SH3 scFv on CML cell survival were assayed.

Transient transfection of K562 cells was performed using Amaxa nucleofection kit described in Section 4.8. Cell viability was assessed by tryphan blue exclusion at 0, 24, and 48 hours post-nucleofection. To determine the effect of electroporation alone, cells were also subjected to nucleofection without plasmid DNA. Results are shown in Figure 5.16. Cells that were electroporated had survival counts reduced following nucleofection. After 48 hours both the K562 and MBP controls maintained a viability above 70%. However, both the Abl-A and Abl-B transfected cells were reduced to below 50%.

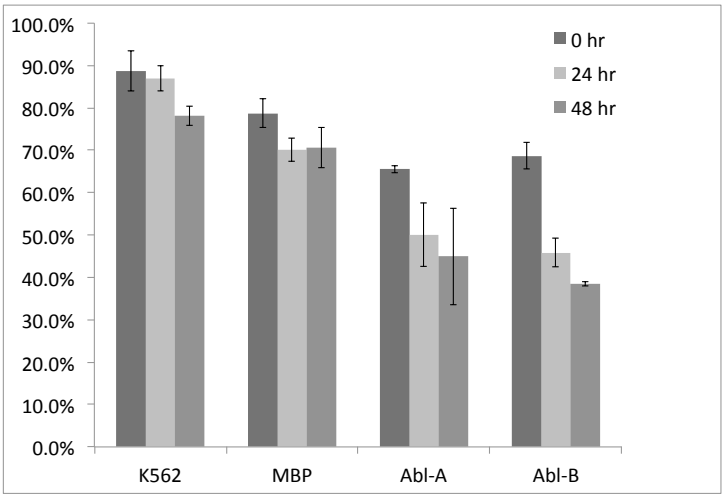

Figure 5.16. Effects of anti-ABL1-SH3 ScFvs on K562 Cell Viability
K562 cells were transiently infected with the retroviral plasmid pMSCV-YFP containing the MBP control and two anti-ABL1-SH3 scFv, ABL-A and ABL-B. To determine effect of

electroporation, cells were also subjected to nucleofection without plasmid DNA (K562). Cell viability was assessed by tryphan blue exclusion at 0, 24, and 48 hours post-nucleofection.

6 Discussion

Antibodies are widely used in both therapeutic and diagnostic applications. However, obstacles such as immunogenicity of animal-derived antibodies, and difficulties in producing antibodies with high quality and sufficient quantity need to be overcome. This has driven the development of alternative systems that can produce antibodies efficiently and cost-effectively. Since the entire antibody is not required for target binding, other development paths have been taken to produce antibody-like molecules that are easier to produce. The development of antibody fragments, such as scFvs, circumvents many of the issues faced with full-length IgG antibody production. However, they are not without their unique set of limitations and obstacles. Still, due to the enormous potential of antibody fragments in diagnostics and therapeutics, there has been considerable interest in overcoming the inherit instability of these fragments. In this thesis, we explored whether increased linkages between the V_L and V_H domains, framework mutations, and specific CDRs could be used to generate stable scFvs.

Experiments to increase the strength of interaction between the V_L and V_H domains were performed first. Preliminary results using permutated scFv designs, Model 1 and Model 3, showed enhanced T_ms that exceed the T_m of the unpermutated scFv. Model 1 and 3 contained two and three linkers joining the V_H and V_L domains, respectively. This result suggested that increasing the number of linkers stabilizes the scFv. In contrast, cyclic and lariat scFvs, where the V_H and V_L were joined by two linkers, were less stable, with T_ms less than that of the unpermutated scFv. However, there was some concern about the accuracy of the T_m values. Assuming equal concentrations of samples in the thermal stability assays, the initial baseline florescence should be similar. However, there were significant differences between control and sample scFvs. This increase in initial fluorescence may be due to impure samples containing partially unfolded proteins, or multiple forms of the scFvs due incomplete processing. Multiple bands on both Coomassie-stained gels (Figure 5.3 and Figure 5.6) indicated that both these scenarios were likely.

Another strategy that we attempted to increase the stability of scFvs was to introduce mutations into framework regions of the scFv. We made a library of framework mutations and used phage display to select for mutations that were tolerated by scFv framework regions. We

hypothesized that Gly to Ala and Pro mutations tolerated by the framework region would increase the stability of scFvs. Conversely, mutations that decreased scFv stability would misfold and be unable to bind the target. Difficulties with creation of a mutant library led us to another strategy involving assaying the ability of specific mutated scFvs ability to bind their target using ELISA. Initial results from the ELISA experiments identified several mutations that were tolerated by the framework region that might also increase scFv stability. However, downstream thermostability assays indicated that this was not the case. First, we could not purify the mutant that had the highest ELISA signal, M23 (G64A and S76/77P). The mutant, M2, with a G64A mutation, was easily purified and therefore, the destabilizing mutations were most likely the S76/77P mutations. To determine that the S76/77P mutation was causing purification difficulties, M3 containing only the S76/77P mutation was cloned into the pET-LP3 expression plasmid. Similar to M23, M3 could not be purified (Figure 5.12). Considering the strong ELISA results, this suggested that the phage stabilizes this mutant. When this mutant was fused to the pIII coat protein in phage display, the scFv was stabilized, which allowed for proper folding. However, when expressed without the pIII fusion, the mutant scFv was not able to fold properly and could not be purified. If this line of experiments were to continue, it would be beneficial to express the M23-pIII fusion scFv with the pET-LP3 plasmid.

The thermostability of remaining scFvs that we could be purified also did not show increased T_ms. As shown in Figure 5.13, there were no significant differences between mutants and the anti-MBP scFv. Considering the promising ELISA results, there are two possible explanations for this discrepancy. First, inspection of the G6A mutant's location on the scFv tertiary structure reveals its close proximity to CDR-L2. Since all mutants tested for stability contained this mutation, it is possible the G64A mutation may have improved the binding of the scFv to MBP through modifications of the binding interface. To determine if this is the case, G64A mutations should be performed on several scFvs containing the same framework, but designed to bind different targets. A lack of improved ELISA signal may indicate that this mutation was only beneficial for anti-MBP scFvs. The second explanation is that there were slight improvements in stabilities of scFvs, but that the SYPRO orange assay was not sensitive enough to measure the differences. Traditionally this assay is used to determine optimal buffer and ligand condition where the differences may be more profound (Crowther *et al.*, 2009; Niesen *et al.*, 2007). Other papers that attempted to increase the thermal stability of scFvs used

other methods for measuring stability such as the thermal challenge assay (Brinkmann *et al.*, 1997; Barthelemy *et al.*, 2008; Young *et al.*, 1995; Kügler *et al.*, 2009; Jespers *et al.*, 2004) or urea denaturation (Wörn and Plückthun, 1998). If we were interested in devoting more resources into characterizing these mutants (and/or future ones) these alternative thermal stability assays may prove useful.

Lastly, it was discovered that variations in protein concentrations affected the melting curves. As shown in Appendix 6, the amplitude of melting curves decreased with decreasing protein concentration. This was not surprising; however, what was unexpected was that when the concentration of protein decreased, the calculated T_m increased. The T_m of the anti-MBP scFv increased from 43.7 ± 0.8ºC at 30 µM to 44.5 ± 0.2ºC at 20 µM, and up to 46.7 ± 0.2ºC at 10 µM. Typically, in melting curve analysis, other conditions such as buffers or ligands are variables. However, scFv melting curve experiments performed in this thesis (Sections 5.1.4, 5.1.6, and 5.2.8), different protein samples were compared. The ability to calculate the concentration following purification was critical as small errors in the concentrations affected the experimental outcome. Diluting samples based on inaccurate initial concentration reading would lead to slight differences in scFv concentrations. These small differences in concentrations could lead to the interpretation of inherent T_m differences that were in fact due to concentration differences. In the permutated scFvs and cyclic/lariat scFv experiments, impure samples were used. Since the Bradford assay calculates the total protein concentration of the sample, impurities would also be included in the calculation. The result would be less of the desired scFv in the thermal melting curve samples. This could explain the significantly higher Model 1 and Model 3 T_ms with the decreased amplitude. This would also cast doubt on any subtle differences of the mutants T_ms, as any variations could be attributed to variations in the concentration. Therefore, the use of differential scanning fluorimetry to determine thermal stability between modified scFvs, or any independently expressed proteins, may not be ideal. Further, if this technique is used, quantitation and purification optimizations are vital to get accurate T_m readings and must be considered for future experiments.

The third aim of this thesis was an alternative approach to stabilize scFvs that did not involve rational design. Instead, it selected for CDRs that stabilized the scFv in intracellular environments. First a large naïve scFv library was enriched for binding to 3bp2-SH2, Abl1-SH3, and Src-SH3 domains by the Sidhu lab at U of T. After four rounds of phage display

selection, an scFv library that was enriched to bind the SH2 and SH3 targets was obtained. This scFv library was screened for binding activity in an intracellular environment using the yeast two-hybrid assay. ScFvs from the phage display selection were cloned into yeast two-hybrid prey plasmids that expressed the scFvs as linear (Figure 4.4) and lariat preys (Figure 4.5).

Although, panning for interactions were successful for all domain targets with both the lariat and linear prey, the lariat was less efficient at screening for binders; **Error! Reference source not found.** shows that for all three of the targets, scFv libraries using the lariat prey plasmid had a lower proportion of interactions than those using the linear plasmid. However, yeast two-hybrid experiments comparing linear and lariat scFvs had been performed previously (Bernhard, 2008). In those experiments, there was a statistically significant increase in binding capacity when using the lariat conformation. This contradicts the result presented in this thesis where the linear scFvs construct was preferred. However, it should be noted that the phage display enrichment performed by Dr. Sidhu's lab used a linear scFv phagemid. If the enrichment was carried out using a lariat scFv design, then the lariat prey plasmid may have been preferred in subsequent yeast two-hybrid screens.

Beyond determining the prey construct that was preferred in the yeast two-hybrid assay, CDRs of scFvs were determined and compared to those isolated by the Sidhu lab. When comparing scFvs to those isolated by phage display, there was some correlation. First, scFvs that had a frequency greater than one were also isolated at a higher frequency by Dr. Sidhu's lab (Table 5.5B). Further, ELISA experiments performed by Dr. Sidhu's lab showed affinity measurements higher than 70% for scFv that were isolated at the highest frequency by both techniques. This result suggests that following phage display panning with the yeast two-hybrid assay can select scFv with favourable CDRs. This combination could provide potentially favourable binders beyond what each technique would be capable individually. Phage display would be able to screen a large naïve library for all possible binder, while removing all members of the library that could not interact with the target. The subsequently reduced library could then be transferred to the yeast two-hybrid system to screen the remaining library for those members that favour binding in a eukaryotic cellular environment.

Although results were positive, further analysis of isolated scFvs need to be performed. Two of the most promising scFvs targeting each domain were identified (Section 0) and cloned

into a retroviral plasmid. Preliminary work was done in our lab using the scFvs developed against Abl1-SH3 domain. Effects of the anti-Abl-SH3 scFvs on CML cell line viability were assessed (Figure 5.16). Ectopic expression of the both anti Abl-SH3 scFvs (Abl-A, Abl-B) caused a significant loss of CML cell viability. Considering this favourable result, further validation of the effectiveness of these scFvs was warranted. Additional downstream experiments are underway; including mouse model studies where mice were injected with a CML cell line expressing the scFvs. In addition, Dr. Rottapel's lab at the U of T is also including these scFvs in their mammalian cell experiments.

Although the results of downstream experiments for these particular targets are not yet known, the techniques described in development of these scFvs should be transferable to a variety of targets. Indeed, phage display and yeast two-hybrid have already been shown useful in with a vast number of targets independently. Experiments presented in this thesis have shown that adapting these techniques to be used in conjunction is possible.

7 References

Afanasieva, T. a, Wittmer, M., Vitaliti, a, Ajmo, M., Neri, D., and Klemenz, R. (2003). Single-chain antibody and its derivatives directed against vascular endothelial growth factor: application for antiangiogenic gene therapy. Gene Ther. *10*, 1850–1859.

Alfthan, K., Takkinen, K., Sizmann, D., Söderlund, H., and Teeri, T. T. (1995). Properties of a single-chain antibody containing different linker peptides. Protein Eng. *8*, 725–731.

Andersen, D. C., and Reilly, D. E. (2004). Production technologies for monoclonal antibodies and their fragments. Curr. Opin. Biotechnol. *15*, 456–462.

Antman, K. H., and Livingston, D. M. (1980). Intracellular neutralization of SV40 tumor antigens following microinjection of specific antibody. Cell *19*, 627–635.

Arndt, K. M., Müller, K. M., and Plückthun, A. (1998). Factors influencing the dimer to monomer transition of an antibody single-chain Fv fragment. Biochemistry *37*, 12918–12926.

Atkins, J. H., and Gershell, L. J. (2002). Selective anticancer drugs. Nat. Rev. Drug Discov. *1*, 491–492.

Barreto, K., Bharathikumar, V. M., Ricardo, A., DeCoteau, J. F., Luo, Y., and Geyer, C. R. (2009). A genetic screen for isolating "lariat" Peptide inhibitors of protein function. Chem. Biol. *16*, 1148–1157.

Barthelemy, P. a, Raab, H., Appleton, B. a, Bond, C. J., Wu, P., Wiesmann, C., and Sidhu, S. S. (2008). Comprehensive analysis of the factors contributing to the stability and solubility of autonomous human VH domains. J. Biol. Chem. *283*, 3639–3654.

Benatuil, L., Perez, J. M., Belk, J., and Hsieh, C.-M. (2010). An improved yeast transformation method for the generation of very large human antibody libraries. Protein Eng. Des. Sel. *23*, 155–159.

Bernhard, W. L. (2008). Engineering Intracellular Antibody Libraries. Masters dissertation, University of Saskatchewan, Saskatoon.

Boder, E. T., and Wittrup, K. . (1997). Yeast surface display for screening combinatorial polypeptide libraries. Nat. Biotechnol. *15*, 553–557.

Boss, M., Kenten, J., and Wood, C. (1984). Assembly of functional antibodies from immunoglobulin heavy and light chains synthesised in E. coli. Nucleic acids *12*, 3791–3806.

Brinkmann, U., Di Carlo, a, Vasmatzis, G., Kurochkina, N., Beers, R., Lee, B., and Pastan, I. (1997). Stabilization of a recombinant Fv fragment by base-loop interconnection and V(H)-V(L) permutation. J. Mol. Biol. *268*, 107–117.

Cole, S., Campling, B., Atlaw, T., Kozbor, D., and Roder, J. (1984). Human monoclonal antibodies. Mol. Cell. Biochem. *62*, 109–120.

Cortez-Retamozo, V. (2004). Efficient Cancer Therapy with a Nanobody-Based Conjugate. Cancer Research *64*, 2853–2857.

Crowther, G. J., Napuli, A. J., Thomas, A. P., Chung, D. J., Kovzun, K. V., Leibly, D. J., Castaneda, L. J., Bhandari, J., Damman, C. J., Hui, R., *et al.* (2009). Buffer optimization of thermal melt assays of Plasmodium proteins for detection of small-molecule ligands. J. Biomol. Screen. *14*, 700–707.

Desplancq, D., King, D. J., Lawson, A. D. G., and Mountain, A. (1994). Multimerization behaviour of single chain Fv variants for the tumour-bindmg antibody B72.3. Protein Eng. *7*, 1027–1033.

Dolk, E., Van Der Vaart, M., Hulsik, D. L., Vriend, G., De Haard, H., Spinelli, S., Cambillau, C., Frenken, L., and Verrips, T. (2005). Isolation of llama antibody fragments for prevention of dandruff by phage display in shampoo. Appl. Environ. Microbiol. *71*, 442–450.

Dong, X., Stothard, P., Forsythe, I. J., and Wishart, D. S. (2004). PlasMapper: a web server for drawing and auto-annotating plasmid maps. Nucleic Acids Res. *32*, W660–4.

Dyer, M. J. S., Hale, G., Hayhoe, F. G. J., and Waldmann, H. (1989). Effects of CAMPATH-1 antibodies in vivo in patients with lymphoid malignancies: influence of antibody isotype. Blood *73*, 1431.

Elbing, K. L., and Brent, R. (2001). Media preparation and bacteriological tools. In Current protocols in protein science, F. M. Ausubel, ed. (Boston, Massachusetts: Clark & Elbing LLP), p. Unit 1.1.

Fellouse, F., and Sidhu, S. S. (2007). Making antibodies in bacteria. In Making and using antibodies, G. C. Howard and M. R. Kaser, eds. (Boca Raton,Fl: CRC Press), pp. 157–180.

Fu, H., Grimsley, G. R., Razvi, A., Scholtz, J. M., and Pace, C. N. (2009). Increasing protein stability by improving beta-turns. Proteins *77*, 491–498.

Ge, M., and Pan, X.-M. (2009). The contribution of proline residues to protein stability is associated with isomerization equilibrium in both unfolded and folded states. Extremophiles *13*, 481–489.

Geyer, C. R., and Brent, R. (2000). Selection of genetic agents from random peptide aptamer expression libraries. Methods Enzymol. *328*, 171–208.

Gietz, R. D., and Schiestl, R. H. (2007). High-efficiency yeast transformation using the LiAc/SS carrier DNA/PEG method. Nat. Protoc. *2*, 31–34.

Glockshuber, R., Schmidt, T., and Plückthun, a (1992). The disulfide bonds in antibody variable domains: effects on stability, folding in vitro, and functional expression in Escherichia coli. Biochemistry *31*, 1270–1279.

Grebien, F., Hantschel, O., Wojcik, J., Kaupe, I., Kovacic, B., Wyrzucki, A. M., Gish, G. D., Cerny-reiterer, S., Koide, A., Pawson, T., *et al.* (2011). UKPMC Funders Group Targeting the SH2-Kinase Interface in Bcr-Abl Inhibits Leukemogenesis. October *147*, 306–319.

Gross, a W., Zhang, X., and Ren, R. (1999). Bcr-Abl with an SH3 deletion retains the ability To induce a myeloproliferative disease in mice, yet c-Abl activated by an SH3 deletion induces only lymphoid malignancy. Mol. Cell. Biol. *19*, 6918–6928.

Hamelinck, D., Zhou, H., Li, L., Verweij, C., Dillon, D., Feng, Z., Costa, J., and Haab, B. B. (2005). Optimized normalization for antibody microarrays and application to serum-protein profiling. Mol. Cell. Proteomics *4*, 773–784.

Hardy, L., and Peet, N. P. (2004). The multiple orthogonal tools approach to define molecular causation in the validation of druggable targets. Drug Discov. Today *9*, 117–126.

Hinman, L. M., Hamann, P. R., Wallace, R., Menendez, A. T., Durr, F. E., and Upeslacis, J. (1993). Preparation and characterization of monoclonal antibody conjugates of the calicheamicins: a novel and potent family of antitumor antibiotics. Cancer Res. *53*, 3336.

Ho, M., Nagata, S., and Pastan, I. (2006). Isolation of anti-CD22 Fv with high affinity by Fv display on human cells. Proc. Natl. Acad. Sci. U. S. A. *103*, 9637–9642.

Hoffman, C. S., and Winston, F. (1987). A ten-minute DNA preparation from yeast efficiently releases autonomous plasmids for transformation of Escherichia coli. Gene *57*, 267–272.

Holliger, P., and Hudson, P. J. (2005). Engineered antibody fragments and the rise of single domains. Nat. Biotechnol. *23*, 1126–1136.

Holliger, P., Prospero, T., and Winter, G. (1993). "Diabodies": small bivalent and bispecific antibody fragments. Proc. Natl. Acad. Sci. U. S. A. *90*, 6444–6448.

Hori, A. (1991). Suppression of solid tumor growth by immuno-neutralising monoclonal antibody against human basic fibroblast growth factor. Cancer Res. *51*.

Jabbour, E., Hochhaus, A., Cortes, J., La Rosée, P., and Kantarjian, H. M. (2010). Choosing the best treatment strategy for chronic myeloid leukemia patients resistant to imatinib: weighing the efficacy and safety of individual drugs with BCR-ABL mutations and patient history. Leukemia *24*, 6–12.

Jespers, L., Schon, O., James, L. C., Veprintsev, D., and Winter, G. (2004). Crystal structure of HEL4, a soluble, refoldable human V(H) single domain with a germ-line scaffold. J. Mol. Biol. *337*, 893–903.

Jung, S., and Plückthun, a (1997). Improving in vivo folding and stability of a single-chain Fv antibody fragment by loop grafting. Protein Eng. *10*, 959–966.

Jäger, M., and Plückthun, A. (1999). Domain interactions in antibody Fv and scFv fragments: effects on unfolding kinetics and equilibria. FEBS Lett. *462*, 307–312.

Kabat, E. A., Wu, T. T., Reid-Miller, M., Perry, H. M., and Gottesman, K. . (1987). Sequences of Proteins of Immunological Interest. In US Department of Health and Human Services (Bethesda, MD: National Institutes of Health).

Kennedy, J. P., Williams, L., Bridges, T. M., Daniels, R. N., Weaver, D., and Lindsley, C. W. (2008). Application of combinatorial chemistry science on modern drug discovery. J. Comb. Chem. *10*, 345–354.

Kim, K. J., Li, B., Winer, J., Armanini, M., Gillett, N., Phillips, H. S., and Ferrara, N. (1993). Inhibition of vascular endothelial growth fac-tor-induced angiogenesis suppresses tumor growth in vivo. Nature *362*, 841.

Koide, A., Gilbreth, R. N., Esaki, K., Tereshko, V., and Koide, S. (2007). High-affinity single-domain binding proteins with a binary-code interface. Proc. Natl. Acad. Sci. U. S. A. *104*, 6632–6637.

Kolonin, M. G., Zhong, J., and Finley, R. L. (2000). Interaction mating methods in two-hybrid systems. Methods Enzymol. *328*, 26–46.

Kügler, M., Stein, C., Schwenkert, M., Saul, D., Vockentanz, L., Huber, T., Wetzel, S. K., Scholz, O., Plückthun, A., Honegger, A., *et al.* (2009). Stabilization and humanization of a single-chain Fv antibody fragment specific for human lymphocyte antigen CD19 by designed point mutations and CDR-grafting onto a human framework. Protein Eng. Des. Sel. *22*, 135–147.

Laemmli, U. K. (1970). Cleavage of Structural Proteins during the Assembly of the Head of Bacteriophage T4. Nature *227*, 680–685.

Lavinder, J., Hari, S., and Sullivan, B. (2009). High-throughput thermal scanning: a general, rapid dye-binding thermal shift screen for protein engineering. J Am Chem Soc. *131*, 3794–3795.

Lee, C. M. Y., Iorno, N., Sierro, F., and Christ, D. (2007). Selection of human antibody fragments by phage display. Nat. Protoc. *2*, 3001–3008.

Liu, C., Tadayoni, B. M., Bourret, L. A., Mattocks, K. M., Derr, S. M., Widdison, W. C., Kedersha, N. L., Ariniello, P. D., Goldmacher, V. S., Lambert, J. M., *et al.* (1996). Eradication of large colon tumor xenografts by targeted delivery of maytansinoids. Proc. Natl. Acad. Sci. U. S. A. *93*, 8618.

Liu, R., Hsieh, C.-Y., and Lam, K. S. (2004). New approaches in identifying drugs to inactivate oncogene products. Seminars in Cancer Biology *14*, 13–21.

Liu, Y., and Mernaugh, R. (2009). Single chain fragment variable recombinant antibody functionalized gold nanoparticles for a highly sensitive colorimetric immunoassay. Biosensors and Bioelectronics *24*, 2853–2857.

Lu, R.-M., Chang, Y.-L., Chen, M.-S., and Wu, H.-C. (2011). Single chain anti-c-Met antibody conjugated nanoparticles for in vivo tumor-targeted imaging and drug delivery. Biomaterials *32*, 3265–3274.

Marasco, W. a (1995). Intracellular antibodies (intrabodies) as research reagents and therapeutic molecules for gene therapy. Immunotechnology *1*, 1–19.

de Marco, A. (2009). Strategies for successful recombinant expression of disulfide bond-dependent proteins in Escherichia coli. Microb. Cell Fact. *8*, 26.

Markiv, A., Anani, B., Durvasula, R. V., and Kang, A. S. (2011). Module based antibody engineering: a novel synthetic REDantibody. J. Immunol. Methods *364*, 40–49.

Matthews, B. W., Nicholson, H., and Becktel, W. J. (1987). Enhanced protein thermostability from site-directed mutations that decrease the entropy of unfolding. Proc. Natl. Acad. Sci. U. S. A. *84*, 6663–6667.

McCafferty, J., Griffiths, A. D., Winter, G., and Chiswell, D. J. (1990). Phage antibodies: filamentous phage displaying antibody variable domains. Nature *348*, 552–554.

Messeguer, a., and Cortés, N. (2007). Combinatorial chemistry in cancer research. Clinical and Translational Oncology *9*, 83–92.

Morino, K., Katsumi, H., Akahori, Y., Iba, Y., Shinohara, M., Ukai, Y., Kohara, Y., and Kurosawa, Y. (2001). Antibody fusions with fluorescent proteins: a versatile reagent for profiling protein expression. J. Immunol. Methods *257*, 175–184.

Morrison, S. L., Johnson, M. J., Herzenberg, L. A., and Oi, V. T. (1984). Chimeric human antibody molecules: Mouse antigen-binding domains with human constant region domains. Proc. Natl. Acad. Sci. U. S. A. *81*, 6851–6855.

Nellis, D. F., Giardina, S. L., Janini, G. M., Shenoy, S. R., Marks, J. D., Tsai, R., Drummond, D. C., Hong, K., Park, J. W., Ouellette, T. F., *et al.* (2005). Preclinical manufacture of anti-HER2 liposome-inserting, scFv-PEG-lipid conjugate. 2. Conjugate micelle identity, purity, stability, and potency analysis. Biotechnol. Prog. *21*, 221–232.

Newton, K., Matsumoto, M. L., Wertz, I. E., Kirkpatrick, D. S., Lill, J. R., Tan, J., Dugger, D., Gordon, N., Sidhu, S. S., Fellouse, F. A., *et al.* (2008). Ubiquitin chain editing revealed by polyubiquitin linkage-specific antibodies. Cell *134*, 668–678.

Ng, S., Jafari, M. R., and Derda, R. (2012). Bacteriophages and viruses as a support for organic synthesis and combinatorial chemistry. ACS Chem. Biol. *7*, 123–138.

Niesen, F. H., Berglund, H., and Vedadi, M. (2007). The use of differential scanning fluorimetry to detect ligand interactions that promote protein stability. Nat. Protoc. *2*, 2212–2221.

Olafsen, T., Tan, G. J., Cheung, C.-W., Yazaki, P. J., Park, J. M., Shively, J. E., Williams, L. E., Raubitschek, A. a, Press, M. F., and Wu, A. M. (2004). Characterization of engineered anti-p185HER-2 (scFv-CH3)2 antibody fragments (minibodies) for tumor targeting. Protein Eng. Des. Sel. *17*, 315–323.

Perrotti, D., Jamieson, C., Goldman, J., and Skorski, T. (2010). Chronic myeloid leukemia: mechanisms of blastic transformation. J Clin Invest *120*, 2254–2264.

Prins, M., Lohuis, D., Schots, A., and Goldbach, R. (2005). Phage display-selected single-chain antibodies confer high levels of resistance against Tomato spotted wilt virus. J. Gen. Virol. *86*, 2107–2113.

Pucca, M., Bertolini, T., and Barbosa, J. (2011). Therapeutic monoclonal antibodies: scFv patents as a marker of a new class of potential biopharmaceuticals. Brazilian Journal of Pharmaceutical Sciences *47*, 31–39.

Quintás-Cardama, A., Kantarjian, H., and Cortes, J. (2007). Flying under the radar: the new wave of BCR-ABL inhibitors. Nat. Rev. Drug Discov. *6*, 834–848.

Reff, M. E., Carner, K., Chambers, K. S., Chinn, P. C., Leonard, J. E., Raab, R., Newman, R. A., Hanna, N., and Anderson, D. R. (1994). Depletion of B cells in vivo by a chimeric mouse human mono-clonal antibody to CD20. Blood *83*, 435.

Reichert, J. M., Rosensweig, C. J., Faden, L. B., and Dewitz, M. C. (2005). Monoclonal antibody successes in the clinic. Nat. Biotechnol. *23*, 1073–1078.

Rimmele, M. (2003). Nucleic acid aptamers as tools and drugs: recent developments. Chembiochem *4*, 963–971.

Robert, R., Dolezal, O., Waddington, L., Hattarki, M. K., Cappai, R., Masters, C. L., Hudson, P. J., and Wark, K. L. (2009). Engineered antibody intervention strategies for Alzheimer's disease and related dementias by targeting amyloid and toxic oligomers. Protein Eng. Des. Sel. *22*, 199–208.

Robinson, C. R., and Sauer, R. T. (1998). Optimizing the stability of single-chain proteins by linker length and composition mutagenesis. Proc. Natl. Acad. Sci. U. S. A. *95*, 5929–5934.

Robinson, M. K., Doss, M., Shaller, C., Narayanan, D., Marks, J. D., Adler, L. P., González Trotter, D. E., and Adams, G. P. (2005). Quantitative immuno-positron emission tomography

imaging of HER2-positive tumor xenografts with an iodine-124 labeled anti-HER2 diabody. Cancer Res. *65*, 1471–1478.

Rodley, P., McDonald, M., and Price, B. (1997). Comparative genomic hybridization reveals previously undescribed amplifications and deletions in the chronic myeloid leukemia□derived K□562 cell line. Genes Chromosomes and Cancer *19*, 36–42.

Roque, a C. a, Lowe, C. R., and Taipa, M. A. (2004). Antibodies and genetically engineered related molecules: production and purification. Biotechnol. Prog. *20*, 639–654.

Schellman, J. a (1997). Temperature, stability, and the hydrophobic interaction. Biophys. J. *73*, 2960–2964.

Scott, C. P., Abel-Santos, E., Wall, M., Wahnon, D. C., and Benkovic, S. J. (1999). Production of cyclic peptides and proteins in vivo. Proc. Natl. Acad. Sci. U. S. A. *96*, 13638–13643.

Shah, N. P., and Sawyers, C. L. (2003). Mechanisms of resistance to STI571 in Philadelphia chromosome-associated leukemias. Oncogene *22*, 7389–7395.

Shawler, D., and Bartholomew, R. (1985). Human immune response to multiple injections of murine monoclonal IgG. Journal of Immunology *135*, 1530–1535.

Sidhu, S. S., and Fellouse, F. a (2006). Synthetic therapeutic antibodies. Nat. Chem. Biol. *2*, 682–688.

Sidhu, S. S., and Koide, S. (2007). Phage display for engineering and analyzing protein interaction interfaces. Curr. Opin. Struct. Biol. *17*, 481–487.

Simmons, L. C., Reilly, D., Klimowski, L., Raju, T. S., Meng, G., Sims, P., Hong, K., Shields, R. L., Damico, L. a, Rancatore, P., *et al.* (2002). Expression of full-length immunoglobulins in Escherichia coli: rapid and efficient production of aglycosylated antibodies. J. Immunol. Methods *263*, 133–147.

Skerra, a, and Plückthun, a (1988). Assembly of a functional immunoglobulin Fv fragment in Escherichia coli. Science *240*, 1038–1041.

Skorski, T., Nieborowska-Skorska, M., Wlodarski, P., Wasik, M., Trotta, R., Kanakaraj, P., Salomoni, P., Antonyak, M., Martinez, R., Majewski, M., *et al.* (1998). The SH3 domain contributes to BCR/ABL-dependent leukemogenesis in vivo: role in adhesion, invasion, and homing. Blood *91*, 406–418.

Smith, G. P. (1985). Filamentous fusion phage: novel expression vectors that display cloned antigens on the virion surface. Science *228*, 1315–1317.

Smith, P. K., Shernan, S. K., Chen, J. C., Carrier, M., Verrier, E. D., Adams, P. X., Todaro, T. G., Muhlbaier, L. H., and Levy, J. H. (2011). Effects of C5 complement inhibitor pexelizumab

on outcome in high-risk coronary artery bypass grafting: combined results from the PRIMO-CABG I and II trials. J. Thorac. Cardiovasc. Surg. *142*, 89–98.

Stijlemans, B., Conrath, K., Cortez-Retamozo, V., Van Xong, H., Wyns, L., Senter, P., Revets, H., De Baetselier, P., Muyldermans, S., and Magez, S. (2004). Efficient targeting of conserved cryptic epitopes of infectious agents by single domain antibodies. African trypanosomes as paradigm. J. Biol. Chem. *279*, 1256–1261.

Tan, P. H., Sandmaier, B. M., and Stayton, P. S. (1998). Contributions of a highly conserved VH/VL hydrogen bonding interaction to scFv folding stability and refolding efficiency. Biophys. J. *75*, 1473–1482.

Testa, L., Van Gaal, W. J., Bhindi, R., Biondi-Zoccai, G. G. L., Abbate, A., Agostoni, P., Porto, I., Andreotti, F., Crea, F., and Banning, A. P. (2008). Pexelizumab in ischemic heart disease: a systematic review and meta-analysis on 15,196 patients. J. Thorac. Cardiovasc. Surg. *136*, 884–893.

Tonikian, R., Zhang, Y., Boone, C., and Sidhu, S. S. (2007). Identifying specificity profiles for peptide recognition modules from phage-displayed peptide libraries. Nat. Protoc. *2*, 1368–1386.

Tung, E. T. K., Ma, H.-W., Cheng, C., Lim, B. L., and Wong, K.-B. (2008). Stabilization of beta-propeller phytase by introducing Xaa-->Pro and Gly-->Ala substitutions at consensus positions. Protein Pept. Lett. *15*, 297–299.

VMaruthachalam, B. (2011). Lariat peptide inhibitors of abl kinase in Vitro. Masters dissertation, University of Saskatchewan, Saskatoon.

Wertman, K. F., Wyman, A. R., and Botstein, D. (1986). Host/vector interactions which affect the viability of recombinant phage lambda clones. Gene *49*, 253–262.

Wong, S., and Witte, O. N. (2004). The BCR-ABL story: bench to bedside and back. Annu. Rev. Immunol. *22*, 247–306.

Wörn, a, and Plückthun, a (2001). Stability engineering of antibody single-chain Fv fragments. J. Mol. Biol. *305*, 989–1010.

Wörn, a, and Plückthun, A. (1998). An intrinsically stable antibody scFv fragment can tolerate the loss of both disulfide bonds and fold correctly. FEBS Lett. *427*, 357–361.

Young, N. M., MacKenzie, C. R., Narang, S. a, Oomen, R. P., and Baenziger, J. E. (1995). Thermal stabilization of a single-chain Fv antibody fragment by introduction of a disulphide bond. FEBS Lett. *377*, 135–139.

8 Appendix

8.1.1 Appendix 1

(a)

GAT ATC CAG ATG ACC CAG TCC CCG AGC TCC CTG TCC GCC TCT GTG
GGC GAT AGG GTC ACC ATC ACC TGC CGT GCC AGT CAG TCC GTG TCC
AGC GCT GTA GCC TGG TAT CAA CAG AAA CCA GGA AAA GCT CCG AAG
CTT CTG ATT TAC TCG GCA TCC AGC CTC TAC TCT GGA GTC CCT TCT
CGC TTC TCT GGT AGC CGT TCC GGG ACG GAT TTC ACT CTG ACC ATC
AGC AGT CTG CAG CCG GAA GAC TTC GCA ACT TAT TAC TGT CAG CAA
TCT TCT TAT TCT CTG ATC ACG TTC GGA CAG GGT ACC AAG GTG GAG
ATC AAA **GGT ACT ACT GCC GCT AGT GGT AGT AGT GGT GGC AGT AGC**
AGT GGT GCC GAG GTT CAG CTG GTG GAG TCT GGC GGT GGC CTG GTG
CAG CCA GGG GGC TCA CTC CGT TTG TCC TGT GCA GCT TCT GGC TTC
AAC TTT TCT TCT TCT TCT ATA CAC TGG GTG CGT CAG GCC CCG GGT
AAG GGC CTG GAA TGG GTT GCA TCT ATT TCT TCT TCT TAT GGC TAT
ACT TAT TAT GCC GAT AGC GTC AAG GGC CGT TTC ACT ATA AGC GCA
GAC ACA TCC AAA AAC ACA GCC TAC CTA CAA ATG AAC AGC TTA AGA
GCT GAG GAC ACT GCC GTC TAT TAT TGT GCT CGC ACT GTT CGT GGA
TCC AAA AAA CCG TAC TTC TCT GGT TGG GCT ATG GAC TAC TGG GGT
CAA GGA ACC CTG GTC ACC GTC TCC TCG GTC

(b)

DIQMTQSPSERSLSASVGDRVTITCRASQSVSSAVAWYQQKPGKAPKLLIYSASSLYSG
VPSRFSGSRSGTDFTLTISSLQPEDFATYYCQQSSYSLITFGQGTKVEIK**GTTAASGSS**
GGSSSGAEVQLVESGGGLVQPGGSLRLSCAASGFNFSSSSIHWVRQAPGKGLEWVASIS
SSYGYTYYADSVKGRFTISADTSKNTAYLQMNSLRAEDTAVYYCARTVRGSKKPYFSGW

Sequence of the anti-MBP ScFv: Anti-MBP scFv nucleotide sequence (a) and amino acid sequence (b). The VL and VH are linked together with the C3 linker indicated in bold.

8.1.2 Appendix 2

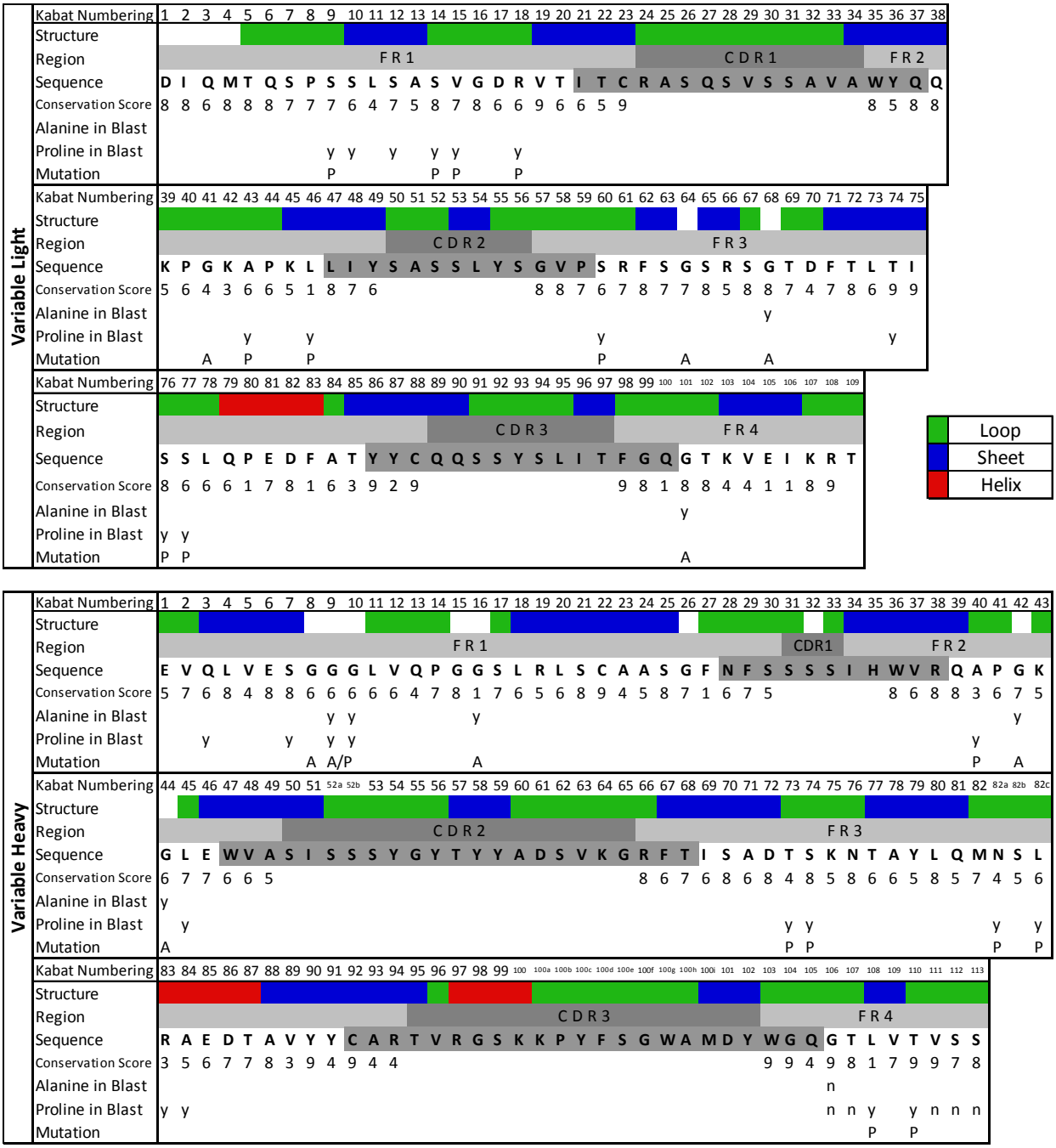

Secondary Structure of the anti-MBP ScFv and Mutation Positions: Glycine positions that contained at least one alanine and proline mutations were determined by the BLAST results and the secondary structure. Only areas of loop conformation (green) were considered for proline substitution. CDR regions (grey) were ignored, as they are responsible for antigen binding. Positions +3 and -3 from all CDRs were also ignored as to not interfere with their antigen binding ability. Blast results were obtained from www.consurf.tau.ac.il with a 250-homologue parameter. The PBI ID used for the blast was 3DVG chain A for the VL region and chain B for the VH region. Sequence alignment and analysis was performed using MacVector. The Kabat

amino acid numbering was used (Kabat *et al.*, 1987). Framework and CDR regions were obtained from Jung and Plückthun (1997). Secondary structure was obtained using the web based program from www.ebi.ac.uk using the crystal structure of K63-specific FAB APU.3A8 (PBI ID 3DVG) (Newton *et al.*, 2008).

8.1.3 Appendix 3

(A)

Sn. #	T_m (°C)	Sequence
3	72	ATG ACC CAG TCC CCG YTC TCC CTG TCC GCC TC
4	78	AGC TCC CTG TCC GCC YCT SYG GGC GAT CSG GTC ACC ATC ACC TG
5	64	ATC AAC AGA AAC CAG SAA AAS CGC CGA AGC TTC TGA TT
6	65	GAA AAG CTC CGA AGC YGC TGA TTT ACT CGG C
7	66	TAC TCT GGA GTC CCT YCA CGC TTC TCT GGT A
8	73	CTT CTC GCT TCT CTG SAA GCC GTT CCG SGA CGG ATT TCA CTC T
9	70	TTC ACT CTG ACC ATC YCC YCC CTG CAG CCG GAA G
10	68	TCA CGT TCG GAC AGG SAA CCA AGG TGG AGA TC
11	76	AGC TGG TGG AGT CTG SCS SAG GCC TGG TGC AGC CAG
12	65	TGG TGC AGC CAG GGG SAT CAC TCC GTT TGT C
13	68	CAC TGG GTG CGT CAG SCG CCG GGT AAG GGC C
14	72	GTG CGT CAG GCC CCG GSA AAG GSC CTG GAA TGG GTT GC
15	65	ACT ATA AGC GCA GAC MCG YCC AAA AAC ACA GCC T
16	69	GCC TAC CTA CAA ATG MMC AGC CYA AGA GCT GAG GAC AC
17	75	GGG GTC AAG GAA CCC YAG TCM CCG TCT CCT CGG TCG

(B)

Library	Pool	Oligonucleotides							
Library A	PA1	8	11	14					
	PA2	5	10	12					
	PA3	4	17	13					
	PA4	6	7	15					
	PA5	3	9	16					
Library B	PA11	3	5	7	9	11	13	15	17
	PA12	4	6	8	10	12	14	16	

Oligonucleotides Used for the Mutant Library Creation: (A) Oligonucleotides were designed with a focus on maximizing annealing potential while maintaining relatively similar T_ms. To ensure we could distinguish between inefficient mutagenesis and a strong selection for wild-type amino acids, silent mutations (yellow) were incorporated into every primer. Blue indicates proline mutation points and red indicates the location of alanine mutations. If a mutation could result in a proline or alanine, it is coloured in green. **(B)** Pools of primers for library A and B creation were determined by matching oligionucleotides with similar T_ms with the condition that they did not overlap.

8.1.4 Appendix 4

	PA11-1	PA11-2	PA11-3	PA11-4	PA11-5	PA11-6
P1	S9F		S9F	S9F		
P3	A43P	Marker	A43P	Marker	Marker	
P5	S60P		Marker			
P7	S76P, S77P	S76P, S77P	Marker	Marker		
P9	G9R		Marker			
P11			Marker			
P13			Marker			T73P,S74P
P15			Marker			V109L

	PA12-1	PA12-2	PA12-3	PA12-4	PA12-5	
P2	-	Marker	R18P	V15A, S14P	-	
P4	Marker	-	L46P	Marker	L46P	
P6	Marker	Marker	-	G68A	-	
P8	-	Marker	-	G101A	-	
P10	-	Marker	-	Marker	-	
P12	-	Marker	-	G42A	-	
P14	-	-	N82aT	L82cP	N82aT, L82cP	

Isolated Mutants from Naïve Library PA11 and PA12: Following creation of the PA11 and PA12 library, the mutagenesis efficiency was determined by sequencing plasmids form each library. Each column indicates the mutations for individual colonies. Rows indicate the corresponding primer for each mutation.

8.1.5 Appendix 5

Sample (Well Bait/Plasmid)	CDR1-VL	CDR2-VL	CDR3-VL	CDR1-VH	CDR2-VH	CDR3-VH
A01 3BP2/pJG4-5	QYY--SY	GASYLYS	QQSYYGYSSLIT	GFNL--YGYGI	YIGSGSSGTY	ARTVRGSKKPYFSGWAMDY
A02 3BP2/pJG4-5	QSY--SY	GASSLYS	QQWYYVSGSPIT	GFNI--GSYGM	YISSYSSGTY	ARTVRGSKKPYFSGWAMDY
A03 3BP2/pJG4-5	QSY--SY	GASSLYS	QQWYWA-SSPIT	GFNI--GSYGM	YISSYSSGTY	ARTVRGSKKPYFSGWAMDY
A04 3BP2/pJG4-5	QYY--SY	GASYLYS	QQSWYAHSGLIT	GFNI--GGGSI	YIYPGYSSTY	ARTVRGSKKPYFSGWAMDY
B01 3BP2/pJG4-5	QYY--SY	GASSLYS	QQWYYVSGSPIT	GFNI--GSYGM	YISSYSSGTY	ARTVRGSKKPYFSGWAMDY
B02 3BP2/pJG4-5	QYY--SY	GASYLYS	QQSFYWGGSLIT	GFNI--GGGSI	YIYPGYSSTY	ARTVRGSKKPYFSGWAMDY
B03 3BP2/pJG4-5	QYY--SY	GASYLYS	QQWYYVSGSPIT	GFNI--GSYGM	CISSYSSGTY	ARTVRGSKKPYFSGWAMDY
B04 3BP2/pJG4-5	QSY--SY	GASSLYS	QQWYYVSGSPIT	GFNI--GSYGM	YIYPGYSSTY	ARTVRGSKKPYFSGWAMDY
C01 3BP2/pJG4-5	QYY--SY	GASYLYS	QQGFWSSYSLIT	GFNL-SYYSSM		
C02 3BP2/pJG4-5	QYY--SY	GASYLYS	QQSYYSSGGLIT	GFNI--GSYGM	YISSYSSGTY	ARTVRGSKKPYFSGWAMDY
C03 3BP2/pJG4-5	QYY--SY	YASYLYS	QQSYYSGHSLIT	GFNL--YGYGI	YIGSGSSGTY	ARTVRGSKKPYFSGWAMDY
C04 3BP2/pJG4-5	QYY--SY	GASYLYS	QQVYW---PLIT	GFNI--GGGSI	YIYPGYSSTY	ARTVRGSKKPYFSGWAMDY
D01 3BP2/pJG4-5	QYY--SY	GASYLYS	QQGYFPYHSLIT	GFNI--GGGSI	YIYPGYSSTY	ARTVRGSKKPYFSGWAMDY
D02 3BP2/pJG4-5	QGY--SY	YASYLYS	QQSYYSSGGLIT	GFNI--GGGSI	YIYPGYSSTY	ARTVRGSKKPYFSGWAMDY
D03 3BP2/pJG4-5	QYY--SY	GASYLYS	QQSYYSSGGLIT	GFNI--GSYGM	YISSYSSGTY	ARTVRGSKKPYFSGWAMDY
D04 3BP2/pJG4-5	QYY--SY	GASYLYS	QQWSF--PSLIT	GFNI--GGGSI	YIYPGYSSTY	ARTVRGSKKPYFSGWAMDY
E01 3BP2/KB41	QYY--SY	YASYLYS	QQSYYGYSSLIT	GFNL--YGYGI	YIGSGSSGTY	ARTVRGSKKPYFSGWAMDY
E02 3BP2/KB41	QYY--SY	GASYLYS	QQSYYSSGGLIT	GFNI--GGGSI	YIYPGYSSTY	ARTVRGSKKPYFSGWAMDY
E03 3BP2/KB41	QYY--SY	GASYLYS	QQSYYSPSSLIT	GFNI--GGGST	YIYPGYSSTY	ARTVRGSKKPYFSGWAMDY
E04 3BP2/KB41	QYY--SY	GASYLYS	QQSWYAHSGLIT	GFNI--GGGSI	YIYPGYSSTY	ARTVRGSKKPYFSGWAMDY
F01 3BP2/KB41	QYY--SY	GASYLYS	QQGFWSSYSLIT	GFNI--GGGSI	YIYPGYSSTY	ARTVRGSKKPYFSGWAMDY
F02 3BP2/KB41	QYY--SY	YASYLYS	QQSYYGHYGLIT	GFNI--GGGSI	YIYPGYSSTY	ARTVRGSKKPYFSGWAMDY
F03 3BP2/KB41	QYY--SY	YASYLYS	QQSYYSGHSLIT	GFNL--YGYGI	YIGSGSSGTY	ARTVRGSKKPYFSGWAMDY
F04 3BP2/KB41	QYY--SY	GASYLYS	QQFYY---PLFT	GFNI--GGGSI	YIYPGYSSTY	ARTVRGSKKPYFSGWAMDY
G01 3BP2/KB41	QYY--SY	GASYLYS	QQSWYAHSGLIT	GFNI--GGGSI	YIYPGYSSTY	ARTVRGSKKPYFSGWAMDY
G02 3BP2/KB41	QYY--SY	GASYLYS	QQSYYSSGGLIT	GFNI--GGGSI	YIYPGYSSTY	ARTVRGSKKPYFSGWAMDY
G03 3BP2/KB41	QYY--FY	GASYLYS	QQSYYGYASLIT	GFNI--GGGSI	YIYPGYSSTY	ARTVRGSKKPYFSGWAMDY
G04 3BP2/KB41	QYY--SY	GTSYLYS	QQSYYSSGGLIT	GFNI--GGGSI	YIYPGYSSTY	ARTVRGSKKPYFSGWAMDY
H01 3BP2/KB41	QYY--SY	GASYLYS	QQHYY---SLIT	GFNI--GGGSI	YIYPGYSSTY	ARTVRGSKKPYFSGWAMDY
H02 3BP2/KB41	QYY--SY	YASGLYS	QQSYYSSGGLIT	GFNI--GGGSI	YIYPGYSSTY	ARTVRGSKKPYFSGWAMDY
H03 3BP2/KB41	QYY--SY	YASGLYS	QQSYYSSGGLIT	GFNI--GGGSI	YIYPGYSSTY	ARTVRGSKKPYFSGWAMDY
H04 3BP2/KB41	QYY--SY	GASYLYS	QQHY---GPLIT	GFNI--GGGSI	YIYPGYSSTY	ARTVRGSKKPYFSGWAMDY
A05 ABL1/pJG4-5	QYG-YSS	GASGLYS	QQYGY---SLIT	GFNL--SYSGM	GIYSSYGYTY	ARYYYG---------AGMDY
A06 ABL1/pJG4-5	QYG-YSS	GASGLYS	QQYGY---SLIT	GFNL--SYSGM	GIYSSYGYTY	ARYFYP---------AGMDY
A07 ABL1/pJG4-5	QYG-YSS	GASGLYS	QQYGY--GWPIT	GFNL--SYSGM	GIYSSYGYTY	ARYYWSS------YGGGMDY
A08 ABL1/pJG4-5	QYG-YSS	GASGLYS	QQYGY--GWPIT	GFNL--SYSGM	GIYSSYGYTY	ARYYWSS------YGGGMDY
B06 ABL1/pJG4-5	QYG-YSS	GASGLYS	QQYGY--GWPIT	GFNL--SYSGM	GIYSSYGYTY	ARYYWSS------YGGGMDY

B07 ABL1/pJG4-5	QYG-YSS	GASGLYS	QQYGY--GWPIT	GFNL--SYSGM	GIYSSYGYTY	ARYYWSS------YGGGMDY
B08 ABL1/pJG4-5	QYYSYGY	YASYLYS	QQAAG---SPIT	GFNIG-SGSSI	YISPGYSYTS	ARGWW----------WAMDY
C05 ABL1/pJG4-5	QYG-YSS	GASGLYP	QQHGW---SLIT	GFNL--SYSGM	GIYSSYGYTY	ARYSGYGSYYYPAPYSGFDY
C06 ABL1/pJG4-5	QYG-YSS	GASGLYS	QQYGY---ALIT	GFNL--SYSGM	GIYSSYGYTY	ARYSYS------YYGAGMDY
C08 ABL1/pJG4-5	QYYSYGY	YASYLYS	QQAAG---SPIT	GFNIG-SGSSI	YISPGYSYTS	ARGWW----------WAMDY
D05 ABL1/pJG4-5	QYG-YSS	GASGLYS	QQYGY--GWPIT	GFNL--SYSGM	GIYSSYGYTY	ARYYWSS------YGGGMDY
D06 ABL1/pJG4-5	QYG-YSS	GASGLYS	QQYGY--GWPIT	GFNL--SYSGM	GIYSSYGYTY	ARYYWSS------YGGGMDY
D07 ABL1/pJG4-5	QSS--GY	GASYLYS	QQYGY---SLIT	GFNL--SYSGM	GIYSSYGYTY	ARYYWSS------YGGGMDY
D08 ABL1/pJG4-5	QYG-YSS	GASGLYS	QQYGY---SLIT	GFNL--SYSGM	GIYSSYGYTY	ARYHYSW-------YSGMDY
E07 ABL1/KB41	QYYSYGY	YASYLYS	QQAAG---SPIT	GFNIG-SGSSI	YISPGYSYTS	ARGWW----------WAMDY
E08 ABL1/KB41	QYG-YSS	GASGLYS	QQYGY---SLIT	GFNL--SYSGM	GIYSSYGYTY	ARYYYY------YGAYGLDY
F05 ABL1/KB41	QYG-YSS	GASGLYS	QQYSY--ASPIT	GFNL--SYSGM	GIYSSYGYTY	ARYYYY------YGAYGLDY
F07 ABL1/KB41	QYG-YSS	GASGLYS	QQYGY---SLIT	GFNL--SYSGM	GIYSSYGYTY	ARYYYAVP------VHGMDY
F08 ABL1/KB41	QYG-YSS	GASGLYS	QQYGY---ALIT	GFNL--SYSGM	GIYSSYGYTY	ARYYYG---------AGMDY
G05 ABL1/KB41	QYYSYGY	GASGLYS	QQYGY---SLIT	GFNL--SYSGM	GIYSSYGYTY	ARYYYG---------AGMDY
G06 ABL1/KB41	QYG-YSS	SASGLYS	QQYGY---ALIT	GFNL--SYSGM	GIYSSYGYTY	ARYSYS------YYGAGMDY
G07 ABL1/KB41	QYG-YSS	GASGLYS	QQHGW---SLTT	GFNL--SYSGM	GIYSSYGYTY	ARYSGYGSYYYPAPYSGFDY
G08 ABL1/KB41	QYG-YSS	GASGLYS	QQYGY---SLIT	GFNL--SYSGM	GIYSSYGYTY	ARYYYFG------SAVGMDY
H05 ABL1/KB41	QYG-YSS	GASGLYS	QQYGY---SLIT	GFNL--SCSGM	GIYSSYGYTY	ARYWYGW-------CAGMDY
H06 ABL1/KB41	QYYSYGY	YASYLYS	QQAAG---SPIT	GFNIG-SGSSI	YISPGYSYTS	ARGWW----------WAMDY
H07 ABL1/KB41	QYC-YSY	CASGLYS	RQYSY--ASPIT	GFNL--SYSAM	GIYSSYCYSY	ARYYWSS------YSDGMDY
H08 ABL1/KB41	QYYSYGY	YASYLYS	QQAAG---SPIT	GFNIG-SGSSI	YISPGYSYTS	ARGWW----------WAMDY
A09 vSRC/pJG4-5	QGYY-GS	YASYLYS	QQAPS---ALIT	GFNI--YYYYI	SISPYSGYTG	ARGGW----------AIDY
A10 vSRC/pJG4-5	QGYY-GS	YASYLYS	QQAPS---ALIT	GFNI--YYYYI	SISPYSGYIG	ARGGW----------AIDY
A11 vSRC/pJG4-5	QGYY-GS	YASYLYS	QQPWH-YSYPIT	GFNI--YYYYI	SISPYSGYTG	AAGGH----------AIDY
A12 vSRC/pJG4-5	Q-YY-GY	GASYLYS	QQYSG---PPIT	GFNI--YYYYI	SISPYSGYTG	ARSSSFHGWV-HYVGALDY
B09 vSRC/pJG4-5	QGYY-GS	YASYLYS	QQSHG---ALFT	GFNI--YYYYI	SISPYSGYTG	AAGGW----------AIDY
B10 vSRC/pJG4-5	QCY--SY	GASYLYS	QQYSG---PPIT	GFNLG-YSSYM	SISSYGGSTG	ARSSSFHGWV-HYVGALDY
B11 vSRC/pJG4-5	QGGY-GY	GASYLYS	QQYSG---PPIT	GFNLG-YSSYM	SISSYGGSTG	ARSSSFHGWV-HYVGALDY
B12 vSRC/pJG4-5	Q-YY-GY	GASYLYS	QQYSG---PPIT	GFNLG-YSSYM	YIYPYGGYTS	ARSSSFHGWV-HYVGALDY
C09 vSRC/pJG4-5	QGYY-GS	YASYLYS	QQPHGGSYYPIT	GFNI--YYYYI	SISPYSGYTG	ARSGW----------AFDY
C10 vSRC/pJG4-5	Q-Y-GGY	GASYLYS	QQYSG---PPIT	GFNLG-YSSYM	SISSYGGSTG	ARSSSFHGWV-HYVGALDY
C11 vSRC/pJG4-5	QGSY-GY	GASYLYS	QQYGY----LIT	GFNLG-YSSYM	SISSYGGSTG	ARSSSFHGWV-HYVGALDY
C12 vSRC/pJG4-5	QGGY-GY	YASYLYS	QQSSY---SLIT	GFNI--YYYYI	SISPYSGYTG	AAGGW----------AIDY
D09 vSRC/pJG4-5	QGYY-GS	YASYLYS	QQAPS---ALIT	GFNI--YYYYI	SISPYSGYTG	ARGGW----------AIDY
D10 vSRC/pJG4-5	Q-Y-GGY	GASYLYS	QQYSG---PPIT	GFNLG-YSSYM	SISSYGGSTG	ARSSSFHGWV-HYVGALDY
D11 vSRC/pJG4-5	Q-YSYGY	GASYLYS	QQPAG-PWHPIT	GFNL--YYGYI	SIYPPYGSTS	ARSVY---------SGLDY
D12 vSRC/pJG4-5	Q-YSYGY	GASYLYS	QQPAG-PWHPIT	GFNL--YYGYI	SIYPPYGSTS	ARSVY---------SGLDY
E09 vSRC/KB41	QGSY-GY	GASYLYS	QQYGY----LIT	GFNI--YYYYI	SISPYSGYTS	ARSSSFHGWV-HYVGALDY
E10 vSRC/KB41	QGYY-GS	YASYLYS	QQSSG----PIT	GFNI--YYYYI	SISPYSGYTG	ARGGF----------AMDY

E11 vSRC/KB41	Q-YY-GY	GASYLYS	QQYSG---PPIT	GFNISSGSYGI	YIYPSYGYTY	ARSSSFHGWV-HYVGALDY
E12 vSRC/KB41	Q-YY-GY	GASYLYS	QQYSG---PPIT	GFNLG-YSSYM	SISPYSGYTG	ARSSSFHGWV-HYVGALDY
F10 vSRC/KB41	Q-YY-SY	GASYLYS	QQYGS----PIT	GFNIYYGYSGI	YIYPYSGYTY	ARSSSFHGWV-HYVGALDY
F11 vSRC/KB41	Q-YY-GY	YASYLYS	QQAPS---ALIT	GFNI--YYYYI	SISPYSGYTG	ARGGW----------AIDY
F12 vSRC/KB41	Q-YY-GS	GASGLYS	QQSHG----PIT	GFNIYYGSYGI	YISSYYGYTS	ARTVRGSKKPYFSGWAMDY
G09 vSRC/KB41	Q-YY-GY	GASYLYS	QQYSG---PPIT	GFNLG-YSSYM	SISSYGGSTG	ARSSSFHGWV-HYVGALDY
G10 vSRC/KB41	Q-YGYSS	GASGLYS	QQFWG-SHSLIT	GFNLS--YSGM	GIYSSYGYTY	ARYVSSS--------GLDY
G11 vSRC/KB41	Q-YY-GY	GASYLYS	QQYSG---PPIT	GFNLG-YSSYM	SISSYGGSTG	ARSSSFHGWV-HYVGALDY
G12 vSRC/KB41	Q-YGYSS	GASGLYS	QQFWG-SHSLIT	GFNLS--YSGM	GIYSSYGYTY	ARYVSSS--------GLDY
H10 vSRC/KB41	Q-YY-GS	GASGLYS	QQAHG----PIT	GFNIYYGSYGI	YISSYYGYTS	ARTVRGSKKPYFSGWAMDY
H11 vSRC/KB41	QDYY-SS	YASYLYS	QQDPS---ARTT			
H12 vSRC/KB41	QGSY-GY	GASYLYS	QQYSG---PPIT	GFNLG-YSSYM	SISSYGGSTG	ARSSSFHGWV-HYVGALDY

CDRs of ScFvs Isolated by Yeast Two-Hybrid: ScFvs that bound to their target were determined by yeast two-hybrid screening as per section 4.5.5. Individual clones were isolated and prepared for sequencing as per section 4.3.4. CDRs were determined by MacVector alignment. Colonies that did not show sugar dependence are indicated in red.

8.1.6 Appendix 6

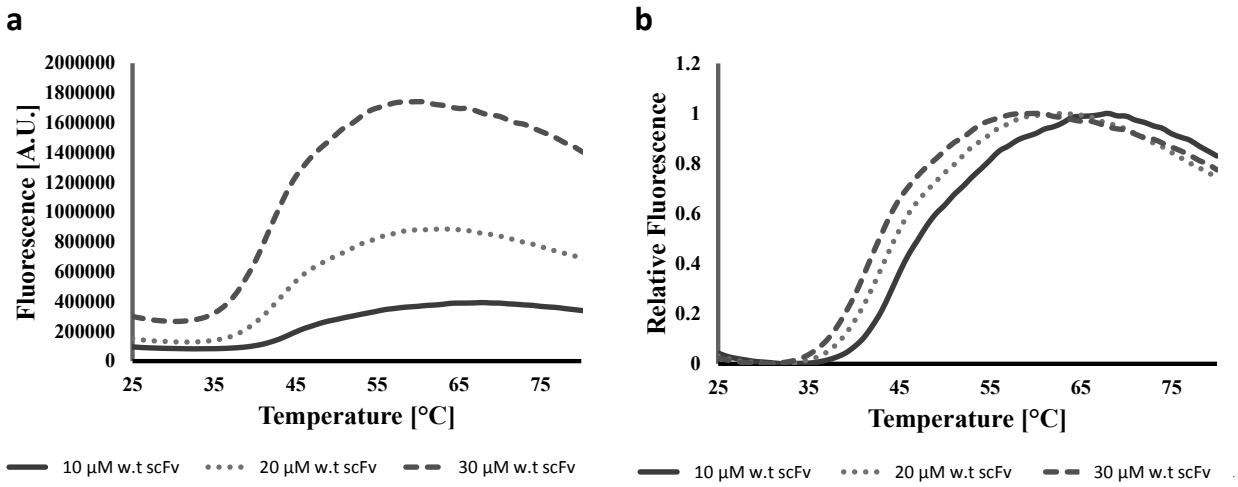

Concentration Dependence of Melt Curves: The thermal stability assay was performed on the anti-MBP scFv as per section 4.7.3. Briefly, scFvs were diluted to a concentration of 10, 20, and 30 µM in Strep-tactin elution buffer. One microliter of 300x SYPRO Orange was added to 19 µL of scFv solution. Samples were loaded in triplicate into a 96-well reaction plate. Thermal denaturation was performed on Step One Plus Real-time PCR system (Applied Biosystems) with 0.2°C per 12 seconds steps. Calculations of the scFv T_ms and visualization of the melt curves were performed using a Differential Scanning Fluorimetry tool. The T_m drops from 46.7 ± 0.2ºC at 10 µM to 44.5 ± 0.2ºC at 20 µM, and down to 43.7 ± 0.8ºC at 10 µM. For comparison, melt curves of the standard scFvs are shown in absolute fluorescence **(a)** and in relative fluorescence **(b)**.